A SEMI-AUTOMATIC REMOTE CONTROLLED SYNTHESIS OF [^{11}C]-2-DEOXY-D-GLUCOSE

S. A. Stone-Elander, E. Ehrin, and J. L. G. Nilsson.
Karolinska Pharmacy, Box 60024, S-104 01 Stockholm, Sweden.

[^{14}C]-2-Deoxy-D-glucose (2-DG) has been used as a substrate for measuring local rates of brain glucose metabolism in animals by quantitative autoradiography (1). The substitution of the 2-hydroxyl group by a hydrogen atom isolates the first step of glucose metabolism with no subsequent loss of labelled metabolic products from the tissues as is true for radioactive D-glucose. To investigate the suitability of 2-DG for "in vivo" studies of local energy metabolism in man by positron emission tomography, we have developed a rapid, semi-automatic synthesis suitable for labelling with carbon-11. Availability of this tracer will enable a comparison with [^{11}C]-D-glucose, the synthesis of which was developed here (2) and is now routinely prepared in our lab.

[^{11}C]-2-DG is synthesized by the reaction of 1-deoxy-1-iodo-2,3:4,5-di-O-isopropylidene-D-arabinotol with Na^{11}CN. H^{11}CN, produced by the ^{14}N (p,α) ^{11}C reaction (3), is trapped by bubbling into a solution of NaOH or NaCN in dry dimethylsulfoxide. A solution of the iodide in DMSO is added and the vial heated at 90° for 5 minutes under N_2-bubbling. At the end of the reaction period, the contents are drawn over onto a dry silica column and the nitrile rapidly eluted with diethylether by "flash chromatography". The ether solution is cooled to -78°C, excess diisobutylaluminum hydride added and the nitrile reduced for 3 minutes. Aqueous ethanol is added to quench the excess hydride, dilute HCl added, and the solution heated at 90° to hydrolyze the intermediate imine and remove the isopropylidene protecting groups. After elution through an ion-exchange column, the aqueous solution is concentrated to 0.5-1.0 ml and injected onto an Aminex HPX-87P HPLC column. The aqueous solution of [^{11}C]-2-DG thus obtained is diluted with saline and passed through a Millipore® filter (0.22μ) yielding a solution suitable for injection 45 minutes after the initial trapping of H^{11}CN and a radiochemical yield of 20-30%.

Synthetic methods have been previously published (4,5) for labelling 2-DG with carbon-11. However, the catalysts used in the reduction of the nitrile were poisoned by any iodo compound remaining in the reaction vessel, thereby requiring the daily synthesis of a triflate precursor immediately prior to the cyanide labelling. Reduction with diisobutylaluminum hydride permits the use of the more stable iodo precursor without the accompanying problems of catalyst poisoning.

(1) Sokoloff L., Reivich M., Kennedy C., et al.
J. Neurochem., 28, 897 (1977).

(2) Ehrin E., Westman, E., Nilsson S.O., et al.
J. Labelled Comp. Radiopharm. 17 (3), 453 (1980).

(3) Christman D.R., Finn R.D., Karlstrom K.I., and Wolf A.P.,
Int. J. Appl. Radiat. Isot., 26, 435 (1975).

(4) Mestelan G., Aubert F., Beaucourt J.P., et al.
J. Labelled Comp. Radiopharm., 16, 661 (1979).

(5) MacGregor R.R., Fowler J.S., Wolf A.P., et al.
J. Nucl. Med., 22, 800 (1981).

SYNTHESIS OF F18-FLUORINE GAS FROM NO CARRIER ADDED F18-HF

M.G. Straatmann, D.J. Schlyer, and J. Chasko.
The Cyclotron Corporation, 950 Gilman Street, Berkeley, CA 94710.

Fluorine-18 in the form of fluorine gas has proven to be of great value in the synthesis of organic compounds with application in positron emission tomography (1). Prior methods of F18-fluorine production required a passivated target chamber and the presence of carrier fluorine in the target gas during irradiation (2). In the system reported here, F18-HF is converted to F18-fluorine gas utilizing a microwave discharge (3). This allows production of F18 from the high yield $^{18}O(p,n)\ ^{18}F$ reaction via recycled O18-oxygen gas which never comes in contact with carrier fluorine. This approach further permits the use of a single F18 target for the production of several different F18-precursors since the F18-activity is removed from the target in the form of HF without passivation or the addition of carrier (4). The eluted activity is trapped in a fluorine-passivated Coors AD 998 alumina tube at liquid nitrogen temperature. While still at -196°C, the alumina tube is closed off from the target and evacuated. The trap is then isolated by valves and allowed to warm to room temperature. A microwave discharge (100 watts, 2450 MHz) is initiated in the tube and a mixture of 5% F_2 in helium is added slowly to a total pressure of 1.5 psia. After about 5 minutes the discharge is extinguished and the tube is pressurized to 1 atmosphere with nitrogen gas. The gas containing the F18-activity is then bubbled through a solution of difluorostilbene in freon-11 (5). The products of the resultant addition reaction are then analyzed by radiogas chromotography to determine the yield of the $^{18}F\text{-}F_2$ conversion reaction.

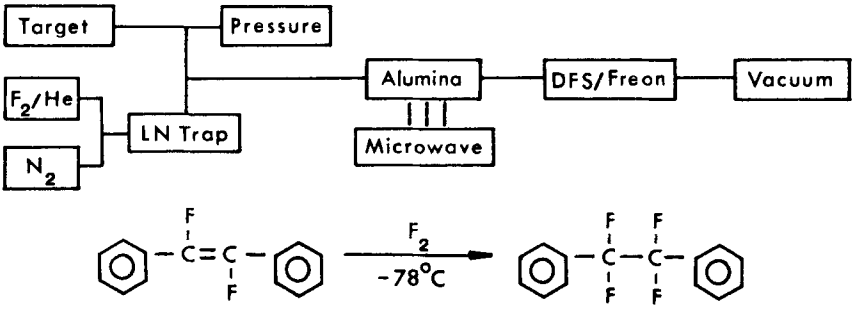

This synthesis has proven to be particularly sensitive to contaminants in the system and to the surface area of the alumina tube. Efforts are underway to improve the conversion yield of this reaction from the present value of 3% (percent of theoretical F18 target yield as F18-DFS adduct). Under optimized conditions, the microwave dissociation/recombination approach may be a route to other F18-precursors containing more than one fluorine atom such as xenon difluoride (6).

(1) Reivich M., Kuhl D., Wolf A.P., et al, Circ. Res., 44, 127 (1979).
(2) Bida G.T., Ehrenkaufer R.L., Wolf A.P., Fowler J.S., MacGregor R.R., and Ruth T.J., J. Nucl. Med., 21, 758 (1981).
(3) Rosner D.E. and Allendorf H.D., J. Phys. Chem., 75, 308 (1971).
(4) Straatmann M.G. and Hendry G.O., Proceedings of 11th International Hot Atom Chemistry Symposium, Davis, California, 1982.
(5) MacGregor R.R., Fowler J.S., and Guzikowski A., private communication (1982).
(6) Firnau G., private communication (1981).

DEVELOPMENT OF AN EQUIPMENT FOR THE AUTOMATIC PRODUCTION OF $^{13}NH_3$ AND L-(^{13}N)-GLUTAMATE

K. Suzuki, K. Tamate, T. Nakayama, T. Yamazaki, Y. Kasida, K. Fukushi, Y. Maruyama, H. Maekawa, and H. Nakaoka.
National Institute of Radiological Sciences, 9-1, 4-Chome Anagawa, Chiba-Shi, Japan.

Up to now, 200~300 mCi of $^{13}NH_3$ have been produced remotely per batch by the $^{16}O(p,\alpha)^{13}N$ reaction by irradiating distilled water with 18 MeV proton beam. Devarda's alloy and sodium hydroxide were used to reduce ^{13}N-labeled oxides formed in the target solution. By manual operation, L-(^{13}N)-glutamate has been produced at a yield of about 90 % by passing distilled $^{13}NH_3$ through a column in which glutamate dehydrogenase was immobilized on an activated Sepharose-4B (1). The L-(^{13}N)-glutamate is purified with an AG-50 cation exchange column.

To achieve the automation in the above procedure, an equipment having following characteristics was developed.

1) It is divided into two units, i.e., working unit and control unit. The working unit is set up inside a hot cell and is composed of electric valves, pumps, reaction vessels, 8 GM tubes, 2 conductivity sensors, etc. which are connected mutually by using teflon tubes. The control unit is located outside the hot cell. It is constructed by connecting a sequential processor to an operation panel, rate meter, CRT, printer, and cassette recorder.
2) The procedures of filling water into a target box, purging out the irradiated solution, preparing and purifying $^{13}NH_3$ and L-(^{13}N)-glutamate, and conditioning the immobilized enzyme column and AG-50 cation exchange column are automatized.
3) The production of $^{13}NH_3$ and L-(^{13}N)-glutamate can be repeated successively 4 times without any additional procedure. When more than 4 repetitions are required, reaction vessels should be changed. In this respect, the method using Devarda's alloy is not so suitable as a reducing agent for the automatic production of $^{13}NH_3$.
4) A sequential processor is used as a controller for the equipment. It contains two CPU, each of which has 32 K bits ROM as an internal program area and 6 K bits RAM as a user's program area. It has a sequencer interface which can control AC power directly and accept two analog inputs and 7 ON-OFF signals. This processor can be used not only for the present purpose but also as an universal processor.
5) The diagram for the system is displayed on the CRT and running lines are distinguished from others by flashing the route.
6) The amounts of ^{13}N formed in the target box during the irradiation, counting rate from the GM tubes and some comments are also displayed on the CRT. By this function, desired amounts of ^{13}N can be produced even after some interruptions of irradiation.
7) The programming sequence is stepped not only by signals from the timer but also by signals from detectors.

It is very important to develop a small and stabilized detector as a line monitor for the radioactivity for an automatic equipment. Although 8 small GM tubes (6 mmϕ x 12 mm, Philips) have been used as line monitors, they have a problem in stability. Therefore, two new types of detectors are now under development. One is a NaI crystal (10 mmϕ x 30 mm) coupled to a photo-multiplier with photo-fibers and the other is also NaI crystal, but coupled to a photo-diode directly. At present, the sensitivity of the latter detector is not enough, but it is most promising since it needs no special equipment for high voltage, counting device, etc.

(1) Gelbard A.S., Benua R.S., Reiman R.E., McDonald J.M., Vomero J.J. and Laughlin J.S., J. nucl. Med., 21, 988-991 (1980).

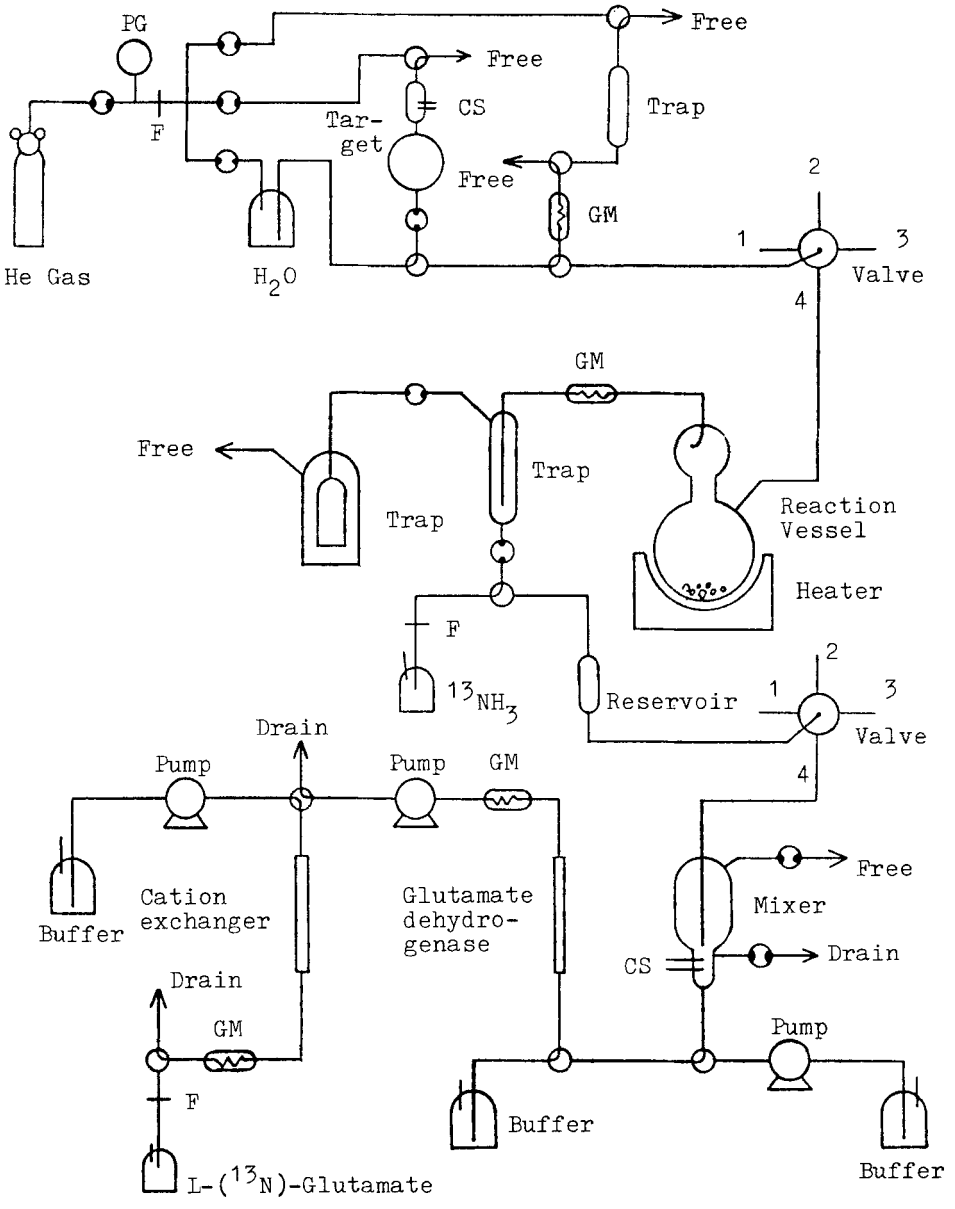

Fig. Diagram for the production of $^{13}NH_3$ and L-(^{13}N)-glutamate

⊖, ⊘, ⊗ ; 2,3,4-way valve, PG; Pressure gauge
CS; Conductivity senser, GM; Geiger Müller tube
F; Filter

OPTIMIZATION OF $^{11}CO_2$ PRODUCTION IN A GAS TARGET

T. Vandewalle and C. Vandecasteele.
Institute of Nuclear Sciences, Proeftuinstraat 86, B-9000 Gent (Belgium).

In general the yield of a radionuclide produced in a gas target is lower than expected from the excitation function. Also, the yield is often not proportional to the beam intensity (1,2,3).

$^{11}CO_2$ is a precursor used for labelling biological active molecules with carbon-11. It is produced in a gas target using the $^{14}N(p,\alpha)^{11}C$ reaction. ^{11}C reacts with traces of oxygen to form $^{11}CO_2$. Practical $^{11}CO_2$ yields are significantly lower than the thick target yields if no attention is paid to the target construction and irradiation conditions. Our purpose is to develop a target with a $^{11}CO_2$ yield close to the thick target yield for 18 MeV protons and intensities up to 20 μA. Therefore the thickness and material of the inlet foil, the diameter of the target and the N_2 pressure must be studied and optimised.

A scheme of the target is represented in Fig. 1 and the experimental conditions shown in Table 1.

Table 1

Target dimension		Entrance windows		Diameter of the collimators	
Internal diameter	Length	[1]	[2]	[4]	[5]
5 cm	40, 50 cm	25 μm Ti	25, 50 μm Ti	20 mm	20, 15 mm
8 cm	20, 30, 40 cm		500 μm Al		

Two collimators [4] and [5] are placed respectively 61 and 2 cm before foil [1]. Between [1] and [2] a helium flow assures the cooling. Behing an exit foil [3] (100 μm Ti) an electrically isolated Faraday cup is placed. The beam intensities on the target and on the Faraday cup are measured separately. Throughout this work 18 MeV protons were used.

First the beam scattering in the inlet foils was studied. A thin copper foil was placed at the exit window and the evacuated target was irradiated. Autoradiographies of the foil were made and the induced ^{62}Zn activity distribution over the foil was measured. For the different entrance foils significant scattering occured, in agreement with the angular distribution calculated according to Marion and Zimmermann (4). To minimize the effect of scattering a large short target with a thin entrance foil made of a low Z material should be used. However, in general a high pressure is required to stoß the beam so that the inlet foil must have a high mechanical strength under irradiation and for fast recovery of the produced activity the target volume must be kept reasonably small. Finally a target of 8 cm internal diameter and 30 cm length and an entrance foil [2] of 50 μm Ti was chosen. To stop the 18 MeV proton beam 10^6 Pa (10 kg/cm^2) is necessary.

The thick target yield for the $^{14}N(p,\alpha)^{11}C$ reaction was determined as a function of the energy (Fig. 2). The results agree satisfactorily with those of Bida et al. (3). Nylon disks were also irradiated at different locations (front-middle-back) in the evacuated target and

in the target filled with nitrogen gas. As appears from Fig. 2, the yields do not differ significantly from the thick target yields at the corresponding energy. Scattering by the entrance foils and by the gas thus does not negatively influence the yield.

For a pressure sufficient to stop the beam at low intensities the current on the Faraday cup was considered as a function of the beam intensity. At a given beam intensity the intensity on the cup rises sharply. Since 4.2 MeV, the proton energy required to penetrate the exit window, corresponds to the practical threshold of the $^{14}N(p,\alpha)^{11}C$ reaction for a given pressure, thick target conditions are in practice only insured up to the point where the current on the cup starts to rise. Calculations show that reduction of the gas density due to beam heating is responsible for this effect. A curve of the breakpoint intensities as a function of the pressure was determined experimentally.

In a final experiment the $^{11}CO_2$ produced under optimal irradiation conditions at different intensities was trapped in a sodium hydroxide solution. The yields were close to the expected ones.

When the scattering of the incident particles by the entrance foils and by the target gas as well as the gas density reduction due to the beam heating are considered, parameters relative to the production can be chosen to allow a reproducible $^{11}CO_2$ production with a maximum yield.

(1) Oselka M., Gindler J.E. and Friedman A.M., Int. J. appl. Radiat. Isotopes, 28, 804 (1977).
(2) Wieland B.W., Schlyer D.J., Ruth T.J. and Wolf A.P., J. Lab. Comp. Radiopharm., XVIII, 27 (1981).
(3) Bida G.T., Ruth T.J. and Wolf A.P., Radiochim.Acta, 27, 181 (1980).
(4) Marion J.B. and Zimmerman B.A., Nucl. Instr. Methods, 51, 93 (1967).

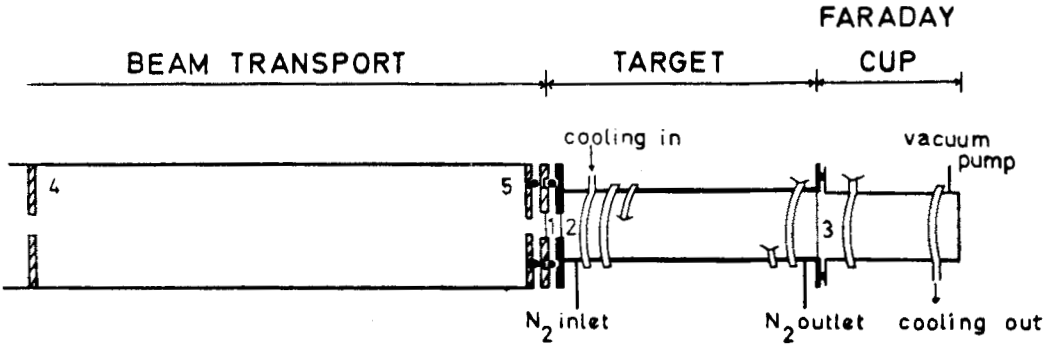

Fig. 1 Target.

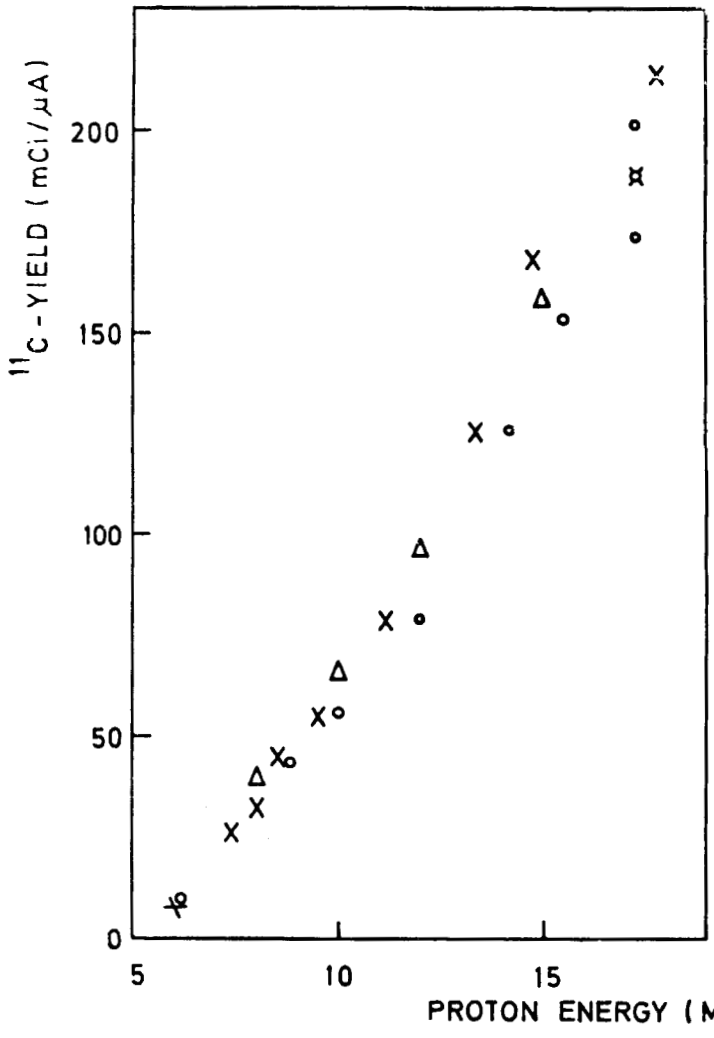

Fig. 2

Thick target yield (at saturation) for the $^{14}N(p,\alpha)^{11}C$ reaction as a function of the energy. (x): Experimentally determined with nylon disks as targets and degrading the energy with Ti and Al foils; (Δ): Results of Bida et al. (3); (o): Experimentally determined with nylon disks irradiated at different locations of the target (see text). The closer the disk is placed to the entrance window, the higher the energy for a target filled with nitrogen gas.

USING A Ge(Li) DETECTOR FOR THE ABSOLUTE ASSAY OF POSITRON EMITTING RADIONUCLIDES, IN PARTICULAR Sr-82/Rb-82

S.L. Waters. M.R.C. Cyclotron Unit, Hammersmith Hospital, London, W12 OHS, U.K.

A prerequisite for quantitative studies involving the positron emission computerised axial tomographic (PECAT) technique, is that the levels of radioactivity being measured are accurately known. In order to achieve this objective, the PECAT and auxiliary counting equipment must be calibrated for the specific radionuclide of interest, and this is most conveniently carried out using radioactive standards. These may be available from a national measurement laboratory; such as sources of Ge-68/Ga-68; or more usually secondary standards have to be prepared and measured "on-site" using a calibrated gamma-ray spectrometer.

The calibration of the spectrometer for gamma-ray detection efficiency generally involves the measurement of a series of standard radioactive sources, with different gamma-ray energies, that often includes Na-22 which provides an efficiency value at 511 and 1275 keV. The efficiency for the annihilation radiation at 511 keV may then be taken as the measured efficiency value for Na-22 or interpolated from a smoothed function drawn through the efficiency values for the range of gamma-ray energies from the other standards (1,2).

It should be noted that substantial errors can be introduced into the radioassay of positron emitters using this approach. This is particularly the case with semi-conductor detectors such as Ge(Li) crystals (2.p.826) and with radionuclides emitting relatively energetic positrons (e.g. Sr-82/Rb-82 β^+ 3.35 MeV.).

Various factors contribute to the overall efficiency of the spectrometer for the 511 keV quanta resulting from positron annihilation, and these have to be carefully standardised before accurate radioassays can be obtained. It is important therefore to take full account of such factors as:

(a) the exact geometry of the source (including source to detector distance, and the type and dimensions of the annihilator).
(b) the absorption of the emitted gamma-rays (by the source, annihilator, air gap, detector, etc.) (3).
(c) the increase in width of the 511 keV gamma-ray peak due to the Doppler broadening effect of the positron annihilation process. (4)

In view of the difficulties and potential inaccuracies in predicting some of the above effects by calculation, we have chosen to make direct measurements in order to assess the magnitude of the problem for our spectrometer arrangement.

We have adopted a fixed geometry for all our radioassay procedures. Standard 1 ml liquid sources sealed in British Standard 2 ml glass ampoules are measured at 25 cm from the detector face. (see Fig. 1). A Ge(Li) crystal (P.G.T., 85cm ^{3} co-axial + RG11A pre-amp) is used as the detector and this is linked via a spectroscopy amplifier (Ortec 570) to a 4096 multichannel analyser (Nuclear Data ND-66). The complete system typically handles total count-rates in the region of 5K sec^{-1} without any artifacts. We also use pure aluminium annihilators in the geometry as shown in Fig. 1.

Measurements were made of the integrated photo-peaks of Sr-85, Na-22, and Ge-68/Ga-68 sources which had been calibrated for absolute activity using pressurised ionisation chambers at the National Physical Laboratory (N.P.L.). A variety of Rb-82 sources were also prepared from the elution of a Sr-82 generator (5); the activity being based on the integration of the 777 keV photo-peak(6) and the Ge(Li) efficiency calibration interpolated from a curve obtained using standards as previously described (1,2). All these sources were examined using a range of aluminium annihilators up to a maximum thickness of 0.8 cm. A thickness of 0.81 cm of aluminium (2.19 g cm^{-2}) is required to completely annihilate the 3.35 MeV positrons from Rb-82 (7). The results of these measurements are shown in the accompanying table and in Fig. 2.

Detector Efficiency for integrated annihilation radiation photopeaks (corrected for γ-quanta) as a function of aluminium annihilator thickness.

Radio-nuclide	Maximum Positron Energy	Aluminium Annihilator Thickness				
		No Annihilator	0.86 gcm^{-2}	1.28 gcm^{-2}	1.71 gcm^{-2}	2.14 gcm^{-2}
^{85}Sr	(514 keV γ-ray)	0.000351 (±0.9%)	0.000329 (±1.1%)	0.000321 (±0.5%)	0.000307 (±0.8%)	0.000294 (±1.3%)
^{22}Na	0.545 MeV	0.000339 (±0.2%)	0.000313 (±1.2%)	0.000303 (±0.8%)	0.000292 (±0.4%)	0.000282 (±0.3%)
^{68}Ga	1.90 MeV	0.000382 (±0.6%)	0.000347 (±0.9%)	0.000334 (±0.4%)	0.000317 (±0.2%)	0.000305 (±0.9%)
^{82}Rb	3.35 MeV	0.000317 (±7.2%)	0.000277 (±7.6%)	0.000270 (±7.5%)	0.000264 (±8.1%)	0.000259 (±7.2%)

It is apparent from the data presented that the efficiency of the detector for the 511 keV annihilation radiation is dependent on the source used to calibrate the spectrometer. In the case of Sr-85 where there is no annihilation process, the reduction in the detector efficiency is due solely to absorption effects. However in the case of Na-22 and Ga-68 where the annihilation process is taking place in a 4Π geometry around the source, considerable deviations from the Sr-85 values were measured.

Even greater effects were measured with Rb-82, where it now appears from this data, that the radioassay based on the intensity of the 777 keV emission as 13.6% and the 511/777 ratio as 14.1 ± 1.0 (6) may be in some doubt, as the authors of the original publication appeared to have made no allowances for the problems outlined above. Further investigations into the Sr-82/Rb-82 decay scheme are progressing.

Acknowledgements: The author is indebted to J.C. Clark (MRC Cyclotron Unit), I.W. Goodier and M.J. Woods (NPL) for much useful discussion.

References

(1) Adams F. and Dams R., "Applied Gamma-Ray Spectrometry", 2nd Ed. Pergamon Press Ltd., 1970, p. 217-220.
(2) Helmer R.G., et al. "Gamma-Ray Energy and Intensity Measurements with Ge(Li) Spectrometers", Ch. 17 of "The Electromagnetic Interaction in Nuclear Spectroscopy" Ed. Hamilton, W.D., North Holland and American Elsevier Pub. Co., 1975, p. 825-834.
(3) Azuelos G., et al. Nucl. Instr. Meths. 142, 491-493 (1977).
(4) Murray G., Phys. Letts., 24B, 268-269 (1967).
(5) Horlock P.L., et al., J. Radioanal. Chem. 64, 257-265 (1981).
(6) Raman S. and Pinajian, J.J, Nucl. Phys. A125, 129-139 (1969).
(7) Nelms A.T. NBS Circular 577. (1956) and Suppl. (1958).

Figure 1

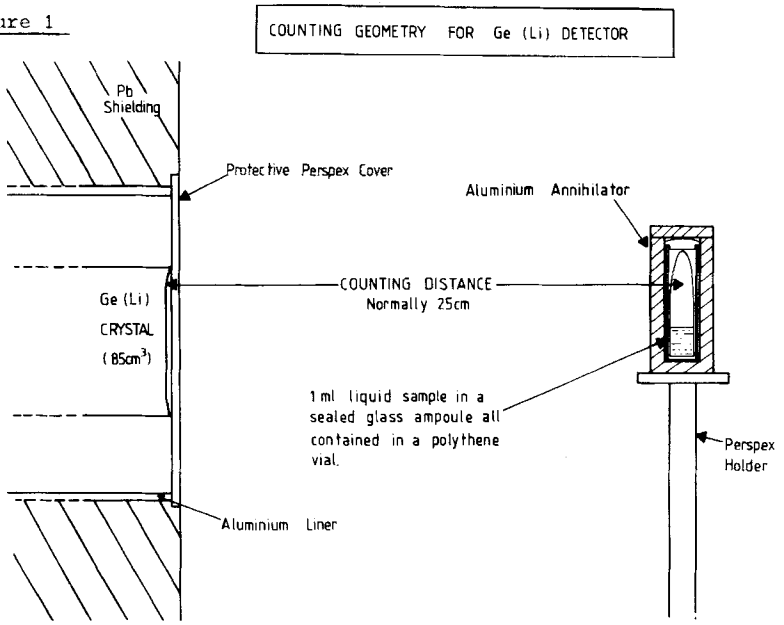

Figure 2

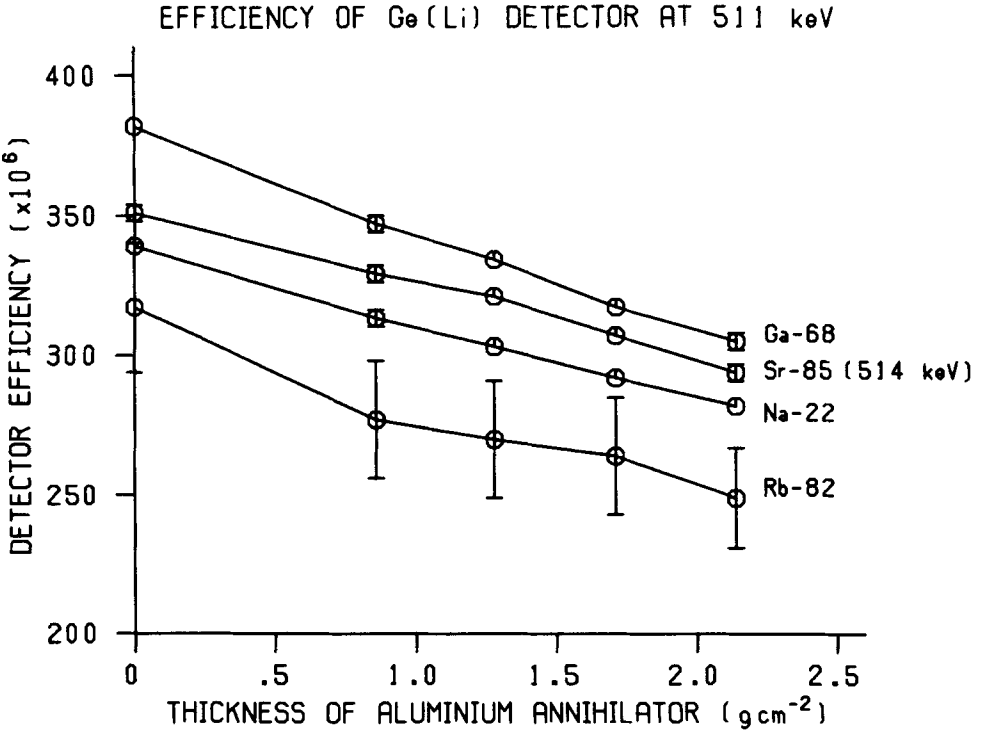

REMOTE SYSTEMS FOR THE ROUTINE PRODUCTION OF SOME CARBON-11 RADIOPHARMACEUTICALS

M.J. Welch, C.S. Dence, and M.R. Kilbourn.
The Edward Mallinckrodt Institute of Radiology, Washington University School of Medicine, St. Louis, MO 63110, USA.

The increasing use of short-lived positron-emitting radiopharmaceuticals for clinical research has necessitated the development of systems which can be utilized to produce these radiopharmaceuticals routinely and with minimal radiation dose to the chemist (1). At Washington University School of Medicine, carbon-11 uniformly labeled glucose is being utilized for studies of brain metabolism (2) while 1-^{11}C-palmitic acid is utilized in studies of myocardial metabolism (3). Remote systems have been developed for the labeling of both of these carbon-11 radiopharmaceuticals. Carbon-11-labeled glucose is produced in our institution photosynthetically utilizing light starved swiss chard plant leaves. In order to produce sufficient amounts (20-30 mCi) of purified labeled glucose, approximately 1 curie of carbon-11-labeled carbon dioxide is needed at the start of the procedure. The remote system for the production of the carbon-11-labeled glucose is contained in a hot cell and consists of two major components. In one of these components the carbon-11 carbon dioxide is trapped at liquid nitrogen temperature; then after warming the activity is circulated utilizing a small peristaltic pump through a reaction vessel containing the light starved leaf. The same reaction vessel is used for illumination, addition of reagents, and evaporation of excess solvent. Following the conversion of the photosynthetic products to a fructose/glucose mixture, the solution is transferred to the second component of the system which is a remotely controlled HPLC system. The carbon-11-labeled glucose is separated from fructose in this system and the effluent monitored using a radiation detector and the glucose peak is transferred into a sterile receiving flask. Total preparation time for the glucose including cyclotron irradiation is approximately 80 minutes and consistently yields of greater than 20 mCi have been obtained utilizing the carbon-11-labeled CO_2 produced with the Washington University School of Medicine Cyclotron Corporation CS-15 cyclotron. The system that we have developed was designed for use with the light starved leaf, however, the system was designed so that it could simply be adapted for use with algae as other investigators have developed preparations of glucose utilizing algae (4).

The remote control system for the production of palmitic acid utilizes a single reaction vessel in which carbon-11 carbon dioxide is reacted with pentadecyl magnesium bromide. The magnesium carboxylate is hydrolyzed, the palmitic acid is extracted into ether, the ether is evaporated, and the final product is solubilized using human serum albumin. As a final step in the procedure, the solution is Millipore filtered using a remote system and a sterile pyrogen free product is obtained. The total production time including cyclotron bombardment is approximately 45 minutes and up to 400 mCi of palmitic acid have been prepared with minimum exposure to the chemist.

Both the systems that we have developed to date require operator interaction, specifically, in the reagent addition, transfer, and organic aqueous extraction steps. We are currently developing techniques for the total automation of the systems described.

REFERENCES

(1) J.S. Fowler, R.R. MacGregor, A.P. Wolf, et al: J. Nucl. Med. 22, 376-380 (1981).
(2) M.E. Raichle, M.J. Welch, R.L. Grubb, Jr., et al: Science 99, 986-987 (1978).
(3) B.E. Sobel, E.S. Weiss, M.J. Welch, et al: Circulation 55, 853-857 (1977).
(4) E. Ehrin, E. Westman, S.O. Nilson, et al: J. Lab. Cpds. Radiopharm. 17, 453-461 (1980).

APPLICATION OF A COMPACT GAMMA-RAY DETECTOR TO AUTOMATIC SYNTHESIS OF RADIOPHARMACEUTICALS LABELLED WITH ^{11}C, ^{13}N, AND ^{18}F

M. Yabe, N. Sato, and K. Matsuno.

Fuji Electric Corporate Research and Development, Ltd., Nagasaka, Yokosuka, Kanagawa 240-01, Japan.

Automatic synthesis of radio pharmaceuticals labelled with ^{11}C, ^{13}N, and ^{18}F are essential in the cyclotron medicine. These radiopharmaceuticals must be promptly synthesized just before their use, because their half-lives are very short. In the course of the synthesis, the close monitoring of positron radioactivity from unit to unit in the synthesizer is essentially needed for its computer control. Since the positron-electron annihilation emits 511 keV gamma-ray photons, gamma-ray detectors are useful for the monitoring. However, since the synthesizer is generally very compactly constructed, existing gamma-ray detectors are too large to fit the tight spaces available for fixing them in it. Therefore, a gamma-ray detector which is sufficiently small, simple in operation, and suitable for obtaining its output signal available for computer processing has been looked for.

Independent of this situation, we developed a compact planar diffused p-n junction type silicon gamma-ray detector by using a ultra-high purity p-type silicon crystal of 10-30 kΩ·cm resistivity in order to make a pocket-size personal gamma-ray monitor (1). Since this detector is encapsulated in a metallic transistor casing 4.8 mm high and 9.1 mm in diameter (Fig. 1) and operable with a 20 volt bias in fully depleted mode at room temperature, it is particularly suitable for solving the above mentioned difficulty. Because the active region is designed to be 140 μm thick for stable operation in the depletion mode at 20 volt, the counting rate of this detector for gamma-rays from ^{241}Am and positron annihilation decreases rather rapidly with their energies as shown in Fig. 2. This characteristic is rather favorable for counting high energy gamma-ray photons with a good linearity versus energy relation.

The applicability of this detector to the monitoring of the automatic pharmaceutical synthesizer has been tested in connection with its sensitivity to the gamma-rays due to positrons from reacting materials, response to the radioactivity change, and attenuation and noise due to cable length. Figure 3 shows the typical response (counts per 2 seconds) of the detector with a 80 cm long cable and the response (instantaneous peak value at every 20 seconds) of a Curie meter(CAPINTEC CRC-10) for a ^{13}N flow carried by NH_3 gas flowing at 50 cm^3/min.

These application data and the characteristics of the detector will be presented along with an exhibition of the detector unit, although the details of the fundamental characteristics have been reported elsewhere.

(1) M. Yabe, N. Sato, H. Kamijo, T. Takechi, and F. Shiraishi, Fifth Symposium on X- and Gamma-Ray Sources and Applications, University of Michigan, Ann Arbor, Michigan, U.S.A., June 10, 1981: Nucl. Instr. Methods, 193 (1982) 63.

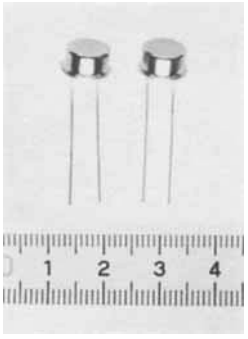

Fig. 1. The silicon gamma ray detector.

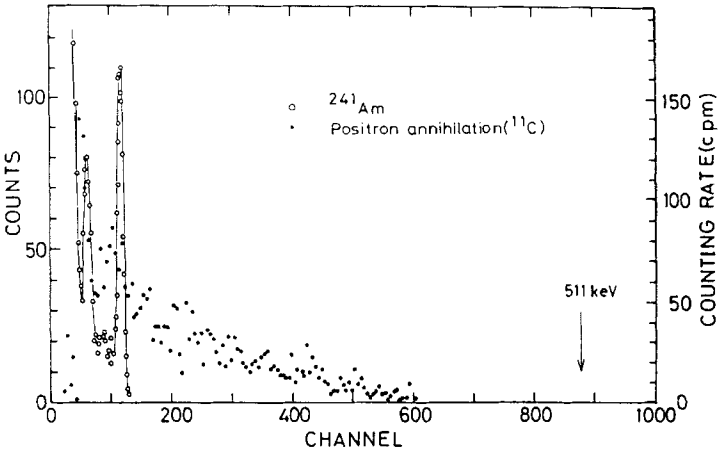

Fig. 2. The gamma-ray spectra of ^{241}Am and positron annihilation due to ^{11}C.

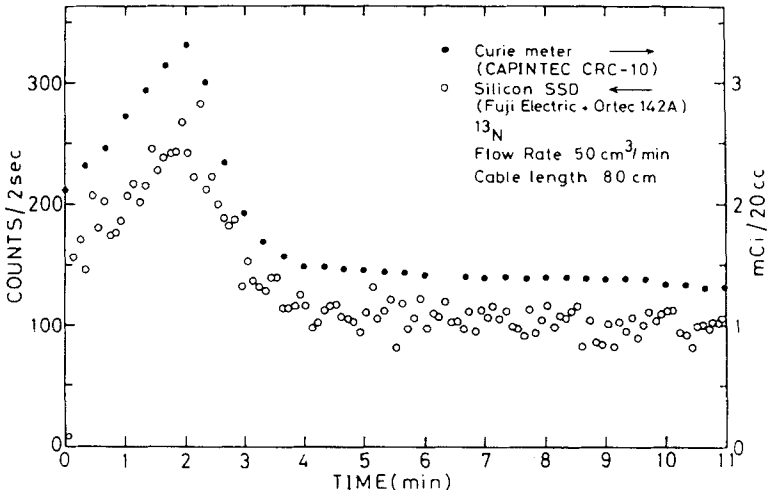

Fig. 3. Comparison of typical response of the silicon detector and a Curie meter to gamma-rays due to positrons emitted from ^{13}N flow carried by NH_3 gas flowing at 50 cm^3/min. The silicon detector was tightly fixed to the piping through which the gas flowed.

A LOW TEMPERATURE IRRADIATION ASSEMBLY FOR THE STUDY OF TECHNETIUM RECOIL IMPLANTATION BY USING CYCLOTRON ACCELERATED PARTICLES

K. Yoshihara, T. Sekine, and T. Ido*.
Department of Chemistry, Faculty of Science, Tohoku University
Sendai 980, Japan.
*Cyclotron Radioisotope Center, Tohoku University, Sendai 980, Japan.

Chemistry of technetium compounds is developing as radiopharmaceuticals of technetium are widely used nowadays. The chemical properties or reaction mechanisms of the technetium complex compounds are not always well elucidated, because of complexity of technetium chemistry.

The authors have been trying to synthesize various technetium complex compounds by recoil implantation and to study their properties and reaction mechanisms. For such purposes, low temperature irradiation is often necessary to suppress thermal and radiation decomposition of irradiation targets and to understand reaction mechanisms accurately.

Therefore, a low temperature assembly was deviced for cyclotron bombardment of the targets. The outline of the assembly is shown in Fig. 1. A stream of cooling gas which is cooled with liquid nitrogen is blown to the target for deuteron irradiation. The temperature attainable was investigated for cooling time. The results are shown in Fig. 2. A temperature of -162°C is obtained with helium, while use of nitrogen gas is less effective than helium under similar conditions. A helium stream (300ℓ/min) for cooling was adopted in the experiments hereafter.

Suppresion of thermal and radiation decomposition by this assembly was much improved compared to the case when the irradiation was done by an ordinary water cooling system. A deuteron beam current of 1μA for 40min. was a standard irradiation condition in our experiments. Phthalocyanines were outstandingly stable, porphyrins were also stable and metal acetylacetonate complexes were fairly stable under this condition.

When the low temperature irradiation was combined with air-free treatment in a glove box, oxidation of implanted technetium to pertechnetate was almost completely avoided. The result is shown in Fig. 3. The target pellet of a mixture of molybdenum and chromium acetylacetonate was irradiated with 24 MeV deuterons under the above condition, and left for 1 day in liquid nitrogen. Then the target was dissolved in benzene and the solution was shaken with perchloric acid of pH 3, and the aqueous extract was passed through a gel chromatography column of Sephadex G-10.

^{95}Tc and ^{99m}Tc produced by the decay of ^{99}Mo were the main objects. Almost all of the technetium is present in reduced forms and not as pertechnetate as is clearly shown in Fig. 3.

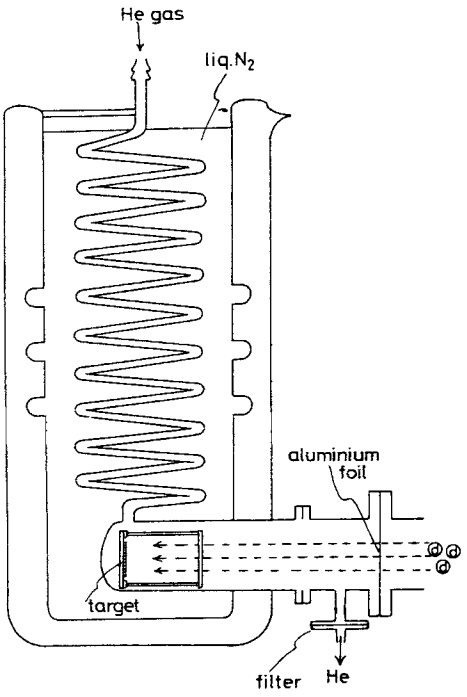

Fig. 1. Irradiation assembly with helium cooling

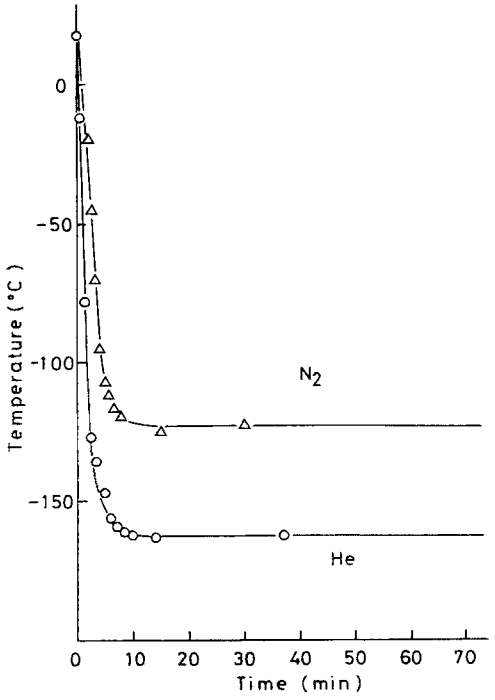

Fig. 2. Temperature vs. cooling time

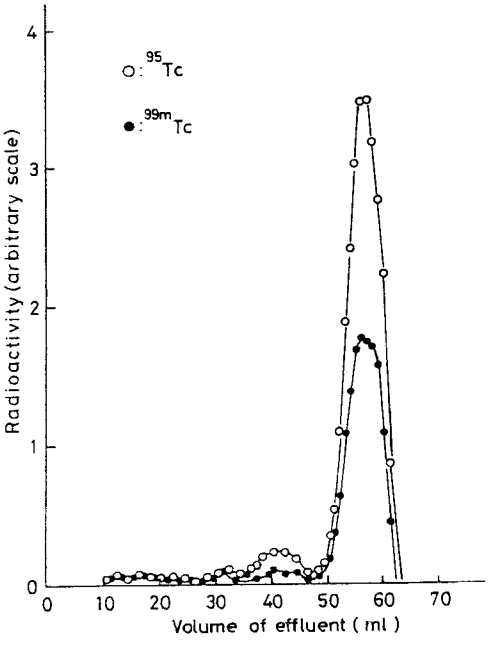

Fig. 3. Gelchromatographic separation of technetium implanted in $Cr(acac)_3$

BIOLOGICAL EFFECTS AND THERAPEUTIC APPLICATIONS OF AUGER AND ALPHA EMITTING RADIONUCLIDES

S.J. Adelstein and W. D. Bloomer.
Departments of Radiology and Radiation Therapy,
Harvard Medical School, Boston, Massachusetts 02115.

The role for unsealed radionuclides in cancer therapy remains largely unrealized, the reasons being the scarcity of carrier molecules with which to achieve differential tumor accumulation and the paucity of appropriate radionuclides . Two types of radioactive decay which satisfy the latter requirement are electron capture with subsequent Auger cascade and alpha emission.

^{125}I decays by electron capture and undergoes internal conversion in 93% of disintegrations. These electron vacancies are filled by outer shell electron rearrangements and ionizations which continue until the valance shell is reached (Auger effect). The number of Auger electrons released per ^{125}I disintegration is substantial and the electrons most frequently produced have a subcellular range (1). Assuming homogeneous distributions of ^{125}I within spherical volumes whose diameters approximate those of the DNA helix and an idealized tumor cell, there is at least an order of magnitude increase in energy deposition within the genome. Consequently one would expect the biological toxicity to be critically dependent on subcellular localization.

Regardless of the assay system used, ^{125}I accumulation within nuclear structures is singularly damaging (2). Much of the supporting data has been obtained from studies where the thymidine analogue $^{125}IUdR$ is incorporated into the DNA backbone. The process is highly efficient; nearly every ^{125}I disintegration produces a double strand break in coliphage and mammalian DNA (3). Considerable evidence exists to suggest that the molecular lesion(s) produced by $^{125}IUdR$ differ from those created by photon irradiation. $^{125}IUdR$ decay leads to marked molecular fragmentation; by comparison, external γ-radiolysis of non-radioactive IUdR results almost exclusively in simple dehalogenation (4). Recent studies using ^{125}I-labeled deoxycytidine located at a single position within a DNA fragment of defined sequence have shown that most radiochemical damage occurs within five nucleotides or 15 to 20 Å of the site of decay (5). Despite possible mechanistic differences, ^{125}I shares a common lethal expression in chromatin with other radiations, at least in terms of morphologically observable phenomena (6).

The use of $^{125}IUdR$ *in vivo* raises a number of potential difficulties: Rapid hepatic dehalogenation, S-phase specificity and high growth fraction are necessary for efficacy. Despite these obstacles, therapeutic doses of carrier-free $^{125}IUdR$ can be administered by intraperitoneal injection to mice bearing ascites tumor cells without producing overt signs of normal tissue toxicity (7). Under these circumstances, tumor cells are exposed directly to $^{125}IUdR$ in the peritoneal cavity before the drug enters the systemic circulation and is degraded. A survival fraction of 10^{-5} can be obtained with 7 injections of 20 uCi each over a 24 hour period.

Alternatives to the use of DNA precursors as carriers of ^{125}I are steroid hormones or their analogues which are translocated from the cytoplasm to the nucleus of cells that contain specific hormone receptors. Once formed, the specific receptor-hormone complex is translocated from the cytoplasm to the nucleus (8,9).

Tamoxifen is a non-steroidal antiestrogen that competes with 17-β-estradiol for the estrogen receptor and is translocated to the nucleus (10). Carrier-free ^{125}I-tamoxifen ($^{125}ITAM$) can be synthesized by the chloramine-T reaction using the tri-*n*-butyltin tamoxifen intermediate (11). An *in vitro* line of human breast cancer cells (MCF-7) derived from a malignant pleural effusion contains biologically active estrogen receptor and is well-suited to investigate ^{125}I cytotoxicity. The specific cytosol estrogen receptor levels for MCF-7 (receptor-rich) and Chinese hamster V-79 (receptor-poor) cell lines are 60 and 4 fmol/mg protein, respectively. When survival is expressed in terms of cellular uptake, $^{125}ITAM$ is differentially cytotoxic to MCF-7 cells (12). There is a two decade difference in surviving fraction

between the two cell lines at the highest doses tested. Although ^{125}IUdR is localized exclusively within DNA, ^{125}ITAM is heterogenously distributed throughout the cell, only a small fraction being associated with nuclear structures. Trichloroacetic acid/ethanol precipitable radioactivity (^{125}ITAM$_{ppt}$) will isolate ^{125}ITAM associated with nucleic acid and protein, specifically or non-specifically bound, from that associated with the whole cell. ^{125}ITAM$_{ppt}$ is just about as toxic as ^{125}IUdR localized within the DNA backbone (13).

Among the currently available alpha emitting radionuclides, astatine-211 appears the most promising. ^{211}At decays by a complex double-branched pathway to lead-207 directly by alpha emission (42%) and indirectly through electron capture (58%) to polonium-211 which almost spontaneously decays by alpha emission. The physical half life is 7.2 hours, the average alpha particle energy is 6.8 MeV, the range in water 60 μm (6 cell diameters) and the linear energy transfer is ∿113 keV/μm. Clonogenic survival assays in V-79 Chinese hamster cells exposed to ionic ^{211}At yield a linear dose response relationship with no shoulder in the low dose region; furthermore, the oxygen enhancement ratio of 1.5 is close to that of other densely ionizing (high LET) particles (14).

We studied the therapeutic efficacy of ^{211}At colloid in experimental malignant ascites and reported that the radiocolloid can be curative with minimal normal tissue toxicity (15). Under the experimental conditions, the therapeutic ratio is favorable because the colloid represents a form of directed administration that physically separates and protects the sensitive mucosal lining of the intestine. Single graded doses of ^{211}At colloid were administered by intraperitoneal injection 24 hours after the intraperitoneal inoculation of 10^6 tumor cells. Mice treated with <50 μCi of the ^{211}At colloid demonstrated a dramatic increase in median survival that was proportional to dose. Doses of 25 and 50 μCi were curative in all animals; although there was some acute morbidity at these doses, there were no acute deaths. The therapeutic efficacy of ^{211}At colloid was compared with that of negatron-emitting ^{32}P as chromic phosphate. Chromic phosphate had no therapeutic efficacy - at doses of 5 to 100 μCi, there was little if any prolongation of median survival, and at higher doses, mice died of toxicity. The most compelling reason for the increased efficacy of the ^{211}At-tellurium colloid is the direct and densely ionizing character of the emitted alpha radiations.

(1) Charlton, D.E., and J. Booz. Radiat. Res., 87, 10 (1981).
(2) Halpern, A., and G. Stöcklin. Radiat. Environ. Biophys., 14, 167, 257 (1977).
(3) Krisch, R.E., and C.J. Sauri. Int. J. Radiat. Biol., 27, 553 (1975).
(4) Stöcklin, G. In S. Okada, M. Imamura, T. Teroshima, and H. Yamaguchi (Eds.), Proceedings of the Sixth International Congress of Radiation Research. Tappan, Tokyo, 382 (1979).
(5) Martin, R.F., and W.A. Haseltine. Science, 213, 896 (1981).
(6) Chan, P.C., E. Lisco, H. Lisco, and S.J. Adelstein. Radiat. Res., 67, 332 (1976).
(7) Bloomer, W.D. and S.J. Adelstein. Nature, 265, 620 (1977).
(8) Jensen, E.V., and H.I. Jacobson. Recent Prog. Horm. Res., 18, 387 (1962).
(9) Senior, M.B. and F.R. Frankel. Cell, 14, 857 (1978).
(10) Heel, R.C., R.N. Brogden, T.M. Speight, and G.S. Avery. Drugs, 16, 1 (1978).
(11) Seitz D.E., G.L. Tonnesen, R.N. Hanson, S. Hellman, and S.J. Adelstein. J. Organomet Chem., 186, C33 (1980).
(12) Bloomer, W.D., W.H. McLaughlin, R.R. Weichselbaum, G.L. Tonnesen, S. Hellman, D.E. Seitz, R.N. Hanson, S.J. Adelstein, A.L. Rosner, N.A. Burstein, J.J. Nove, and J.B. Little. Int. J. Radiat. Biol., 38, 197 (1980).
(13) Bloomer, W.D., W.H. McLaughlin, R.R. Weichselbaum, R.N. Hanson, S.J. Adelstein, and D.E. Seitz. J. Radioanal. Chem., 65, 209 (1981).
(14) Harris, C.R., S.J. Adelstein, T.J. Ruth, and A.P. Wolf. Radiat. Res., 74, 590 (1978).
(15) Bloomer, W.D., W.H. McLaughlin, R.D. Neirinckx, S.J. Adelstein, P.R. Gordon, T.J. Ruth, and A.P. Wolf. Science, 212, 340 (1981).

SYNTHESIS AND BIO-DISTRIBUTION OF AN ^{211}At-ASTATINATED AROMATIC ANTITUMOUR DRUG

Ian Brown*.
The Research Laboratories, The Radiotherapeutic Centre, University of Cambridge School of Clinical Medicine, Addenbrooke's Hospital, Cambridge CB2 2QQ, United Kingdom.

The development of potential endoradiotherapeutic drugs represents an alternative approach towards the management of refractory and metastatic malignant disease.(1) Substituted naphthoquinol phosphate salts selectively concentrate in certain tumours,(2) both *in vitro* and *in vivo*. In particular, 6-^{211}At-astato-2-methyl-1,4-naphthoquinol bis(dilithium phosphate), abbreviated 6-^{211}At-astato-MNDP, is being investigated as an antitumour drug; its cytotoxic action is due to the *in situ* radiotherapeutic effect of the highly ionizing decay products of ^{211}At. The resultant α-particle emission, of mean energy 6.8 MeV and range 60 μ can achieve immense subcellular damage and cell death within a significant tissue volume.

Although 6-^{211}At-astato-MNDP has been synthesized over periods of 5 - 7 h, by a five-stage preparation, in yields of 28 - 32%;(3) it is preferable, in view of the short half-life of ^{211}At, to investigate more direct synthetic routes. Thermal heterogeneous isotopic exchange methods are well established;(4) several ^{211}At-astato-aromatic compounds have been prepared from both bromo- and iodo-analogues.(5) Here, isotopic exchange has been attempted for 6-iodo-MNDP (d.pt 180°C) and ^{211}At$^-$ at 170°C.

Astatine-211 was produced via the ^{209}Bi(α,2n)^{211}At reaction at the Birmingham University Nuffield 1.52 m cyclotron. Bismuth, melted onto supporting copper foils was irradiated with a 28 MeV α-beam. ^{211}At was extracted from the irradiated target by dry distillation at 560°C, into 100 mM NaOH.

To a solution of Na^{211}At (100 μCi) was added 1 mg 6-iodo-MNDP; the solution was evaporated to dryness, *in vacuo*. The mixture was heated *in vacuo*, at 170°C for time periods ranging from 2 - 30 m, followed by cooling to room temperature. The residue was dissolved in 30 μl distilled water. Excess ^{211}At$^-$ was removed by ion-exchange chromatography (DEAE-Sephadex); 0.9% aqueous NaCl was used as an eluant. The final solution of 6-^{211}At-astato-MNDP was sterilized by membrane filtration (0.2 μ), ready for injection. The product was identified by tlc-radiochromatography using: cellulose/UV_{254} and n-BuOH/MeCOOH/H_2O (v/v 10:3:7) solvent system. R_F values were 0.45 and 0.90 for 6-^{211}At-astato-MNDP and ^{211}At$^-$ respectively. Activity was determined by measuring X- and γ-ray emission, using a 2 in NaI well crystal. Isotopic exchange efficiency (Fig. 1) appeared to plateau at 40-50%, for periods in excess of 5 m. Heating for 10 m, enabled a rapid and efficient preparation of 6-^{211}At-astato-MNDP to be achieved, in sufficient amounts for bio-distribution and therapeutic studies.

Bio-distribution studies were carried out in C57Bl male mice with a transplanted murine rectal adenocarcinoma. 6-^{211}At-astato-MNDP solution (5 - 10 μCi) was administered by an intra-peritoneal route, to mice whose thyroid activity has been blocked by the prior subcutaneous injection of $KClO_4$. Mice were sacrificed at 30 m, 1 h, 3 h and 6 h. Tissue uptake was expressed in terms of the Mean Biological Concentration (MBC = 100% x Specific activity of organ/specific activity of the whole body). The MBC for tumour was found to range

* Beit Memorial Fellow for Medical Research

from 150 - 230%, over the first 3 h post-injection (Fig. 2); these values parallel those obtained for 6-^{125}I-iodo-MNDP in the same system.(6) Tumour:blood ratio was 2.8 ± 0.7 : 1 over the 6 h studied. Activity was principally excreted via the renal system. Important in any radiotherapeutic treatment is the radiation dose delivered to critical organs; in this respect, kidney, liver and bone marrow are pertinent. Uptake into kidney was 100 - 110%, reflecting the plasma clearence of the drug and its metabolites. Liver and whole blood exhibited a similar pattern of MBC (65 - 75%). For bone marrow, the MBC is 25 - 40% over 6 h; although it is likely that bone marrow toxicity would not be a major problem, it is probable that therapy would involve several successive injections of 6-^{211}At-astato-MNDP. Further data is being accrued in view of the possibility of a cumulative haemapoetic impairment.

Whilst 6-^{211}At-astato-MNDP is known to be stable in vitro,(3) it is important that the ^{211}At-carbon bond is not labile in vivo. Parallel studies with ^{211}At$^-$ have indicated a high uptake of activity into macrophage-laden tissue, such as lung and spleen. There is a significantly lower uptake ($P < 0.001$) of 6-^{211}At-astato-MNDP into spleen and lung, compared with that for ^{211}At$^-$. This suggests that the C-^{211}At bond is stable in vivo, at least over the first 3 h post-injection.

References

(1) Mitchell J.S., Brown I. and Carpenter R.N., Int. J. Radiat. Oncol. Biol. Phys. In press (1982).
(2) Marrian D.H., Marshall B. and Mitchell J.S., Chemotherap. 3, 225 (1961).
(3) Brown I., Int. J. Appl. Radiat. Isotopes. 33, 75 (1982).
(4) Elias H. and Lotterhos H.F., Chem. Berichte. 109, 1580 (1976).
(5) Shiue C.-Y., Meyer G.-J., Ruth T.J. and Wolf A.P., J. Lab. Comp. Radiopharm. 18, 1039 (1981).
(6) Brown I. unpublished results.

Fig. 1

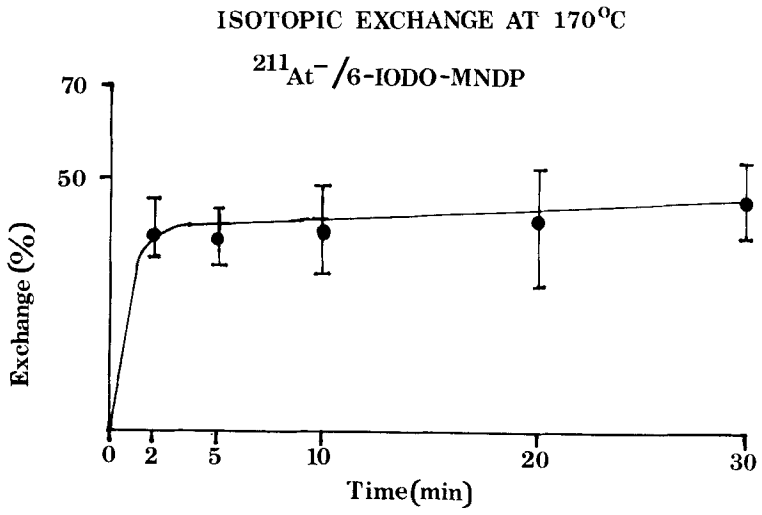

Fig. 2

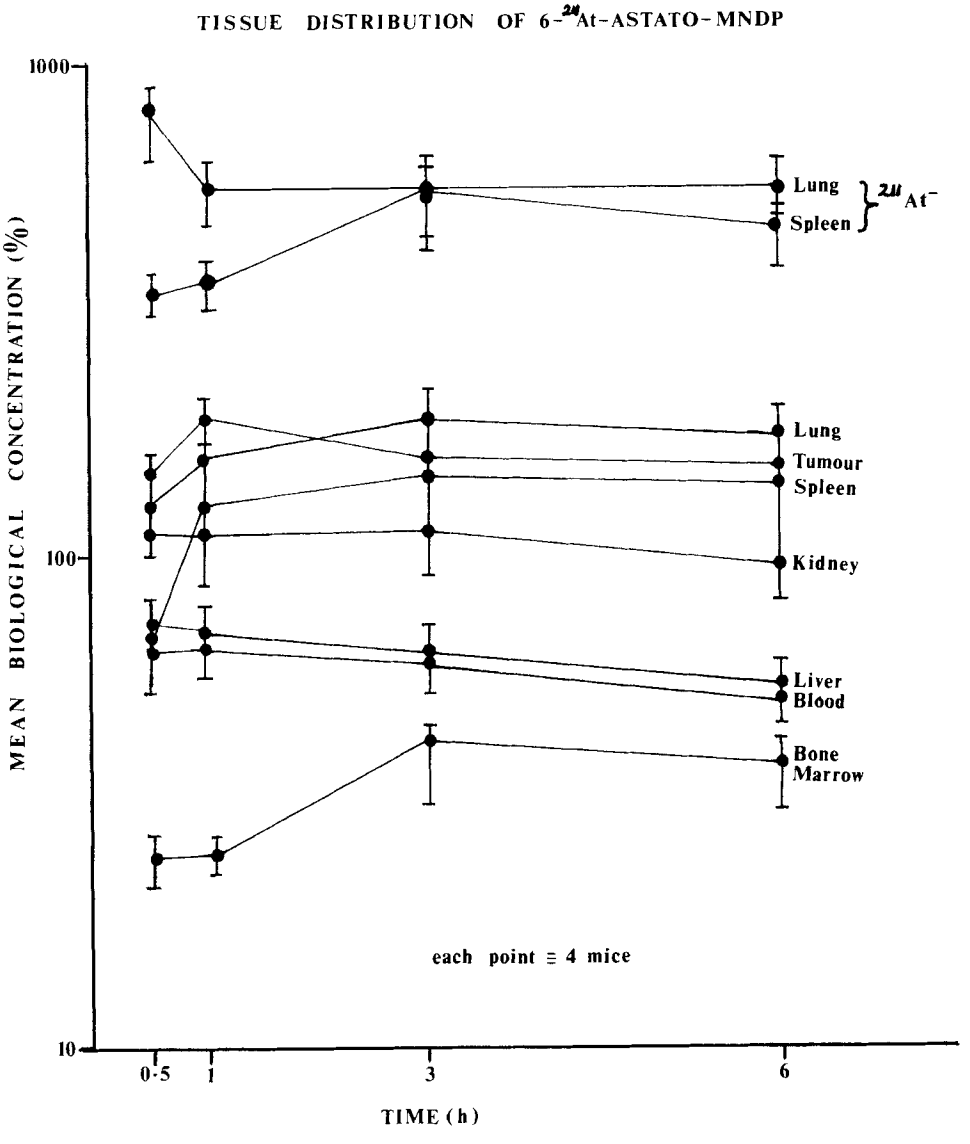
TISSUE DISTRIBUTION OF 6-^{211}At-ASTATO-MNDP
MEAN BIOLOGICAL CONCENTRATION (%)
1000
100
10
Lung
Spleen
^{211}At$^-$
Lung
Tumour
Spleen
Kidney
Liver
Blood
Bone
Marrow
each point ≡ 4 mice
0·5
1
3
6
TIME (h)

PALLADIUM-109 LABELED LYMPHOCYTES - A NEW AGENT FOR LYMPHOID ABLATION

S.C. Srivastava, R.A. Fawwaz, T.S.T. Wang, T. Prach, P. Richards, and P.O. Alderson. Medical Department, Brookhaven National Laboratory, Upton, New York 11973.

Palladium-109 has favorable radionuclidic properties ($t_{½}$ 13.4 hr, β^- 1.028 MeV max.) for use in lymphatic ablation therapy prior to organ transplantation. Earlier work has demonstrated the effectiveness of ^{109}Pd complexes of porphyrins (that localize in lymph nodes) at preventing allograft rejection in dogs and rats, presumably as a result of irradiation from the beta emission of palladium-109 (1-3). Labeled lymphocytes should prove superior for this application since higher and more selective concentration in lymphatic tissue can be achieved than what is generally achieved using porphyrin derivatives.

This study was carried out to: (i) develop a method for preparing ^{109}Pd-8-hydroxyquinoline (Pd-oxine) complex suitable for cell labeling; (ii) optimize conditions for labeling lymphocytes with Pd-oxine; (iii) determine biodistribution of Pd-oxine-labeled lymphocytes (Pd-L) and compare localization results with those obtained with ^{111}In-labeled lymphocytes (In-L); and (iv) evaluate the potential of Pd-L for selective lymphoid ablation relative to that of ^{109}Pd-porphyrins.

Neutron bombardment of enriched $^{108}PdCl_2 \cdot 2H_2O$ (2.03 mg) in a sealed quartz ampule for 16 hr using the Brookhaven High Flux Reactor (5.5×10^{14} n s^{-1} cm^{-2}) produced 1.52 Ci of ^{109}Pd. The material was dissolved in 1.0 ml DMSO with gentle heat and stirring. An aliquot of this solution containing 45 mCi of ^{109}Pd was transferred into a 30 ml multi-injection bottle containing 5 ml of a 0.1 M acetate buffer, pH 3.95, followed by the addition of 234 μg oxine dissolved in the same buffer to give a molar ratio of oxine to palladium of 2.6. The solution was stirred for 30 min and the complex extracted with 5 ml chloroform by vortex mixing (~90% extraction). The chloroform layer was separated and the solvent evaporated under a N_2 stream. The residue was dissolved in 3.0 ml warm absolute ethanol and filtered through a 0.45 μm Nylon-66 filter. The specific activity of ^{109}Pd-oxine complex at the time of experiments was 122 mCi ^{109}Pd/mg Pd-oxine.

Lymph nodes obtained from Lewis rats were passed through a mesh. The cells were washed twice with medium 199 and suspended in phosphate buffered saline, pH 7.4. ^{109}Pd-oxine was added dropwise to the cell suspension and incubation carried out for 30 min. The cells were washed once with medium 199 and resuspended in 1 ml of medium 199. The yield varied between 40 and 65% which is comparable to the yield obtained for ^{111}In oxine labeling of lymphocytes. Pd-L or In-L was injected into animals (n = 3/group) i.v. The animals were sacrificed at 3 hr post injection and % injected dose (ID)/g determined in various tissues by counting. Tissue histology was also obtained. The results are summarized in Table 1.

In tracer doses Pd-L and In-L had similar distributions. Pd-L showed 72 ± 5% of activity in spleen, 15 ± 0.6% in lymph nodes, and 3 ± 0.4% in bone marrow. However, Pd-L showed higher uptake in kidney (9 ± 0.9%) than In-L. An increase in the amount of Pd-oxine (>0.5 μg/10^8 cells) or an increase in Pd-109 activity to >55 μCi/10^8 cells resulted in a significant drop in activity in lymph nodes to 0.5% ID. Histologic studies showed that therapeutic doses of Pd-L (800 μCi Pd-109, 1.2 μg Pd-oxine, and 300 μCi Pd-109/10^8 cells) resulted in marked splenic lymphopenia by day 4, but no lymph node lymphopenia.

This study shows that localization of ^{109}Pd-labeled lymphocytes in lymphatic tissue is indeed much higher and more selective as compared to ^{109}Pd-labeled porphyrins. The results also suggest that splenic lymphoid ablation can be achieved by Pd-109 lymphocytes. However, in order to achieve high lymph node localization and more generalized lymphatic ablation, the ratio of μg Pd-oxine or μCi of ^{109}Pd to cells that are administered must be kept sufficiently low. This entails use of larger numbers of labeled cells at modest (55 μCi/10^8 cells) Pd-L activity concentrations. Presently this is a limiting factor that remains to be solved.

(1) Fawwaz R.A., Frye F., Loughman W. and Hemphill W., J. Nucl. Med. 15, 997 (1974).
(2) Fawwaz R.A. and Hardy M.A., Surgery 86, 194 (1979).
(3) Doi J.D., Lavallee D.K., Srivastava S.C., Prach T., Richards P. and Fawwaz R.A., Int. J. Appl. Radiat. Isotop., 32, 877 (1981).

Table 1
Biodistribution of Pd-109 and In-111-Labeled Lymphocytes

μCi ^{109}Pd/ 10^8 Cells	μg Pd(oxine)/ 10^8 Cells	% Administered Dose Per Gram Tissue 3 hrs					
		Spleen	Liver	Lymph Node	Kidney	Bone Marrow	Intestinal Mucosa
10	0.06	68.1 ± 5.4	6.7 ± 0.7	15.6 ± 0.7	9.7 ± 0.9	4.0 ± 0.6	0.14 ± 0.009
10	0.30	72.0 ± 5.8	5.4 ± 0.6	15.6 ± 0.6	6.5 ± 0.7	3.2 ± 0.4	0.18 ± 0.012
10	0.50	79.1 ± 4.2	4.9 ± 0.4	13.6 ± 0.7	5.6 ± 0.7	3.3 ± 0.2	0.14 ± 0.008
10	1.20	61.1 ± 7.1	5.5 ± 0.4	0.72 ± 0.07	7.7 ± 0.6	0.6 ± 0.03	0.19 ± 0.016
30	0.06	61.3 ± 8.2	9.6 ± 0.5	12.8 ± 0.8	4.1 ± 0.3	4.4 ± 0.7	0.11 ± 0.013
55	0.06	61.8 ± 5.4	6.7 ± 0.9	16.17 ± 0.8	4.5 ± 0.4	4.6 ± 0.4	0.14 ± 0.014
114	0.06	55.1 ± 6.9	6.1 ± 0.7	0.46 ± 0.03	6.2 ± 0.4	1.4 ± 0.05	0.16 ± 0.01
1*	10**	82.3 ± 6.7	5.6 ± 0.7	18.2 ± 0.9	1.1 ± 0.09	5.3 ± 0.6	0.11 ± 0.16

*μCi In-111 and **μg oxine, per 10^8 cells.

Research at Brookhaven National Laboratory supported under U.S. Department of Energy Contract #DE-AC02-76CH00016. Research at Columbia University supported by a grant from the National Heart, Lung and Blood Institute.

^{11}C AND ^{13}N LABELLED BCNU AND ITS IN VIVO PHARMACOKINETICAL STUDY WITH PET *

M. Diksic, S. Farrokhzad, Y.L. Yamamoto, and W. Feindel.
Montreal Neurological Institute, McGill University, Montreal, Canada, H3A 2B4.

1,3-bis(2-chloroethyl)-1-nitrosourea (BCNU) is well known as an antitumor drug (1). We have synthesized ^{13}N and ^{11}C-labelled BCNU and made it suitable for *in vivo* studies with positron emission tomography (PET).

^{13}N has been produced in the form of $^{13}NO_3^-$ by irradiating high purity water with ~9.5 MeV protons (at target material) and a beam current of 50 μA. The volume of the target chamber is 10 ml. The water is kept in the target during irradiation with helium over pressure of one atmosphere.

^{11}CO was produced by proton irradiation of research purity nitrogen in a continuous mode. Irradiated gases are carried through Zn-oven at 400°C where CO_2 is reduced to CO. Any traces of CO_2 are removed with NaOH trap. The Japan Steel Works medical cyclotron has been used as the source of accelerated protons.

After irradiation of water, $2x10^{-2}$ mmol of HNO_3, the hold-back carrier, was added and water was evaporated to dryness. The labelling is done in the same flask by adding a solution of 1,3-bis(2-chloroethyl) urea (BCU) in acetic acid and Cu-dust. This reaction time was about 5 min. In general the labelled ^{13}N-BCNU is available for IV-injection 30 min after the end of irradiation.

Typical specific activity of ^{13}N-BCNU at the time of injection is about 5 mCi/mg or about 1 Ci/mmol.

^{11}C-labelled BCNU (no carrier added) was prepared by nitrosation of ^{11}C-labelled BCU with $NaNO_2$ in CH_3COOH or formic acid. ^{11}C-labelled BCU was synthesized from $^{11}COCl_2$ (no carrier added) and ethylenimine by adopting the method described by Bestion (2) for nonradioactive BCU. ^{11}CO is delivered to the hot cell at a rate of about 25 mCi/min. The gas is mixed with research purity chlorine at a flow rate of ~10 ml/min. A low pressure mercury lamp (450 W) is used to irradiate gas mixture in a quartz spiral. The quartz in the spiral has ID of 3 mm. Nonreacted chlorine is removed from the reaction gas by Sb-trap. ^{11}C-phosgene is collected in a cold solution of dry ethylenimine in acetone. After enough of ^{11}C-phosgene has been collected reaction mixture is warmed up to about 40°C. The best radiochemical yield for BCU obtained so far is ~30%. After 5 min acetone is evaporated and nitrosation is done as mentioned earlier. The final product (^{11}C-BCNU) is separated by HPLC on a Partisil PAC column by using 70% ether in hexane as elution mixture. ^{11}C-BCNU fraction is collected and after evaporation of the solvent dissolved in saline and sterilized by filtering it through 0.2 μ Millipor. This makes 10-15 mCi of ^{11}C-BCNU readily available for patients use. Maximum specific activity achieved so far is 40 Ci/mmol of BCNU at the time of injection. Synthesis time is about 15 min after $^{11}COCl_2$ delivery is stopped.

The optimisation of the labelling procedures will be discussed with an emphasis on the radiochemical yield and specific activity of the final product.

The PET scans have been taken immediately after IV-injection and continued for 60 min. During scanning, the blood samples are taken every 5 min and analysed for intact BCNU. The PET scans in conjunction with blood samples were used in the pharmacokinetics studies.

REFERENCES

(1) Johnston, T.P., G.S. McCaleb, and J.A. Montgomery. J. Med. Chem., 6, 669 (1963).
(2) Bestion, H. Ann. Chem., 566, 210 (1950).

* This work has been supported in part by the grant from National Cancer Institute and Medical Research Council of Canada, Killam fellowships to one of us (M.D.) and the Cone Memorial Research Fund of the Montreal Neurological Institute.

SYNTHESIS OF 5'-DEOXY-5-[^{18}F]FLUOROURIDINE AS A PROBE FOR MEASURING TISSUE PROLIFERATION IN VIVO

C.-Y. Shiue, A.P. Wolf, and M. Friedkin.
Department of Chemistry, Brookhaven National Laboratory, Upton, NY 11973.

The rapid development of positron emission tomography (PET) coupled with a rational choice of radiopharmaceuticals has made it possible to carry out the in vivo study of dynamic biochemical processes. This technique has been used for the measurement of regional glucose metabolism in a variety of human diseases as well as in the localization and quantitation of normal cortical activity by the application of 2-^{18}FDG and PET (1-4). The principles of this technique could also apply to measuring tissue proliferation in vivo by using suitably labeled probes. ^{14}C, ^{3}H and ^{11}C-Labeled thymidine has been used as a tracer to study DNA synthesis in mice and tumor bearing animals (5,6). The use of labeled uridine or uridine analogs could also provide an index of tissue proliferation via increased transport and increased intracellular phosphorylation and incorporation into RNA (7,8). Therefore, if we label uridine or its analog with a positron emitting nuclide, such as ^{18}F, it might be feasible to measure tissue proliferation in vivo.

^{18}F-Labeled 5-fluorouracil (9), 5-fluorouridine (10) and 5-fluorouridylate have been synthesized chemically and enzymatically and used to study the differences in the biodistributions in normal and tumor bearing mice (11). Recently, a new fluorinated nucleoside, 5'-deoxy-5-fluorouridine has been synthesized and has shown equal or better cytostatic activity at lower levels of toxicity than 5-fluorouracil or 2'-deoxy-5-fluorouridine (12,13). The unlabeled compound was prepared from 5-fluorouridine by isopropylidination and iodination, followed by reduction and deprotection (14).

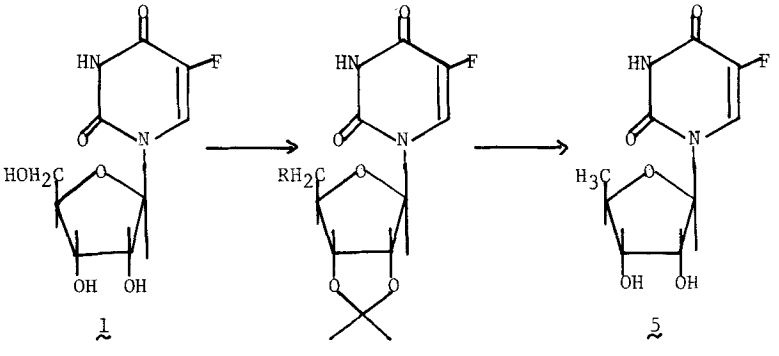

(Eq 1)

1

2 R=OH

3 R=I

4 R=H

5

The method, however, is not suitable for the synthesis of the ^{18}F labeled compound. We report here the synthesis of

5'-deoxy-5-[^{18}F]fluorouridine from either [^{18}F]acetyl hypofluorite (15,16) or [^{18}F]F_2.

Reaction of 5'-deoxy-2',3'-di-O-acetyluridine (6) with [^{18}F]acetyl hypofluorite in acetic acid gave [^{18}F]-5'-deoxy-2',3'-di-O-acetyl-5,6-dihydro-5,6-difluorouridine (7) in ~ 30% radiochemical yield (based on recovered ^{18}F). Hydrolysis of 7 with NaOMe/MeOH followed by purification with column chromatographs (cation exchange and silica gel) gave 5'-deoxy-5-[^{18}F]fluorouridine (8) in 20-25% radiochemical yield in a synthesis time of ~ 80 min from EOB.

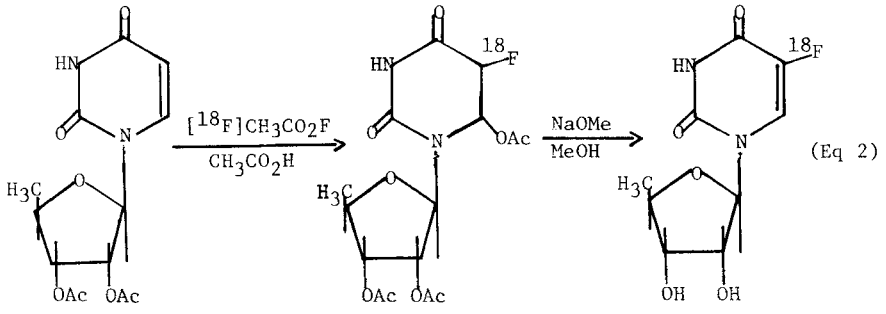

6 7 8 (Eq 2)

Reaction of 5'-deoxy-2',3'-di-O-acetyluridine with [^{18}F]F_2 in acetic acid gave 5'-deoxy-5-[^{18}F]fluorouridine in a yield comparable to that from [^{18}F]acetyl hypofluorite since there are no isomeric separations, in contrast to the synthesis of 2-deoxy-2-[^{18}F]fluoro-D-glucose from the reaction of 3,4,6-tri-O-acetyl-D-glucal with [^{18}F]F_2 (17).

In order to achieve the maximum radiochemical yield of 5'-deoxy-5-[^{18}F]fluorouridine and without the contamination of 5'-deoxyuridine, the molar ratio of [^{18}F]F_2 (or [^{18}F]CH_3CO_2F) with substrate should keep at ~ 2. The identity of compound 8 was checked by tlc (silica gel, EtOAc-  -H_2O, 70:40:5), Rf = 0.65, and in comparison with the authentic sample.

In summary, we report here a convenient synthesis of 5'-deoxy-5-[^{18}F]fluorouridine from either [^{18}F]F_2 or [^{18}F]CH_3CO_2F in high radiochemical yield.

This work was carried out at Brookhaven National Laboratory under contract with the U. S. Department of Energy and also by the Office of Health and Environmental Research. The authors wish to thank Dr. A. F. Cook of Hoffmann-LaRoche for the gifts of 5'-deoxy-2',3'-di-O-acetyluridine and 5'-deoxy-5-fluorouridine.

(1) Reivich, M., Kuhl, D., Wolf, A.P., et al., Circ. Res. 44, 127 (1979).
(2) Greenberg, J., Reivich, M., Alavi, A., et al., Science 212, 678 (1981).
(3) Phelps, M., Kuhl, D., and Mazziotta, J. C., Science 211, 1445 (1981).

(4) Alavi, A., Reivich, M., Greenberg, J., et al., Sem. Nucl. Med. 11, 24 (1981).
(5) Christman, D., Crawford, E., Friedkin, M., et al., Proc. Nat. Acad. Sci. U.S. 69, 988 (1972).
(6) Crawford, E., Christman, D., Friedkin, M., et al., Int. J. Nucl. Med. Biol. 5, 61 (1978).
(7) Stambrook, P., Siskin, J., and Ebert, J., J. Cell. Physiol. 82, 267 (1973).
(8) Rozenquist, E., Mierzejewski, E., Wigglesworth, N., J. Cell. Physiol. 97, 241 (1978).
(9) Fowler, J., Finn, R., Lambrecht, R., et al., J. Nucl. Med. 14, 63 (1973).
(10) Shiue, C.-Y., Fowler, J., MacGregor, R., et al., Radiopharmaceuticals II, 259 (1979).
(11) Crawford, E., Friedkin, M., Wolf, A.P., et al., manuscript in preparation.
(12) Armstrong, R., and Diasio, R., Cancer Res. 40, 3333 (1980).
(13) Bollag, W., and Hartman, H., Europ. J. Cancer 16, 427 (1980).
(14) Cook, A., Holman, M., Kramer, M., et al., J. Med. Chem. 22, 1330 (1979).
(15) Rozen, S., Lerman, O., and Kol, M., J. C. S. Chem. Comm., 443 (1981).
(16) Shiue, C.-Y., Salvadori, P., Wolf, A.P., et al., manuscript in preparation.
(17) Ido, T., Wan, C.-N., Casella, V., et al., J. Label. Cmpds. Radiopharm. 14, 175 (1978).

SYNTHESIS AND ANIMAL STUDIES WITH ^{123}I LABELLED 1-(3'-IODO-3'-DEOXY-β-D-ARABINOFURANOSYL)URACIL

J.R. Mercer, L.I. Wiebe, E.E. Knaus, W. Maier-Borst, and F. Helus.
Faculty of Pharmacy, University of Alberta, Edmonton, Alberta, Canada.

In an ongoing study to evaluate the potential of synthetic nucleosides for use in non-invasive diagnostic oncology, we have prepared a variety of radiohalogenated analogues of naturally occurring nucleosides (1). The nucleoside epoxide (I) proved to be a valuable precursor for a high-yield one-step synthesis of radiohalogenated 1-(3'-halogeno-3'-deoxy-β-D-arabinofuranosyl)uracils (II).

Compounds with structure II did not significantly inhibit the growth of leukemia cells in vitro (2). The apparent absence of therapeutic properties did not preclude the possibility of in vivo uptake of the nucleosides II into tumor or normal tissue. It was therefore of interest to prepare the radiolabelled compounds II and to investigate their potential as non-invasive diagnostic agents.

The epoxide (I) was prepared in 30% overall yield in 5 steps from uracil using a known procedure (3,4). The iodo compound (II-a) was readily prepared in greater than 90% yield when equimolar quantities of epoxide and HI were heated at 93°C for 2 hours in a minimal volume of solvent. This represents a significant improvement over existing methods of synthesis of II-a (5). For radiochemical syntheses, ^{123}I was prepared by proton irradiation of an enriched ^{124}Te target using the D.K.F.Z. Heidelberg compact cyclotron. After reaction and work-up a product of greater than 99% radiochemical purity was obtained with a radiochemical yield in excess of 90%. Injection-ready samples of (^{123}I) II-a with specific activities of 0.37 GBq/mg (0.127 GBq/μmole) were prepared. The compound II-a was also prepared using (^{131}I) NaI.

The radiolabelled compounds (^{123}I and ^{131}I) II-a were used in whole body distribution and elimination studies with normal and tumor-bearing Wistar rats. The data suggests rapid excretion of unchanged iodo compound and an absence of tumor or normal tissue localization of radioactivity. Compounds (^{82}Br) II-b and (^{36}Cl) II-c have also been synthesized and show similar results in animal experiments (6).

(1) Abrams, D.N., Knaus, E.E., Mercer, J.R. and Wiebe, L.I., J. Label. Cmpds. Radiopharm., 16, 12 (1979).
(2) Hollenberg, D.H., Watanabe, K.A. and Fox, J.J., J. Med. Chem., 20, 113 (1977).
(3) Codington, J.F., Fecher, R. and Fox, J.J., J. Org. Chem., 27, 163 (1962).
(4) Codington, J.F., Fecher, R. and Fox, J.J., J. Amer. Chem. Soc., 82, 2794 (1960).
(5) Cushley, R.J., Codington, J.F. and Fox, J.J., Can. J. Chem., 46, 1131 (1968).
(6) Lee, Y.W., Knaus, E.E. and Wiebe, L.I., Unpublished results.

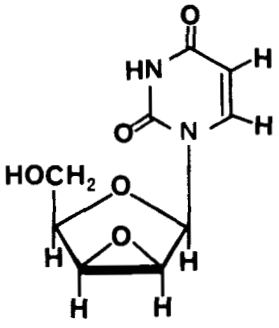

I

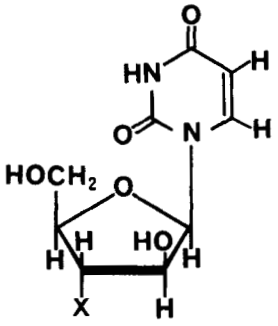

II

a X=I
b X=Br
c X=Cl

STUDIES WITH PT-195M LABELED PLATINUM COMPLEXES

W. Cole, J. Wiza, B. Odenheimer, and W. Wolf, Radiopharmacy Program, University of Southern California, Los Angeles, CA 90033;
J.D. Hoeschele and T.A. Butler, Oak Ridge National Laboratory, Oak Ridge, TN 37830; and
R.D. Smyth, Bristol Laboratories, Syracuse, NY 13201.

Cisplatin (cis-dichloro-diammine-platinum(II)) is the first of a new family of inorganic pharmaceuticals that have significant chemotherapeutic potential, in cancer and in other major diseases. Cisplatin has been approved as an antitumor drug, and is most effective in testicular, ovarian, head and neck and transitional bladder cancer, although it is also proving useful in other forms of cancer (1). One major problem in its use, however, is the severe nephrotoxicity that it can induce, a problem which has spurred the search for other drugs of that family devoid of this most undesirable side effect. Platinum possesses several radionuclides, of which Pt-195m has proven to be the most desirable so far. Numerous articles have been published describing the use of Pt-195m labeled cisplatin in biodistribution, metabolism and radiopharmacokinetic studies.

Pt-195m is made by neutron activation of Pt-194, and is obtained at specific activities ranging from 0.7 to 1.2 mCi/mg. Inasmuch as natural platinum contains only 32.9% of Pt-194, the material irradiated is usually a target of highly enriched (97.41%) Pt-194. The crude Pt-195m is then dissolved in aqua regia, and traces of Au-199 (produced by decay of the 30-minute Pt-199) are removed by liquid/liquid extraction. The next step involves the reduction of Pt(IV) to Pt(II), probably the most delicate step in this process. Once the tetrachloroplatinate has been obtained, further syntheses will depend on the nature of the carrier ligand that will be attached. Probably the most widely used method involves conversion of the tetrachloroplatinate to the tetraiodoplatinate, so as to use the high trans-directing effect of the iodine ligand to produce as pure as possible a cis-diammine complex, devoid of any trans-diammine impurities (2,3).

QSAR studies at the leaving ligand had suggested that dicarboxylic ligands capable of forming a chelate might be of particular interest, and we have chosen the cis-diammine-ethylmalonato Pt(II) as a model for initiating QSLR (Quantitative Structure Localization Relationship) studies (4). The ethylmalonato complex is prepared by the stoichiometric addition of ethylmalonic acid to cis-diammine-diaquo Pt(II). The latter, which in the synthesis of cisplatin is obtained following the removal of iodine with silver nitrate, can also be generated in the same way from Pt-195m cisplatin itself. The latter process appears to be more advantageous when small quantities of complexes need to be synthesized, inasmuch as Pt-195m cisplatin appears to be a better starting material than either the Pt-195m tetrachloroplatinate or the diaquo complex itself, possibly due to the oligomerization of the diaquo complex during shipping.

Synthesis of cis-diammine-ethylmalonato Pt(II): The ionic chloride content of the solution of Pt-195m cisplatin in isotonic saline is measured. A solution of silver nitrate is prepared containing in 0.1 ml the stoichiometric amount of silver ion required for 2 ml of the Pt-195m cisplatin solution; following mixing of these two solutions, the reaction mixture is centrifuged for 30 seconds in a Beckman Microfuge, the silver chloride pellet is washed and combined with the supernatant and this material is labeled as solution A. Solution B is prepared as follows: 0.2 ml containing 2 molar-

equivalents of silver nitrate and 1 of ethylmalonic acid, corresponding to the cisplatin in solution A, are adjusted to pH 4.5-5. Solution A and B are mixed and incubated at 40-50 C for three hours, and then centrifuged. Chromatographic analysis of the material documented that better than 97% of the activity corresponded to the ethylmalonato complex, and this solution was stable for 14 days.

Chemical reactivity studies: Given that chlorine forms a more stable bond with class (b) metals (such as Pt) than oxygen, displacement of the chloro ligands by ethylmalonic acid is unlikely, as verified experimentally. However, we have also observed that the ethylmalonato is strongly bound, and that its displacement by chloride ions is slow, probably because of the stabilization afforded by the chelate ring. In addition, this displacement is highly pH dependant. It is particularly slow at pH 7, suggesting that it is unlikely that the free ethylmalonato complex may be converted *in vivo* into cisplatin. Details of the kinetic studies are shown in figures 1 and 2.

Biodistribution studies: Pt-195m ethylmalonato was administered to Sprague-Dawley rats, 150-200 g, which were sacrificed at times ranging from 5 min. to 96 hrs. post-injection. Clearance of Pt-195m from the blood and tissues is significantly higher following administration of the Pt-195m ethylmalonato complex than that of cisplatin. As an example, at 3 hrs. post-administration, the comparative % retained per organ is given in Table I, following comparable therapeutic doses (8 mg and 1 mg/kg, respectively).

In conclusion, the present studies with Pt-195m cis-diammino-ethylmalonato Pt(II) have documented some of the chemical and biological properties of this compound that are important in understanding its chemotherapeutic activity and why it may (or may not) possess undesirable side-effects. Such Pt-195m labeled complexes will also be important in assessing non-invasively the biological disposition of platinum complexes in individual patients.

(1) Prestayko, A.W., Crooke, S.T. and Carter, S.K., "Cisplatin: Current Status and New Developments", Academic Press, New York, 1980.
(2) Wolf, W. and Manaka, R.C., J. Clin. Hematol. Oncol. 7, 79, (1977).
(3) Hoeschele, J.D., Butler, T.A., Roberts, J.A. and Guyer, G.E., submitted to Radiochim. Acta
(4) Manaka, R.C. and Wolf, W., in "Radiopharmaceuticals: Structure-Activity Relationships", R. Spencer, ed. Academic Press, New York, 1981. p. 183.

Table I

% Injected/Organ of Pt-195m at 3 hrs following the IV administration of 1 mg/Kg of cisplatin and 8 mg/Kg of cis-diammino-ethylmalonato Pt(II) to Sprague Dawley rats.

Organ	cisplatin	ethylmalonato
Whole Blood	2.86 ± 0.50	0.80 ± 0.08
Kidney	3.24 ± 0.24	0.64 ± 0.06
Liver	4.06 ± 0.09	0.77 ± 0.03
Skin	23.73 ± 7.97	2.45 ± 0.30
Muscle	6.88 ± 0.25	1.50 ± 0.17

Fig:1

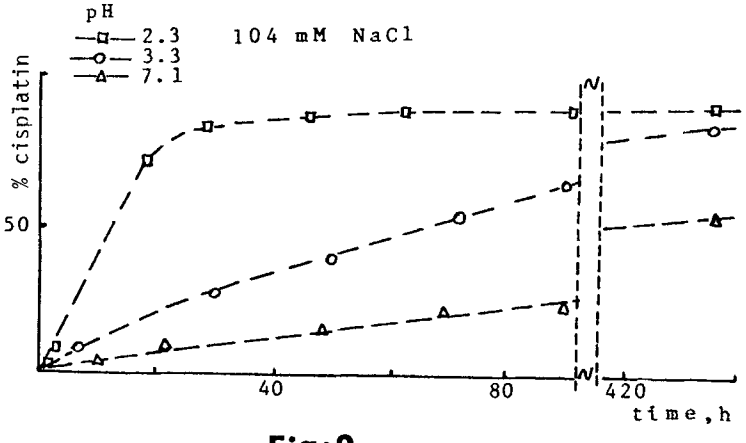

Fig:2

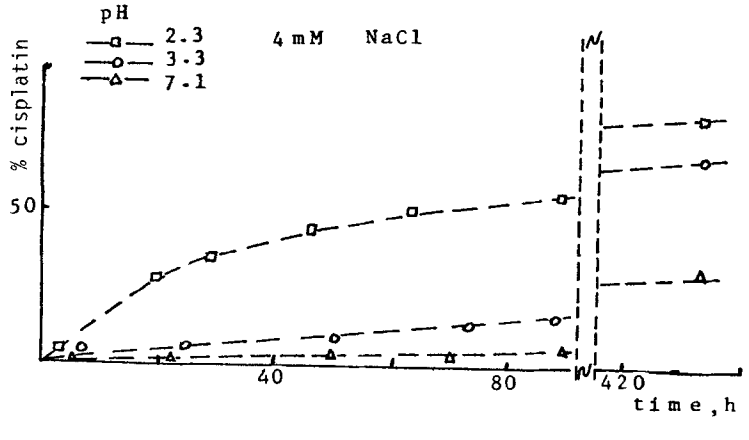

AN IMPROVED METHOD FOR THE PREPARATION OF DTPA-COUPLED PROTEINS

D.J. Hnatowich, W.W. Layne, R.L. Childs, P.W. Doherty, D. Lanteigne, and J. Ansell. Departments of Nuclear Medicine, Radiology, and Medicine, University of Massachusetts Medical Center, Worcester, MA 01605.

Although a few proteins such as transferrin form stable chelates with metallic radionuclides such as ^{67}Ga and ^{111}In, most proteins do not possess this property. Perhaps the only reasonable approach to the radiolabeling of these proteins with metallic radionuclides is by covalently attaching a strong chelating group to the protein. This has been considered by many investigators in the past (1-6) and does provide a protein capable of chelating metals. However, each method requires either a complicated multi-step synthesis of the coupling agent, harsh coupling conditions, and/or lengthy and involved purification procedures because of low coupling efficiencies. We have developed a new method of coupling proteins which appears to be superior to previously reported methods. We are coupling proteins with diethylenetriaminepentaacetic acid (DTPA) through the use of the cyclic anhydride of this acid.

The anhydride is prepared by reacting acetic anhydride with DTPA. Characterization by NMR and IR indicate that the anhydride is cyclic and that the central acetic acid-amine group is a zwitterion. The anhydride is stable for at least several months at room temperature in moisture-free environments.

Coupling is achieved by adding solutions of the protein in pH 7 buffer to the solid anhydride. The reaction is completed in about 1 min at room temperature. Hydrolyzed control experiments are performed in which the intentional hydrolysis of the anhydride before adding to the protein is the only procedural change. We have determined that the constants for the formation of ^{111}In labeled free DTPA and protein-bound DTPA are similar, therefore coupling efficiency is equivalent to the percentage of ^{111}In activity bound to protein following the addition of ^{111}In acetate and may be measured either by exhaustive dialysis, Sephadex or Sepharose chromatography, or by high performance liquid chromatography.

Initial work was performed with serum albumin as the model protein (7). The influence of anhydride:protein molar ratio and protein concentration on coupling efficiency was determined. Under optimal conditions (i.e., protein concentrations of about 10 mg/ml or greater and anhydride:protein ratios of about 1:1 or less) coupling efficiencies are 65 $\pm$ 5% with controls showing 7 $\pm$ 3% bound activity. Because of the efficient coupling, purification of the coupled protein from free DTPA is accomplished by a single passage through a Sephadex G50 column. Biodistributions at 45 min were determined in mice for ^{111}In-DTPA-albumin and commercial ^{125}I-albumin; accumulation in each tissue type and blood agree to within two standard deviations and most agree to within one standard deviation.

In order to investigate the effect of coupling on protein viability, we have coupled fibrinogen, a protein for which both in vitro and in vivo assays of clotability are available. Under the conditions of the study, coupling efficiency is 13 $\pm$ 3% with controls showing zero bound activity (8). The in vivo properties of ^{111}In-DTPA-fibrinogen were compared to those of commercial ^{125}I-fibrinogen in dogs. Over 130 hrs blood clearance of both labels was identical within experimental error. Using a dog thrombogenic catheter model, the clot:blood ratios were also in agreement and images obtained at 24 hrs clearly show the clot along the length of a catheter in the jugular vein.

Because of our interest in radioimmunodiagnosis, we have also investigated the coupling to antibody. Using human non-specific IgG, the same trends are observed with respect to the influence of protein concentration and anhydride:protein molar ratio as is observed with albumin but the maximum coupling efficiency in this case is 35 $\pm$ 5%. Coupling efficiency was also found to be optimum at pH 7. Similar coupling efficiencies were obtained for bovine non-specific IgG and for monoclonal

anti-CEA and anti-PAP antibody. Preliminary studies of the viability of ^{111}In-DTPA-anti-CEA antibody show that when coupled at 0.03 groups per molecule this protein is still capable of binding with CEA.

(1) Sundberg M.W., Meares C.F., Goodwin D.A., et al., J. Med. Chem., 17, 1304-1307 (1974).
(2) Yeh S.M., Meares C.F. and Goodwin D.A., J. Radioanal. Chem., 53, 327-336 (1979).
(3) Krejcarek G.E. and Tucker K.L., Biochem. Biophys. Res. Comm., 77, 581-585 (1977).
(4) Wagner S.J. and Welch M.J., J. nucl. Med., 20, 428-433 (1979).
(5) Pritchard J.H., Ackerman M., Tubis M. and Blahd W.H., Proc. Soc. Exp. Biol. Med., 151, 297-302 (1976).
(6) Yokoyama A., Omomo Y., Horiuchi K., Saji H., Yamamoto K., Ishii Y., Tanaka H. and Torizuka K., J. nucl. Med., 22, P32 (1981) (Abstract).
(7) Hnatowich D.J., Layne W.W. and Childs R.L., Int. J. appl. Radiat. Isotopes (in press).
(8) Layne W.W., Hnatowich D.J., Doherty P.W., Childs R.L., Lanteigne D. and Ansell J., J. nucl. Med. (in press).

LABELING STUDIES OF PROTEINS USING BIFUNCTIONAL CHELATES: THE DESFERRIOXAMINE-HUMAN SERUM ALBUMIN (DF-HSA) CONJUGATE

Gy. A. Janoki, J. F. Harwig, and W. Wolf
Radiopharmacy Program, University of Southern California, Los Angeles, CA 90033.

Biologically important proteins labeled with various radiometals which have favorable decay characteristics are of significant value in diagnostic studies. The in vivo stability of such radiometal-protein complexes is generally low, however, due to the absence of specific metal binding receptors which form stable bonds. One approach towards improving the stability of such complexes involves the concept of "bifunctional chelates", first introduced into radiopharmaceutical studies by Sundberg et. al. (1). Various chelons and coupling methods have been tried which lead to compounds having a higher labeling yield and a superior in vivo stability compared to the directly labeled proteins. However, while numerous papers have been published using such techniques, a number of key problems remain to be solved. Primary among these is the low specific activity reported by most workers, usually in the 5 - 50 uCi/mg range. These results fall far short of the theoretical specific activities for such bifunctional chelates, which exceed 500 mCi/mg, and raise the question of why the theoretical yields cannot be attained.

We have chosen desferrioxamine-mesylate (DF) as the chelating agent for this study. DF forms a 1:1 complex with trivalent metal ions such as Fe, Ga, In, etc. and has a free amino group which is not involved in metal binding. With ferric ions, DF forms complexes of high stability (log K = 30.6) (2). The relative stability of the Ga-DF complex is apparently even higher, given that DF at relatively low concentration can remove Ga-67 from the Ga-Transferrin complex. Coupling of DF to a protein (human serum albumin, HSA) was effected using either 1-ethyl-3-(3-dimethylaminopropyl)carbodiimide HCl (ECD), to yield a carboxy-modified protein, or glutaraldehyde (GL), to yield an amino-modified protein. Both methods offer the advantages of mild and simple reactions.

Synthesis of DF-HSA conjugate using ECD: In a typical synthesis, 0.2 umole of the purified HSA monomer in 1 ml isotonic saline were mixed with 10 umole ECD (solid) at pH 4.7 and 10, respectively, and 0.1 mmole DF in 1 ml saline were added. The reaction was stopped by addition of 1 ml of 1M acetate buffer pH 4.7, which quenched any excess of unreacted ECD. The resulting DF-HSA conjugates were then dialysed at 4°C for 24 hours against 0.1M acetate buffer pH 5.0 and for another 24 hours, also at 4°C, against 0.15M sodium chloride pH 7.4, using a dialysis membrane tube that retained molecules above 12,000-14,000 daltons. The conjugates were purified further on Sephadex G-150 columns. The fractions corresponding to the albumin monomer peak were combined and concentrated by ultrafiltration. The two conjugates obtained, following coupling at pH 4.7 and pH 10, will be referred to as compounds I and II, respectively. The coupling efficiency of this reaction was also determined by using DF which had been complexed with Ga before coupling ("prelabeled DF") (3).

Synthesis of DF-HSA conjugate using GL: 1 ml of a 0.2 M solution of DF in 0.15 M phosphate buffered saline (PBS) at pH 7.8 was stirred with 12 ul of 25% glutaraldehyde. The HSA monomer (100 mg, 0.15 mmoles, in 10 ml PBS) was then added and was stirred for 2 hours at room temperature. The crude conjugate was purified as described above to yield compound III.

Radiolabeling of the DF-HSA conjugates: With constant stirring 1 mg

of each of the purified DF-HSA conjugates in 0.2-0.5 ml of 0.15M NaCl pH 7.4 was mixed with 0.1 ml of a 0.05M $NaHCO_3$ solution pH 7.4, and 0.01-1 mCi of Ga-67-citrate was added. This solution was stirred at room temperature for 1 hour, and was analyzed by gel filtration on a Sephadex G-50 column eluted with 0.15M NaCl pH 7.4 at a flow rate of 0.8 ml/minute. The radioactivity of the eluate and its absorbance at 280 nM were monitored. The labeled conjugates were also assayed using paper chromatography on Whatman No.1, using methanol 85% as the developing solvent.

Urea treatment of the conjugates: Either before or after the labeling step, urea was added to the conjugates to yield a final concentration that was 7.5 M in urea. The relative changes in labeling efficiency were determined as described above.

Biodistribution of the Ga-67-citrate labeled conjugates: The biodistribution of the labeled conjugates was studied in rabbits using a scintillation camera. The blood clearance of the labeled conjugates was compared to that of the folllowing reference compounds: Ga-67-citrate, Ga-67-DF, Tc-99m-HSA, Tc-99m-RBC (labeled in vivo). In addition, I-125-HSA was administered to each rabbit conjointly with the test substance studied.

The kinetics of the reaction of Ga-67-citrate with the conjugates were studied between 30 minutes and 5 hours of incubation. At 60 minutes more than 95% labeling had been achieved (Figure 1). The stability of the conjugates was measured daily over a one week period. After one week of storage the protein retained 90% of its original activity. The labeling efficiency was affected little by changes in pH from 4-8 (Figure 2). The typical elution profile of the conjugates is shown in Figure 3. More than 95% of the applied activity eluted from the column with the same elution profile as HSA, as verified both by radioactivity and UV determinations. The specific activities of the conjugates ranged from 5 to 50 uCi/mg; following urea treatment the metal binding capacity increased significantly, with specific activities ranging from 100 to 1500 uCi/mg (Figure 4). The Ga-DF-HSA conjugates localized predominantly in the central blood pool and the liver, with a very small fraction localizing in the kidneys. The blood clearance of the conjugates studied was slower than that of Ga-67-citrate, Ga-67-DF or Tc-99m-HSA, but faster than that of Tc-99m-RBC and of I-125-HSA (Figure 5). Among the conjugates, compound II localized least in the liver and had the slowest blood clearance. Liver localization, specially in the case of compound I, was significantly higher than expected from the blood perfusion of liver.

These results show that such labeled conjugates have excellent in vitro and in vivo stability and acceptable biological properties. The specific activity of the various labeled conjugates was lower than expected based on the coupling efficiency (3), but was increased following urea treatment, a fact that is consistent with the notion that numerous coupled chelons are hidden as a consecuence of intra-molecular non-covalent cross-linking between the protein and the chelon substituents. Hence, the full potential of proteins labeled with bifunctional chelates will only be realized when such macromolecules can be labeled at their theoretical specific activities.

(1) Sundberg, MW, Meares, CF, Goodwin, DA, et. al., J. Med. Chem., 17, 1034 (1974).
(2) Goodman, MM, Thakur, ML, Hoffer, PB, et. al., J. Label. Compds. Radiopharm., 16, 1 (1979)
(3) Janoki, GyA, Harwig, JF, Chanachai, W and Wolf, W, Submitted to Int. J. Appl. Rad. Isotop.

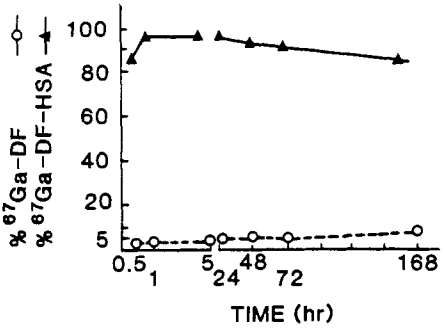

Figure 1

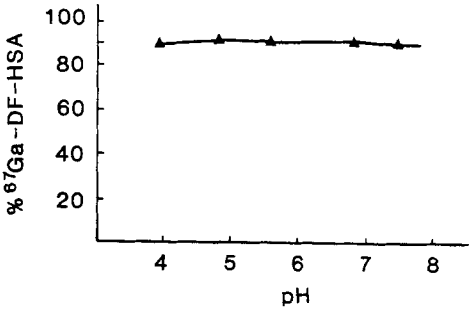

Figure 2

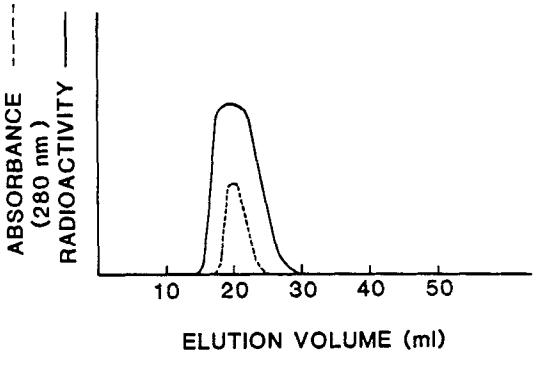

Figure 3

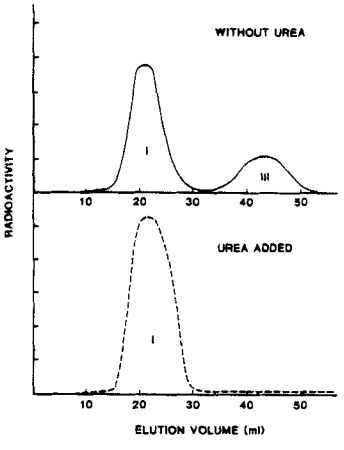

Figure 4

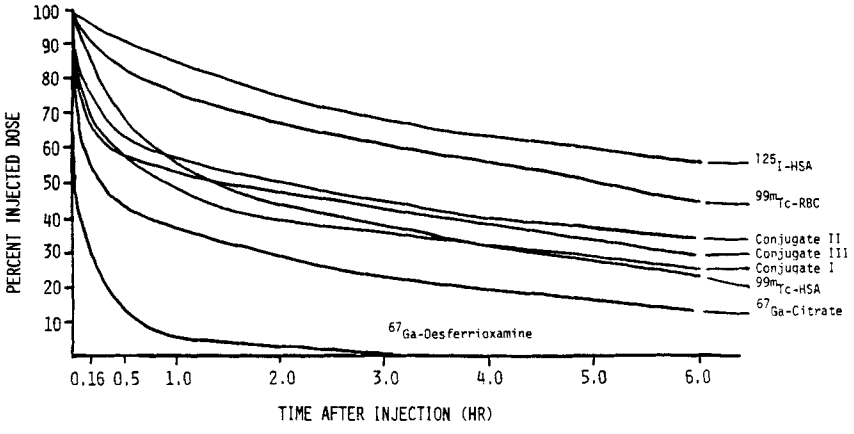

Figure 5

PHENOLIC AMINOCARBOXYLIC ACIDS - NEW CHELATING AGENTS FOR MODIFYING GALLIUM-67 BIODISTRUBUTION

F.C. Hunt and D.J. Maddalena.
Isotope Division, Australian Atomic Energy Commission, Lucas Heights Research Laboratories, Private Mail Bag, Sutherland, NSW, 2232, Australia.

The limitations of Ga-67 tumour and abscess imaging due to high uptake by blood and normal tissue, have led to a variety of strategies to remove background activity, thereby enhancing lesion to normal tissue ratios.

The methods used to lower Ga-67 blood and tissue radioactivity include intravenous iron administration to displace Ga from transferrin (1,2) or treatment with chelating agents such as desferrioxamine (3,4) and tricatecholamides (5). All these methods rely on the similarity in ionic radii and properties of the ferric and gallic ions.

Other types of chelating agents with a high affinity and stability constant for ferric ion are the phenolic aminocarboxylic acids, previously suggested for the treatment of iron overload in thalassaemia patients (6). The use of these chelators for in-vivo gallium chelation and scintigraphic image enhancement was therefore attempted.

The chelating agents, ethylenediamine di(o-hydroxyphenylacetic acid), EDDHA (I), and N,N'-bis(2-hydroxybenzyl) ethylenediamine N,N'-diacetic acid, HBED (II), were synthesized by literature methods (7,8) with carboxy or sulphonyl groups in the phenolic ring, to favour the urinary excretion route on complexation with gallium.

The ability of these compounds to chelate Ga-67 in-vivo was tested in rats bearing transplanted lymphatic leukaemias.

Administration of carboxy EDDHA as the sodium salt (25 mg/kg, I.V.) to tumour bearing rats 2 hours post Ga-67 citrate injection induced a decrease in Ga-67 concentration in all tissue. The tumour concentration decreased to half that in the untreated control animals. There was a tenfold decrease of Ga in the blood compared with controls and an eleven fold increase in urinary excretion 1 hour post injection of the chelating agent. The tumour to blood ratio increased four fold. The results are shown in Table 1.

Scintigraphic images of rats treated as above with carboxy EDDHA, showed a decreased body background and clearer delineation of tumour compared with controls.

It is concluded that the phenolic aminocarboxylate chelating agents are capable of chelating gallium in-vivo, promoting its urinary excretion and enhancing tumour images by increasing tumour to blood ratios.

The similarity of gallium and indium chemistries suggests a potential application of these chelating agents as gallium-67 or -68, and indium-111 radiopharmaceuticals, particularly as the phenolic ring can be readily substituted with lipophilic groups. The phenolic aminocarboxylates have already been formulated into technetium-99m hepatobiliary radiopharmaceuticals (9).

(1) Sephton R.G. and Martin J.J., Brit. J. Radiol., 53, 572 (1980).
(2) Smith F.W. and Dendy P.P., Brit. J. Radiol. 54, 398 (1981).
(3) Sephton R.G. and DeAbrew S., Proc. Soc. Exptl. Biol. Med. 161, 402 (1979).
(4) Oster Z.H., Som P., Sacker D.F., and Atkins H.L., J. Nucl. Med. 21, 421 (1980).
(5) Moerlein S.M., Welch M.J., Raymond K.N., and Weitl F.L., J. Nucl. Med. 22, 710 (1981).
(6) Pitt G.G. and Martell A.E., Inorganic Chemistry in Biology and Medicine. American Chemical Society, Washington, 1980, p.279.
(7) Dexter M. and Cranston R.I., U.S. Patent 2,824,128 (1958).
(8) Geigy J.R. (A-G), British Patent 843,003 (1960).
(9) Hunt F.C., Wilson J.G., Maddalena D.J., Bautovich G.J., and Hutcherson R., Proc. 1st Asia & Oceania Cong. Nucl. Med. Sydney, Australia, Sept. 1976 p.140.

Effect of Carboxy - EDDHA on the Biodistribution of

Ga-67-Citrate in Tumour Bearing Rats*

	Liver	Kidneys	Muscle	Skin	Femur	Blood	Urine	Intestines	Tumour
Control	9.1	1.52	23.5	14.3	0.66	22.8	4.9	4.5	1.74
Treated	4.2	1.58	8.53	7.86	0.42	2.4	54.9	3.11	0.79

	Control	Treated
Tumour/Muscle	6.7	7.9
Tumour/Blood	0.99	4.10

*Ga-67 injected at t = 0, COOH - EDDHA at t = 2 hrs, sacrificed at t = 3 hrs (% I.D./organ. Means for 5 rats)

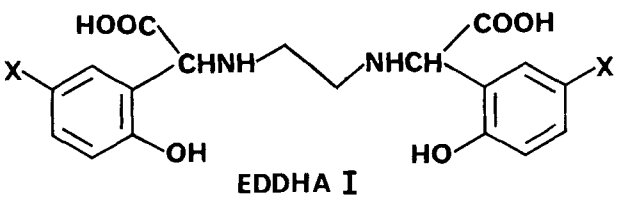

EDDHA I

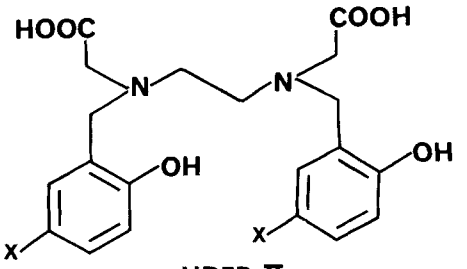

HBED II

X = H, COOH, SO_3^-

PREPARATION AND EVALUATION OF A NEW INDIUM-111 AGENT FOR EFFICIENT LABELING OF HUMAN PLATELETS IN PLASMA

M.L. Thakur and M.J. Barry, Department of Diagnostic Radiology, Yale University School of Medicine, 333 Cedar St., New Haven, Connecticut 06510.

Since the introduction of ^{111}In oxine cell labeling technique in 1976, (1), a number of methods for labeling of human platelets have been reported (2-6). The most efficient incorporation of ^{111}In into platelets occurs when the cells are suspended in media, other than plasma. Platelets suspended in such media, however, suffer from reduced aggregability. Agents such as ^{111}In-acetyl acetone (7) or ^{111}In-tropolene (8) have provided no solution to the problem due to the inability of the agents to preserve their integrity in presence of plasma transferrin.

We have developed a new agent (^{111}In-M) that labels platelets in plasma efficiently (82 $\pm$ 4%) with no apparent loss of platelet aggregability (100% of control platelets, Fig. 1a). The agent which compares favorably with ^{111}In-oxine is formed almost quantitatively in aqueous solutions of a wide range of pH and is extractable in chloroform (Fig. 2). It can be prepared in isotonic saline, stored at 22°C for longer than a week (Table 1) and be used for labeling platelets in plasma without any further treatment.

The incorporation of radioactivity into platelets is related to the platelet concentration (Fig. 3), pH of the medium (Table 2) and to the time and temperature of incubation (Fig. 1b). Platelets separated from 33 ml venous human blood and suspended in 1.5 ml autologous plasma at pH 6.5 to 6.9, yielded 82 $\pm$ 4% labeling efficiency in 10 minutes incubation at 37°C. Analogous to oxine, an increasing concentration of M[+] reduces platelet labeling efficiency but has little effect on platelet aggregability (Fig. 1a). Canine platelets labeled with this agent had 70% recovery and 7.8 days survival.

Ruthenium-103-M and ^{99m}Tc-M complexes had been also prepared. Under identical conditions these agents incorporated 24% and 5.7% radioactivity respectively, into platelets suspended in plasma.

The new ^{111}In-agent is promising for an efficient labeling of human platelets in plasma and justifies continuation of further investigations.

(1) McAfee, J.G. and Thakur, M.L., J. Nucl. Med., 17, 480 (1976).

(2) Thakur, M.L., Welch, M.J., Joist, J.H. and Coleman, R.E., Thrombosis Res., 9, 345 (1976).

(3) Scheffel, U., Tsan, M.F. and McIntyre, P.A., J. Nucl. Med., 20, 524 (1979).

(4) Heaton, A.W., Davis, H.H., Welch, M.J., Mathias, C.J., Joist, H.J., Sherman, L.A. and Siegal, B.A., Br. J. Hematology, 42, 613 (1979).

(5) Hawker, R.J., Hauker, L.M. and Wilkinson, A.R., Clinical Science, 58, 243 (1980).

(6) Thakur, M.L., Walsh, L., Malech, H.L. and Gottschalk, A., J. Nucl. Med., 22, 381 (1981).

(7) Sinn, H. and Silvester, D.J., Br. J. Radiol., 52, 758 (1979).

(8) Dewanjee, M.K., Rao, S.A. and Didisheim, P., J. Nucl. Med., 22, 981 (1981).

[+] M = 2-Mercaptopyridine 1-oxide.

Table 1

Stability of ^{111}In-M prepared in 0.9% NaCl

Days after Preparation	% Extracted
0	99
1	99.3
2	99.2
3	99.4
6	99.0
13	97.9
14	98.4

M - concentration 10 μg/ml

Table 2

Effect of pH on platelet labeling efficiency

pH	% Yield
4.46	28.9
6.36	81.2
6.46	90.7
6.97	98.4

Platelets (8×10^8) were suspended in 0.9% NaCl and pH was adjusted with citric acid or Na-Citrate

INFLUENCE OF M, TIME AND TEMPERATURE

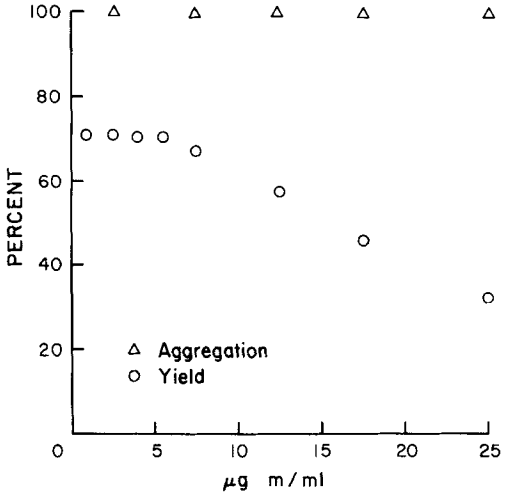

Fig. 1.a.

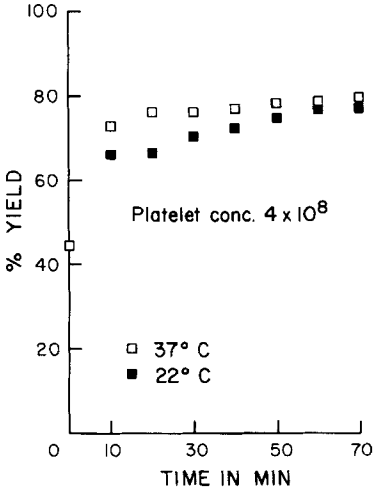

Fig. 1.b.

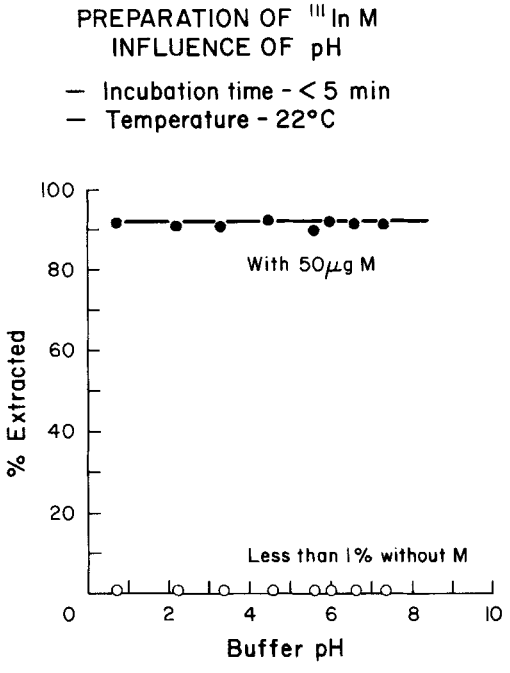
PREPARATION OF ^{111}In M
INFLUENCE OF pH
— Incubation time - < 5 min
— Temperature - 22°C
100
80
60
40
20
0
% Extracted
With 50μg M
Less than 1% without M
2
4
6
8
10
Buffer pH

Fig. 2.

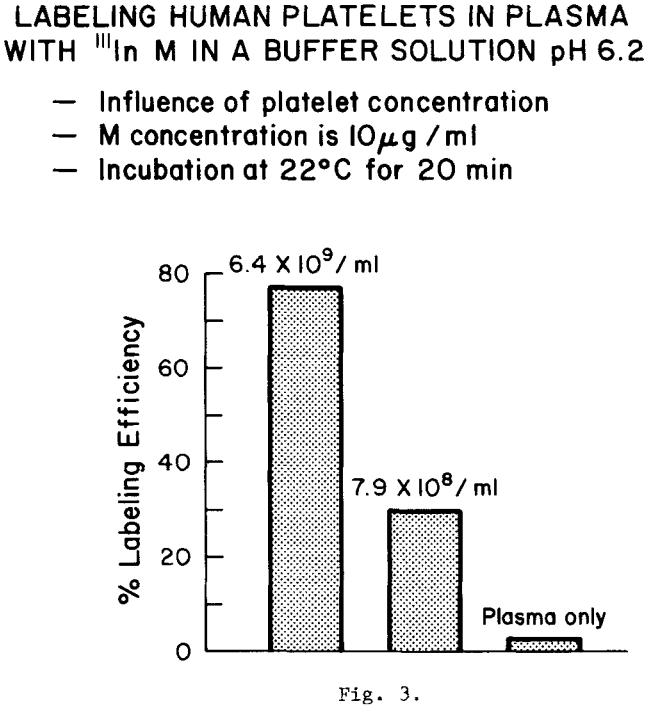
LABELING HUMAN PLATELETS IN PLASMA
WITH ^{111}In M IN A BUFFER SOLUTION pH 6.2
— Influence of platelet concentration
— M concentration is 10μg / ml
— Incubation at 22°C for 20 min
80
60
40
20
0
% Labeling Efficiency
6.4 X 10^9/ ml
7.9 X 10^8/ ml
Plasma only

Fig. 3.

FATE OF ^{111}In IN ^{111}In-LABELED PLATELETS LABELED VIA TROPOLONE AND OXINE CARRIER IN RABBITS AND DOGS

S.A. Rao, M.K. Dewanjee, and P. Didisheim.
Division of Nuclear Medicine and Hematology, Mayo Clinic and Mayo Foundation, Rochester, Minnesota 55905, U.S.A.

Fate of ^{111}In in ^{111}In-labeled platelets was studied by a) analyzing the subcellular distribution of ^{111}In in cytoplasmic proteins, organelles and membrane, b) biodistribution of lysate of ^{111}In-labeled autologous platelets in rabbits at 3 and 24 hours and c) biodistribution of ^{111}In-labeled autologous platelets at 1 day and 4 days after intervenous administration.

Dog and rabbit platelets were labeled with ^{111}In-tropolone (20µg tropolone) and ^{111}In-oxine (50µg oxine) in ACD-saline and ACD-plasma media (1-3). Lipid soluble ^{111}In-tropolone or ^{111}In-oxine binds with cytoplasmic platelet proteins, membrane and organelles; ^{111}In-bound radioactivity in these fractions was determined by sucrose gradient separation (25%, 45%, and 60% sucrose density).

^{111}In-Platelets were lysed by six repeated freezing and thawing (freezing - 26°C, thawing: 37°C). A fraction was centrifuged at 28000 g for 1 hour at 8°C. The supernatant was filtered with 0.22µmeter millipore filter paper. The amount of organelles and membrane bound ^{111}In accounted for (55±5)% of total ^{111}In in platelets; about (25±5)% of this is bound to membrane. A fraction of filtered platelet lysate was chromatographed (Sephadex G-100). Major fraction (85% of ^{111}In) was bound to a platelet protein of molecular weight 50,000±5000 daltons (4-6), (Fig. 1). Fraction of ^{111}In-labeled autologous platelet lysate of rabbit without filtration was administered to rabbits. Results of biodistribution was shown in Table 1. Biodistribution of intact platelet labeled with oxine or tropolone carrier in ACD-saline or ACD-plasma media at 1 day and 4 days are shown in Table 2.

As platelets undergo lysis, these ^{111}In-bound membrane fragments, organelles and proteins localize in the reticuloendothelial system; 30-40% in liver, 2% in spleen, 6-8% in bone marrow. Only 9-11% are in systemic circulation. By administration of labeled platelet lysate and separation of cell and plasma bound labeling media carrier ^{111}In at 3 and 24 hours we found that medium of ACD-saline, ACD-plasma or carrier of oxine or tropolone did not significantly alter biodistribution. This 24 hour biodistribution of labeled platelet lysate is similar to the 96 hour distribution of intact labeled platelets in rabbits. These studies clearly demonstrate that ^{111}In radioactivity in spleen is mainly due to platelet pooling, that in marrow is due to accumulation of labeled platelet fragments and platelet proteins and that in liver is due to a combination of pooling and sequestration.

(1) Thakur M.L., Welch M.H., Joist J.H., et al., Thromb. Res. 9, 345-357 (1976).
(2) Heaton W.A., Davis H.H., Welch M.J., et al., Indium-111: a new radionuclide label for studying human platelet kinetics. Br. J. Hematol. 42, 613-622 (1979)
(3) Dewanjee M.K., Rao S.A., Didisheim P., Indium-111 Tropolone, a new high-affinity platelet label: preparation and evaluation of labeling parameters. J. Nucl. Med. 22, 981-987 (1981).
(4) Hudson E.M., Ramsey R.B., Evatt B.L., Subcellular localization of indium-111 labeled platelets. J. Lab. Clin. Med., 97, 577-582 (1981).
(5) Mathias C.J., Welch M.J., Labeling mechanism and localization of ^{111}In in human platelets. J. Nucl. Med., 20, 659 (1979) abst.
(6) Joist J.H. and Baker R.K., Loss of ^{111}Indium as indicator of platelet injury. Blood, 58, 350-353 (1981).

TABLE 1. (MEAN ± S.D.)OF BIODISTRIBUTION (% I.D.) OF ^{111}IN-CHLORIDE AND LYSATE OF ^{111}IN-LABELED AUTOLOGOUS PLATELETS LABELED IN ACD-SALINE AND ACD-PLASMA MEDIA AT 3 AND 24 HOURS AFTER I.V. ADMINISTRATION IN NEW ZEALAND ALBINO RABBITS

	^{111}Indium Chloride		Lysate of ^{111}In-Platelets (Tropolone)			Lysate of ^{111}In-Platelets (Oxine)	
Sacrifice Time (hr) Number	3 (n=4)	24 (n=5)	3 (n=4)	24 (n=5)	24 (n=5)	24 (n=5)	24 (n=5)
Labeling Media			ACD-Saline	ACD-Saline	ACD-Plasma	ACD-Saline	ACD-Plasma
Blood	47.88 ± 10.90	11.74 ± 4.41	55.54 ± 3.92	8.74 ± 1.46	11.95 ± 3.35	11.05 ± 0.82	10.14 ± 1.33
Liver	5.78 ± 1.64	5.72 ± 0.99	9.98 ± 0.65	32.64 ± 11.14	41.43 ± 3.68	20.21 ± 1.45	45.57 ± 7.02
Spleen	0.09 ± 0.02	0.13 ± 0.08	0.16 ± 0.01	1.76 ± 0.67	1.23 ± 0.39	0.81 ± 0.69	1.92 ± 1.07
Lungs	1.17 ± 0.26	0.54 ± 0.19	2.17 ± 0.18	0.78 ± 0.13	0.76 ± 0.07	1.35 ± 0.78	0.49 ± 0.06
Kidneys	4.21 ± 0.14	5.26 ± 1.79	4.15 ± 0.44	10.34 ± 2.64	7.57 ± 2.72	5.78 ± 1.38	5.68 ± 2.64
Stomach GI Tract	6.53 ± 0.51	7.30 ± 2.78	7.17 ± 0.31	5.42 ± 1.23	4.97 ± 0.61	6.94 ± 0.64	4.32 ± 0.58
Skeletal Muscle	16.12 ± 0.65	15.95 ± 1.45	6.28 ± 0.85	9.87 ± 1.08	7.05 ± 2.00	13.59 ± 1.84	6.45 ± 1.06
Bone	2.25 ± 0.93	4.63 ± 2.78	2.05 ± 0.04	4.67 ± 0.89	2.25 ± 0.95	4.65 ± 1.62	1.76 ± 0.63
Bone Marrow	5.67 ± 1.53	4.26 ± 3.05	7.88 ± 1.85	6.89 ± 1.34	6.09 ± 2.17	7.02 ± 3.09	6.38 ± 2.75
Total % Retained	90.43 ± 11.20	56.28 ± 7.13	95.00 ± 4.90	81.30 ± 11.76	83.60 ± 6.50	71.40 ± 4.65	83.05 ± 8.28
Plasma/ Cell	3.93 ± 0.42	3.94 ± 0.72	3.14 ± 0.49	3.25 ± 0.37	3.07 ± 0.44	4.20 ± 1.07	4.41 ± 1.19

TABLE 2. BIODISTRIBUTION (MEAN ± S.D.) OF PERCENT OF ADMINISTERED DOSE OF ^{111}IN-LABELED PLATELETS (ACD-SALINE) VIA TROPOLONE AND OXINE LIGAND IN NEW ZEALAND ALBINO RABBITS AT 24 AND 96 HOURS AFTER INTRAVENOUS ADMINISTRATION

	Percent of injected dose			
	Tropolone		Oxine	
Tissue	24 hours (n = 5)	96 hours (n = 5)	24 hours (n = 5)	96 hours (n = 5)
Blood	55.12 ± 5.67	6.02 ± 2.42	50.24 ± 6.67	4.38 ± 0.78
Liver	17.56 ± 5.88	32.24 ± 9.09	21.15 ± 2.49	42.05 ± 7.29
Spleen	8.17 ± 1.85	17.94 ± 10.50	10.88 ± 3.58	15.68 ± 2.30
Lungs	1.38 ± 0.36	0.49 ± 0.33	1.32 ± 0.27	0.30 ± 0.02
Kidneys	1.03 ± 0.30	2.07 ± 0.78	1.05 ± 0.33	2.30 ± 1.38
Heart	0.16 ± 0.02	0.28 ± 0.22	0.22 ± 0.05	0.08 ± 0.30
Skeletal muscle	2.59 ± 0.58	1.84 ± 0.68	2.13 ± 0.23	3.48 ± 0.43
Bone	1.27 ± 0.66	1.17 ± 0.39	1.71 ± 0.61	2.12 ± 0.67
Bone marrow	10.55 ± 4.59	12.82 ± 3.54	9.27 ± 2.45	16.48 ± 2.03
Gastrointestinal tract	2.27 ± 0.42	2.68 ± 0.35	2.33 ± 0.41	2.42 ± 0.29

FURTHER STUDIES ON TRANSLOCATION OF Ga-67 FROM TRANSFERRIN TO FERRITIN

R.E. Weiner, B.-S. Hung, G.J. Schreiber, and P.B. Hoffer.
Departments of Diagnostic Radiology and Pharmacy Practice, University of Kansas Medical Center, Kansas City, KS 66103, U.S.A.

Ga-67 is known to localize in tumors and abscesses although the mechanism is obscure. There is evidence that the iron transport protein, transferrin (TF), may participate in the delivery of this radionuclide (1-4). Ferritin (FE), the iron storage protein which is largely present intracellularly, may act as a sequestering agent for Ga-67. We have shown, using the equilibrium dialysis technique (5), that certain low molecular compounds enhance the translocation of Ga-67 originally TF bound to FE. Since the dialysis membrane may slow translocation (6,7), we have investigated this transfer in the abscence of a membrane and also examined the mechanism of this transfer.

For the transfer experiments, Ga-67 citrate was complexed with TF and dialyzed overnight at 4 °C to rid non-bound activity. Aliquots of a mediating ion and a FE solution were added to a 30 µM TF solution and the mixture incubated at 37 °C. At desired times, 250 µl of this sample was chromatographed on a column containing AG 1x4 resin to separate TF bound Ga-67 from FE•Ga-67 and non-protein bound activity (7). To obtain the amount of non-protein bound Ga-67, an additional 250 µl was placed on a column containing Sephadex G-50. Control experiments showed that less than 0.1% of the added activity chromatographed with albumin or immunoglobulin G on this column. The transfer rate (TR) of Ga-67 from TF to FE was determined from the initial slope of the % bound vs. time plot. To investigate the role of mediating ions on Ga-67 binding to FE, an aliquot of a mediating ion and Ga-67 citrate solution were added to a 3 µM FE solution and the mixture incubated at 37 °C. At desired times, 250 µls of this sample was chromatographed on a G-50 containing column and the percentage bound determined. Paper chromatography was performed according to Hnatowich (8) using ITLC-SG and solvent systems A and B.

Figure 1 shows that in the abscence of any mediator there was a significant transfer of Ga-67 from TF to FE. At 50 hrs, FE had bound about 45% of the activity while the TF bound activity had decreased from 86% to 43%. In contrast, the addition of adenosine triphosphate (ATP) at 1mM, to the incubation media had greatly enhanced the TR. 42% of the Ga-67 was bound to FE in less than half the time (20 hr). The TR for ATP was -2.6 %/hr compared to -0.83 without any mediator. The other compounds examined, 30 µM citrate, 1mM lactate, 1mM AMP and 0.1mM pyrophosphate (PP_i), had a TR similar (range -0.52 to -0.85) to the TR in abscence of any mediator.

To investigate the mechanism of transfer, the ability of ATP to enhance FE•Ga-67 formation was examined. This command did not appear to augment the binding of Ga-67 to FE (Fig. 2). Initially, the reaction with and without ATP was examined at 37 °C. Since the reaction was rapid compared to the time required for chromatography, the temperature was lowered to slow the reaction and enhance any possible differences. At both temperatures there appears to be no stimilatory effect due to the presence of ATP.

To help explain the influence of these phosphate containing compounds, we examined the relative affinity of PP_i compared to EDTA. We have shown earlier (Weiner et al., unpublished data) that PP_i was more effective than ATP in removing Ga-67 from TF. However, even at a 10:1 PP_i (R_f=0) to EDTA ratio, > 98% of the activity migrated with the EDTA (R_f=1.0) suggesting at least compared to EDTA, PP_i had a lower affinity for Ga-67.

In conclusion, it is likely that ATP enhances translocation of Ga-67 from TF to FE by its ability to destablize the TF•Ga-67 complex. This increased rate is probably not due to a high affinity ATP•Ga-67 complex removing Ga-67 from TF or ATP facilitating the binding to FE. Postulates that may explain this phenomena (9) are 1. ATP may bind to the TF and causing a conformational change which has a lower affinity for gallium, 2. interaction of ATP with the HCO_3^- ligand at the metal binding site that disrupts the site, and 3. ligand-exchange initiated at the coordinated water site.

The presence of a membrane did appear to slow the translocation of the radionuclide between proteins. In previous dialysis experiments (Weiner et al., unpublished data) the transfer in the presence of ATP required about 60 hrs while only 20 hrs were required when

the two proteins were in contact. Whether these two proteins came in contact or interacted through the membrane of the cell or vesicle is unknown at present. However, in either case, our results show that the cytoplasmic constitutents would facilitate the movement of Ga-67 into the cell.

This research was supported in part by DOE contract DE-AC02-78EV04625.

(1) Hayes R.L., Rafter J.J., Carlton J.E. and Byrd B.L., J. Nucl. Med. 23, 8 (1982).
(2) Noujaim A.A., Lentle B.C., Hill J.R., Terner U.K. and Wong H., Int. J. Nucl. Med. Biol. 6, 193 (1979).
(3) Harris A.W. and Sephton R.G., Cancer Res. 37, 3634 (1977).
(4) Larson S.M., Rasey J.S., Allen D.R., Nelson N.J., Grunbaum Z., Harp G.D. and Williams D.L., J. Nat. Can. Inst. 64, 41 (1980).
(5) Weiner R.E., Schreiber G.J. and Hoffer P.B., J. Nucl. Med. 22, P33 (1981).
(6) Miller J.P.G. and Perkins D.J., Eur. J. Biochem. 10, 146 (1969).
(7) Harris D.C., Biochem. 17, 3071 (1978).
(8) Hnatowich D.J., J. Nucl. Med. 16, 764 (1975).
(9) Aisen P. and Listowsky I., Ann. Rev. Biochem. 49, 357 (1980).

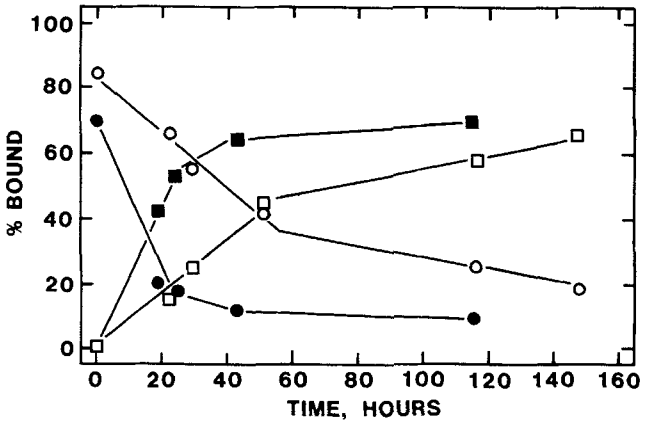

Figure 1. Influence of ATP on Ga-67 transfer from TF to FE as a function of time. Thirty μM TF•Ga-67 complex was prepared and then incubated with 3μM FE at 37 °C with (●,■) and without (○,□) 1mM ATP. At times indicated two 250μl aliquots of sample were chromatographed on an AG1x4 and Sephadex G-50 columns as described, and the percentage of activity bound to TF (●,○) and FE (■,□) was determined.

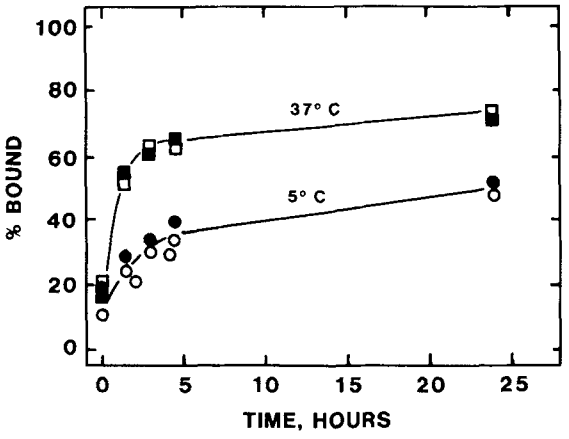

Figure 2. Efect of ATP and temperature on Ga-67 binding to FE with time. A 3μM FE solution was incubated with 10 μCi Ga-67 citrate in the presence (●,■) and absence (○,□) of 1 mM ATP at 5 °C (●,○) and 37 °C (■,□). At indicated times, 250 μl of sample was chromatographed on a G-50 column as described and the percent of activity bound to FE determined.

COMPARISON OF Ge-68/Ga-68 GENERATOR SYSTEMS FOR RADIOPHARMACEUTICAL PRODUCTION

K.D. McElvany, K.T. Hopkins, T.J. Hanrahan, H.A. Moore, Jr., and M.J. Welch.
The Edward Mallinckrodt Institute of Radiology, Washington University School of Medicine, St. Louis, Missouri 63110.

Several germanium-68/gallium-68 generator systems have been proposed over the past several years in an effort to provide a source of the positron-emitter gallium-68 that can readily be converted into radiopharmaceuticals for use with positron emission tomography. The first Ge-68/Ga-68 generator to be described consisted of Ge-68 adsorbed onto an alumina column; the daughter radionuclide was eluted with 0.005 M EDTA (1). In order to produce radiopharmaceuticals other than ^{68}Ga-EDTA, it is first necessary to break the stable EDTA complex and remove all traces of EDTA; this procedure adds several steps and a significant amount of time to procedures for preparing ^{68}Ga-radiopharmaceuticals. Comar and co-workers (2) more recently described an ionic Ge-68/Ga-68 generator system utilizing a tin dioxide column eluted with 1 M HCl. Another ionic Ge-68/Ga-68 generator system - an alumina column that is eluted with 0.1 M NaOH to yield Ga-68 as the gallate ion - has also been described (3).

Long term testing of 20-30 mCi generators of each of these three types has been carried out to evaluate Ga-68 elution yields, Ge-68 breakthrough levels, chemical contaminants, and the ease of ^{68}Ga-radiopharmaceutical preparation. The elution characteristics of these three generators are summarized in Table 1.

Table 1. Elution Characteristics of 20-30 mCi Germanium-68/Gallium-68 Generators

	Alumina/ 0.005 M EDTA	Alumina/ 0.1 M NaOH	Tin Dioxide/ 1 M HCl
^{68}Ga Elution Efficiency	70-80%*	50-60%	70-80%
^{68}Ge Breakthrough	<0.01%	<0.003%	<0.003%
Chemical Contaminants	<5 ppm Al^{3+}	20-50 ppm Al^{3+}	<2 ppm Sn^{2+}

*decreases dramatically over a period of 6-12 months

Of the three Ge-68/Ga-68 generators, the alumina/0.005 M EDTA system has the least favorable properties. The gallium-68 elution yield drops off considerably with time; in addition, the extra steps required to prepare ^{68}Ga-radiopharmaceuticals other than EDTA are a major disadvantage. Both of the ionic generators have very low levels of Ge-68 leakage coupled with reasonably good Ga-68 elution yields; the tin dioxide/1 M HCl system produces somewhat higher yields of gallium-68 with lower levels of chemical contaminants.

In an effort to determine which generator would provide Ga-68 best suited for labeling proteins and antibodies via bifunctional chelating groups, a study was carried out to determine the amount of a chelating group required to efficiently bind the radionuclide. The ionic generator eluants were used both directly and following extraction into diethyl ether from 6 M HCl to label different amounts of EDTA; the eluant from the alumina/0.005 M EDTA generator was first extracted into ether from 6 M HCl and washed to remove all traces of EDTA. Table 2 summarizes the data from these experiments.

The gallium-68 obtained from all three generator systems has been used to label a variety of compounds with potential uses in nuclear medicine; these include ^{68}Ga-EDTA, ^{68}Ga-EDTMP, ^{68}Ga-transferrin, ^{68}Ga-human serum albumin microspheres, ^{68}Ga-red blood cells, and ^{68}Ga-platelets. However, for applications involving trace amounts of chelating groups, such as antibodies or proteins linked to bifunctional chelates, studies such as those described above are required to evaluate generator eluants.

Table 2. Effect of Chelate Concentration on the Preparation of ^{68}Ga-EDTA

Amount of EDTA (mg)	Percent Binding* (per total generator elution) Alumina/0.005 M EDTA EX+	Alumina/0.1 M NaOH EX	Alumina/0.1 M NaOH NEX	Tin Dioxide/1 M HCl EX	Tin Dioxide/1 M HCl NEX
10	100	100	100	100	100
5	100	100	100	100	100
2	100	100	92	100	95
1	100	100	61	100	88
0.5	86	91	64	100	75
0.25	60	75	-	78	45

*determined by thin layer chromatography (ITLC-SG with pyridine:ethanol:water::1:2:4)
+EX=extracted into diethyl ether from 6 M HCl; NEX=not extracted

These preliminary results suggest the superiority of the ionic generator systems with respect to sustained Ga-68 elution yields and ^{68}Ge breakthrough levels over long periods of time. It appears, however, that it may be necessary to first purify the gallium-68 by extraction when trace amounts of chelates are to be labeled.

(1) Greene M.W. and Tucker W.D., Int. J. Appl. Radiat. Isotop., 12, 62 (1961).
(2) Lewis R.E. and Camin L.L., J. Lab. Comp. Radiopharm., 18, 164 (1981).
(3) Loc'h C., Maziere B., and Comar D., J. Nucl. Med., 21, 171 (1980).

FACTORS AFFECTING THE CEREBRAL UPTAKE OF GALLIUM COMPLEXES

S.M. Moerlein, D.D. Dischino, K.N. Raymond, F.L. Weitl, and M.J. Welch.
The Edward Mallinckrodt Institute of Radiology, Washington University School of Medicine, St. Louis, Mo. 63110.

There is currently great interest in the use of positron emission tomography for the quantitation of regional cerebral hemodynamics. The development of a freely-diffusible Ga-68 complex for this purpose is desirable due to the availability of this positron-emitting isotope from several generator systems(1-4). Linear tricatecholamide (LICAM) ligands have been shown to coordinate Ga(III) with large formation constants(5,6), so their applicability as Ga-68 binding cerebral perfusion agents was investigated.

Only compounds which are lipophilic are able to penetrate the blood-brain barrier(7). The octanol/water partition coefficient (log P) of Ga-LICAM complexes can be increased by lengthening the terminal N-alkyl substituent R on the ligand's spermidine backbone. LICAM analogs with various substituents (R = H, $(CH_3)_2CH$, $C_6H_5CH_2$, C_6H_{11}, $CH_3(CH_2)_7$, and $CH_3(CH_2)_9$) were synthesized as previously reported (8). The measured log P of Ga-67 LICAM complexes ranged from 0 to ca. 170 and were found to be in agreement with estimates made using the fragment constant approach(9,10).

Incubation of the Ga-67 LICAM complexes in human plasma or 5% human serum albumin followed by analysis using gel permeation chromatography indicated that the gallium-LICAM complexes bind to high molecular weight plasma proteins independent of the complex log P. The Ga-67 LICAM complexes were inert to exchange with the iron transport protein transferrin as shown by the absence of Ga-67 transferrin when plasma samples were analyzed using anti-human transferrin affinity chromatography.

The cerebral extraction fraction in Rhesus monkey brain was determined by the internal carotid injection of 0.2 ml of ethanol/normal saline solution containing Ga-68 LICAM complex(11). Blood components were excluded in the injectate to avoid adverse effects caused by plasma protein binding of the lipoidal Ga-68 LICAM complexes. When the cerebral extraction fractions of the Ga-68 LICAM chelates were compared to those of lipophilic C-11 benzyl alkyl ethers, it was concluded that the molar weight/size as well as the log P of the complex are important determinants of blood-brain barrier penetration. Further details will be presented, including the extrapolated characteristics of the ideal Ga-68 complex for cerebral perfusion studies.

(1) Loc'h C., Maziere B., Comar D., J. Nucl. Med. 21, 171 (1980).
(2) Neirinckx R.D., Davis M.A., J. Nucl. Med. 20, 1075 (1979); 21, 81 (1980).
(3) Ehrhardt G.J., Welch M.J., J. Nucl. Med. 19, 925 (1978).
(4) Greene M.W., Tucker W.D., Int. J. Appl. Radiat. Isotopes 12, 62 (1965).
(5) Moerlein S.M., Welch M.J., Raymond K.N., Weitl F.L., J. Nucl. Med. 22, 710 (1981).
(6) Pecoraro V.L., Wong G.B., Raymond K.N., Polyhedron (in press).
(7) Oldendorf W.H., Proc. Soc. Exp. Biol. Med. 147, 813 (1974).
(8) Weitl F.L., Raymond K.N., J. Org. Chem. 46, 5234 (1981).
(9) Nys G.G., Rekker R.F., Chim. Therap. 9, 361 (1974).
(10) Leo A., Jow P.Y.C., Silipo C., Hansch C., J. Med. Chem. 18,

(11) Eichling J.O., Raichle M.E., Grubb R.L., Larson K.B., Ter-Pogossian M.M., Circ. Res. 37, 707 (1975).

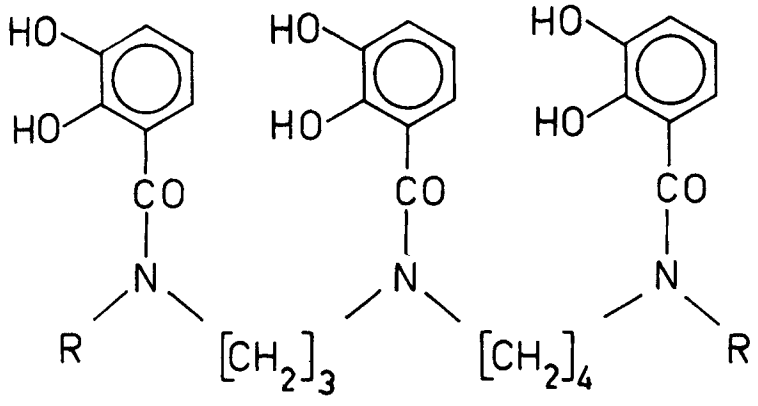

Partition Coefficients of Gallium-LICAM Complexes

R	Calculated[a]	Measured[b]
H	3.6×10^{-11}	0.00 ± 0.01
$(CH_3)_2CH$	1.6×10^{-6}	0.00 ± 0.01
$C_6H_5CH_2$	3.7×10^{-5}	0.00 ± 0.01
C_6H_{11}	1.8×10^{-3}	0.03 ± 0.02
$CH_3(CH_2)_7$	1.1	3.2 ± 0.8
$CH_3(CH_2)_9$	---	163 ± 30

(a) Based on the measured log P for R = $CH_3(CH_2)_9$ using the methods of references 9 and 10.
(b) 1-Octanol / 0.01 M Citrate Buffer, pH 7.0 .

EXTRACTION CHROMATOGRAPHY IN ISOTOPE PRODUCTION: APPLICATION IN THE PRODUCTION OF ^{67}Ga AND ^{201}Tl*

R. Weinreich+, Deborah F.S. Chamma, A. de Costa e Silva, Lizete Fernandes++, and Ana M.S. Braghirolli.
Instituto de Engenharia Nuclear, Caixa Postal 2186, Rio de Janeiro, Brazil.

Extraction chromatography is a rapid and selective separation method (1) in which the complexing agent is first deposited on a carrier material such as fine-grained powder and an aqueous solution is then percolated rapidly through this material. This method combines the main advantage of solvent extraction (its high selectivity) with those of column techniques (their easy use and technical simplicity). It is mostly used for ultra-rapid and selective separation and identification of radioisotopes (2). Despite its evident advantages, to our knowledge this method has not been applied to isotope production procedures.

For practical use, columns of optimized length and diameter were constructed allowing selective separation with a minimum volume of liquid. As carrier material, Voltalef 300 LD powder (Polymonochlorotrifluoroethene) was used which is chemically inert and has good adhesivity for a complexing agent such as TBP. The extraction behaviour of many ions in TBP is already well-known from reprocessing of nuclear fuel elements; other ions have been investigated in tracer experiments.

For the production of 78-h ^{67}Ga citrate, a target of natural zinc electroplated onto a nickel covered copper backing was irradiated by 24 MeV protons at the external beam of the compact cyclotron CV 28 of IEN Rio de Janeiro. The separation of the no-carrier-added ^{67}Ga was carried out by extraction chromatography from 6 N HCl into TBP. The general extraction behaviour of Ga^{3+} and Zn^{2+} as studied in tracer experiments is shown in Fig. 1. Ga^{3+} is extracted practically 100 %, as indicated in the literature (3). Zn^{2+}, however, is separated selectively from acid concentrations higher than 4 M. In remote hot-cell handling, a 6.5 cm long column of 8 mm diameter is used and the separation is carried out from 6 M HCl. Cu^{2+}, Ni^{2+} and Co^{2+} do not interfere, since they are not extracted with TBP.

The behaviour of iron was of particular interest because it seems to block the accumulation of ^{67}Ga citrate in tumor cells. It could be shown that Fe^{2+} is not extracted, but Fe^{3+} accompanies gallium. Consequently, the apparatus in contact with the solution was generally made from teflon to present oxidation. Dissolution of target material occurs in a reducing medium in which no Fe^{3+} is present. On the column itself, less than 5 % of Fe^{2+} is oxidized to Fe^{3+}. Thus, the quality control showed iron concentrations far below the tolerable limit of 10 µg per 3 mCi ^{67}Ga citrate (4).

The gallium activity was eluted in 6 ml of water. The solution was evaporated to dryness, dissolved in a citrate solution, and sucked through a Millipore filter. Besides the regular quality control, particular attention was paid to the presence of TBP or their decomposition products in the solution. Although the raw solution eluted from the column contains TBP, nothing was found in the final citrate solution.

Even though the CV 28 is not particularly well-suited for ^{201}Tl-production, it was used for this purpose. Because of the maximum proton energy of 24 MeV, only poor yields can be obtained when

applying the commonly-used production method via the lead precursor. Therefore, the production from mercury was studied, about which not much is known.

Again, the chemical separation process chosen was extraction chromatography. The general extraction behaviour of Tl^{+}, Tl^{3+} and Hg^{2+} into TBP-benzene (1:1) as studied in tracer experiments is shown in Fig. 2. Tl^{3+} is extracted from HCl into TBP solution over the entire acidity range (3). In general, the same effect was observed with HNO_3 solutions. Tl^{+}, however, is practically non-extractable from both HNO_3 and HCl solutions at acid concentrations less than 4 M. The partition coefficient of Hg^{2+} from HCl solutions lies between that of Tl^{3+} and Tl^{+}. In HNO_3 solution, however, the partition coefficient of Hg^{2+} shows a distinct minimum at the molarity of 7 M acid. Thus, the separation of ^{201}Tl from mercury can be carried out by extraction chromatography in two ways:

(i) Separation of Tl^{+} from mercury in 7 M HNO_3, elution with water,
(ii) Separation of Tl^{3+} from mercury in 2 M HCl, reduction to Tl^{+} on the column, elution with water.

With an efficient high-current mercury target, the extraction chromatography method will be used for the production of ^{201}Tl at IEN Rio de Janeiro.

---

* Work performed by support of the Brazilian National Atomic Energy Commission (CNEN) and the International Atomic Energy Agency (IAEA), Vienna.

+ On leave of absence from KFA Jülich GmbH, FRG.
++On leave of absence from IPEN São Paulo, Brazil.

(1) Siekierski S. and Fidelis I., J. Chromatogr., 4, 60 (1960).
(2) Trautmann N., Kaffrell N., Behlich H.W., Folger H., Herrmann G., Hübscher D. and Ahrens H., Radiochim. Acta, 18, 86 (1972).
(3) De A.K. and Sen A.K., Talanta, 14, 629 (1967).
(4) Silvester D.J. and Thakur M.L., Int. J. appl. Radiat. Isotopes, 21, 630 (1970).

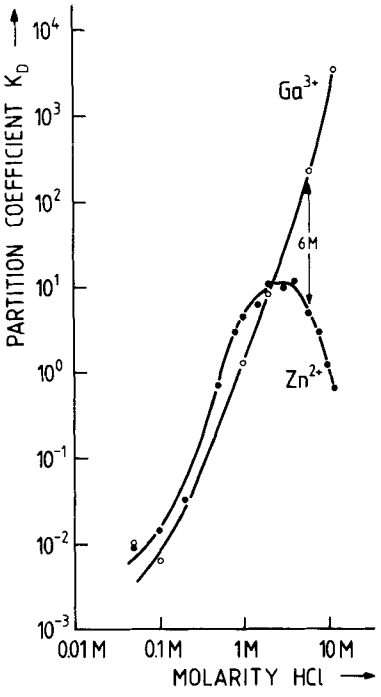

Fig. 1 Extraction behaviour of Ga^{3+} and Zn^{2+} between TBP/benzene 1:1 and HCl solution.

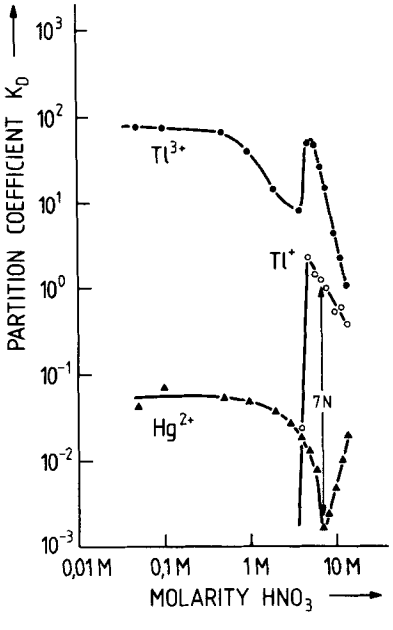

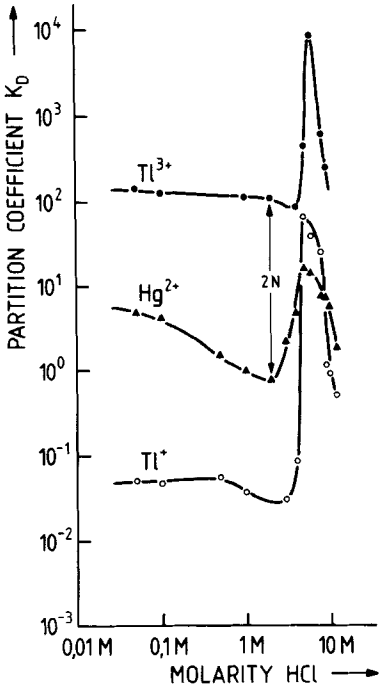

Fig. 2 Extraction behaviour of Tl^+, Tl^{3+} and Hg^{2+} between TBP/benzene 1:1 and HNO_3 solutions (left) and HCl solutions (right), respectively.

RECENT DEVELOPMENTS IN THE PRODUCTION OF SOME SHORT-LIVED NEUTRON DEFICIENT RADIOISOTOPES OF HEAVY HALOGENS

S.M. Qaim.
Institut für Chemie 1 (Nuklearchemie), Kernforschungsanlage Jülich GmbH, D-5170 Jülich, FRG.

The heavy halogens (especially Br and I) form strong covalent bonds with C. Some of the short-lived neutron deficient radioisotopes of those elements are therefore very useful for labelling biomolecules which are eventually applied for regional functional studies using either single photon tomography (e.g. ^{123}I) or positron emission computed tomography (e.g. ^{75}Br). In developing radiopharmaceuticals for regional functional imaging radiohalogens lend themselves to the analogue approach (1).

In this paper some of the new developments in the production of ^{75,77}Br and ^{123}I will be reviewed. Besides discussing the status of nuclear data of commonly used nuclear reactions (cf. 2), a summary of the most recent measurements on some further important or potentially important nuclear processes will be given. Particular emphasis will be given to the positron emitter ^{75}Br (3-7). For the production of ^{123}I the use of the (p,n) and (d,n) reactions on highly enriched ^{123}Te and ^{122}Te, respectively, will be discussed.

Some of the recent advances in the construction of high current targets as well as in the automation of the production processes, absolutely necessary for the large scale production of those radioisotopes, will be outlined. Large scale production methods are now available for the promising positron emitter ^{75}Br (7). The radiochemical aspects of separation and quality control will be discussed briefly.

(1) Stöcklin G. and Kloster G., "Metabolic Analogue Tracers in Computed Emission Tomography" (Ell and Holman eds.), Oxford University Press 1982.
(2) Qaim S.M., "Nuclear data relevant to cyclotron-produced short-lived medical radioisotopes", Radiochimica Acta, in press.
(3) Weinreich R., Alfassi Z.B., Blessing G. and Stöcklin G., Proc. 17th Int. Annual Meeting of Soc. Nucl. Medicine, Innsbruck 1979, p. 209.
(4) Paans A.M.J., Welleweerd J., Vaalburg W., Reiffers S. and Woldring M.G., Int. J. appl. Radiat. Isotopes, 31, 267 (1980).
(5) Qaim S.M. and Weinreich R., Int. J. appl. Radiat. Isotopes, 32, 823 (1981).
(6) Alfassi Z.B. and Weinreich R., Radiochimica Acta, 30, 67 (1982).
(7) Blessing G., Weinreich R., Qaim S.M. and Stöcklin G., Int. J. appl. Radiat. Isotopes, 33, 333 (1982).

PREPARATION OF ^{75}Br BY THE $^{78}Kr(p,\alpha)$ ^{75}Br REACTION*

A.M. Friedman, O. J. DeJesus, P. Harper, and C. Armstrong.
Chemistry Division, Argonne National Laboratory, 9700 South Cass Avenue, Argonne, Illinois 60439 USA.

^{75}Br is a potentially useful isotope for positron emission tomography but its preparation in high purity has required the use of a relatively large cyclotron. We have found that quantities of the order of 30-40 millcuries can be prepared by the $^{78}Kr(p,\alpha)$ reaction at energies between 12 and 15 MeV and the product contains less than 0.1% of ^{76}Br contamination.

Bromine isotopes have been used with increasing frequency in halogenated radiopharmacueticals during the past few years (1-3). This has been due to the greater stability of the C-Br bond, the lower steric hindrance of Br atoms when compared to I atoms, and the absence of thyroid localization of the free ion. The most suitable isotope for positron emission tomography (PET) is ^{75}Br (90% positron decay and half life of 100 minutes). Unfortunately, the usual method of preparation, by the $^{75}As(^{3}He, 3n)$ reaction requires 30-50 MeV ^{3}He ions to prepare ^{75}Br with low levels of ^{76}Br contamination; an energy beyond the range of most medical cyclotrons.

In order to eliminate this problem a theoretical investigation of other preparative methods was undertaken. A calculation of the $^{78}Kr(p,\alpha)$ cross section, using a simple statistical model for compound nuclear formation and using particle emission widths and binding energies common to nuclei in this region (4), indicated a cross section of 10-50 millibarns at proton energies of 12-15 MeV. Since, at these energies, little ^{76}Br would be produced an attempt was made to test the theoretical prediction as this would be a promising production method.

An aluminum gas target holder was used which was 6 cm internal diameter at the rear and which tapered to 2 cm internal diameter at the front and was 31 cm in length. This was filled to a pressure of 1/2 atmosphere with a mixture of 20% ^{78}Kr and 80% ^{80}Kr, or 99% ^{78}Kr; the beam of the FMI CS-15 cyclotron entered the target after having its energy modified by passing through a set of aluminum foils to an energy between 12 MeV to 15 MeV. After each irradiation, the Kr target was cryopumped from the target volume. About 80 ml of water was condensed in the target and this was pumped through a Dowex 50 cation column to remove Rb isotopes and thru a Dowex A-1 (10%) anion exchange column or alumina column (acid washed) to absorb the bromide ions. The yield was obtained by assaying an aliquot of the anion column eluent or the anion feed solution by placing it in a calibrated scintillation spectrometer and counting the 511 keV radiation; the γ-ray spectra of the Br isotopes were measured in a 5" NaI scintillation detector and pulse height analyzer.

The decay curves of the annihilation peaks were used to determine the yields of both ^{74}Br isomers, ^{75}Br, and ^{76}Br. No ^{74}Br was observed (starting 20 minutes after bombardment); the total amount of ^{76}Br or ^{77}Br observed was less than 0.1%.

In Table 2 we list the yields of ^{75}Br which would be formed at these energies under standard conditions (100% ^{78}Kr target, 2 atmospheres of pressure, and 30 μamps of beam current). We have also listed in Table II the cross sections observed for the (p,α) reaction at the various beam energies.

Several conclusions can be drawn by examination of Table 2.

First, the yield of ^{75}Br is sufficient for production of most radiopharmaceuticals.

Second, the amount of ^{76}Br produced will be very small. Therefore, ^{75}Br produced in this fashion will be potentially valuable for preparation of a number of radiophamaceuticals for human use.

*The work was performed under the auspices of the Division of Biological and Environmental Sciences of the United States Department of Energy and the National Institute of Health, grant number NS16835-01.

Third, since ^{75}Br can be produced by this technique and since the ^{78}Kr target gas can be reused, this technique provides an inexpensive method of obtaining ^{75}Br and is available to every facility having a small medical cyclotron.

TABLE 1. Yields of ^{75}Br at End of Bombardment.[a]

E(MeV)	Current μa	Time sec	^{75}Br μCi
12	3	600	0.780
13	3	600	7.83
13	3	300	3.60
14	3	120	2.92
15	3	120	4.10
15	3	120	4.70

[a]Target gas was 20% ^{78}Kr, 80% ^{80}Kr, pressure was 1/2 atmosphere, target length was 31 cm.

TABLE 2. Extrapolated Yields[a] of ^{75}Br at Saturation

E MeV	^{75}Br[a] mCi	Cross Section for ^{75}Br (mbarns)
12	2.4	7.0
13	23.3	68.0
13	21.2	61.9
14	42.4	123.8
15	33.9	99.0
15	47.2	138.0
15	68.2	199.1

[a]Calculated for 31 cm target length, 2 atmospheres of 100% - ^{78}Kr gas, 30 μa beam current.

(1) Kulmala H., Huang C.C., Dinerstein R.J., and Friedman A.M., "Specific In Vivo Binding of ρ-Bromospiperone", Life Science 28, 1911 (1981).
(2) Katzenellenbogen, J.A. et al. (77-Br)-16a-bromoestradiol-17b, a Gamma Emitting Estrogen; 3rd Inter. Sympos. Radiopharm. Chem. St. Louis, June, 1980.
(3) Spicer et al., "A Case for 77-Br Labelled Radiopharmaceuticals", Int. Jour. Appl. Rad. Isotopes 28, 163 (1977).
(4) A good discussion of the statistical model and its relation to the calculation of cross sections is given in Chapters 16 and 17 of "Physics of the Nucleus" by M.A. Preston, Addison Wesley, New York, 1962.

COMPACT CYCLOTRON PREPARATION OF 38.1 MINUTE ZINC-63 FOR POSITRON TOMOGRAPHY

R.E. Bigler, J.R. Dahl, L.S. Rothman, and P.B. Zanzonico.
Biophysics Laboratory, Memorial Sloan-Kettering Cancer Center, New York, NY 10021.

We have developed a relatively simple procedure for the preparation of very large amounts (up to 100 Curies) of zinc-63 ($T_{\frac{1}{2}}$=38.1 min, 93% positron emission) (1) using a small, compact, medical and in-hospital cyclotron. We expect this isotope will find extensive use as a label for compounds for medical research and diagnosis, especially those compounds for human studies which require quantitative positron tomography. The yield for the

$$^{63}Cu(p,n)^{63}Zn$$

reaction is 125 mCi/microampere at the end of a saturation bombardment, using 15 MeV hydrogen ions provided by a Cyclotron Corporation Model CS-15 cyclotron. In a typical production procedure, 1 Ci of Zn-63 is prepared in a 8 minute and 50 microamp bombardment of a copper target mounted on a water cooled internal probe (2) within the cyclotron. The probe can withstand beam currents in excess of 800 microamps. No radiocontaminants were observed between 1.5 min and about 6 hours. Two radiocontaminants are found beyond that time; copper-64 ($T_{\frac{1}{2}}$=12.70 h) at about 0.5% of the total activity at the end-of-bombardment (EOB), which by the chemical processing required to separate zinc from the copper target (discussed below) is removed; and zinc-65 ($T_{\frac{1}{2}}$=244.1 d, 1.46% positron emission) at about 0.002%. The zinc-65 contamination can be reduced if needed by use of a copper-63 enriched target (natural abundance 69.2%). The current cost for copper enriched to 99.89% Cu-63 is about $150.00 per gram (Union Carbide Corp., Oak Ridge National Laboratory, Oak Ridge, TN 37830).

Our automated chemical preparation procedure for providing zinc-63 in a form suitable for direct use in humans or as a precursor for further chemical labeling procedures is given here. The irradiated copper disc is dissolved in concentrated hydrochloric acid containing hydrogen peroxide as a catalyst. After dissolution, the solution is boiled for ten minutes to insure removal of the hydrogen peroxide and cooled. The solution is then diluted to reduce the concentration of HCl to 2.5 Molar. This solution is passed through a 1 cm diameter by 30 cm long column of anion exchange resin (AG-1-X8) equilibrated with 2.5 Molar HCl (3). Copper is removed from the column by washing with 200 ml of 2.5 Molar HCl. To elute the zinc, the column is rinsed with distilled water. Radioactivity content and purity of the sample were measured with a calibrated GeLi gamma-ray spectrometer. The ionic strength of the solution is adjusted to isotonicity (0.9% NaCl) and the pH to pH 6.8-7.1 when the solution is intended for human use. The solution is sterilized by filtration through a 0.22 micron Millipore filter. Pyrogen testing on each batch prior to human use is performed using the Limulus amebocyte lyrate (LAL) assay (Associates of Cape Cod, Inc., Woods Hole, MA 02543) (4). The total time required for this chemical preparation after EOB is about 1 hour. The total copper administered with each dose of Zn-63 does not exceed 15 micrograms as proven by a rapid spot test (5). The spot test is based on the formation of a violet precipitate upon addition of $(NH_4)_2Hg(CNS)_4$ to a solution containing Cu^{+2} and Zn ions (zinc must be added to the test solution). The lowest dose of copper to cause gastrointestinal toxicity (nausea) when administered orally to humans is 120 micrograms per kilogram of body weight. The zinc non-radioactive content is derived from trace quantities contained within the copper target and is insignificant for this purpose. It should be possible to approach the theoretical maximum specific activity of 4.9 x 10^9 Ci/mmol for Zn-63 for purposes involving syntheses of high specific activity radiolabeled compounds.

The schema described by Loevinger and Berman (6) as modified by Bigler (7) was used for radiation absorbed dose estimates. The absorbed radiation dose to the ovaries, liver and total body is 120, 91, and 9.5 mrads/mCi, respectively, for intravenously injected Zn-63; and 100, 48, and 8.0 mrads/mCi for orally admin-

istered Zn-63. The radiation dose contribution from the 0.002% Zn-65 radiocontaminant for the ovaries, liver and total body is 0.2, 1.3, and 0.3 mrad/mCi Zn-63, respectively, for intravenously administered doses; and 0.05, 1.0 and 0.07 mrads/mCi Zn-63 for orally administered doses. We are indebted to E.E. Watson and J.L. Coffey of the Radiopharmaceutical Dosimetry Center, Oak Ridge Associated Universities, for providing the equilibrium dose constants needed for Zn-63 dose calculations.

The foregoing estimates of the radiation dose of Zn-63 and Zn-65 were generated with respect to EOB. Because the half-life of Zn-65 is much longer than that of Zn-63, the amount of the radiocontaminant Zn-65 relative to Zn-63 will increase rather rapidly. Consequently, since large (i.e. multiple Curie) amounts of Zn-63 can be produced, it is the progressively increasing radiation hazard of the Zn-65 which may ultimately limit the useful "shelf-life" of the Zn-63 preparation. We propose a generally applicable solution to this type of situation. The useful "shelf-life"is defined as the time at which the radiocontaminants will give to the critical or dose limiting organ a total dose considered acceptable. We illustrate this procedure for a Zn-63 preparation by choosing a dose doubling as acceptable. The dose due to Zn-63 will equal the dose due to Zn-65 at 6 hours for the ovaries and an intravenous administration of activity.

$$120\, e^{-\frac{(\ln 2)t}{38.1}} = 0.2\, e^{-\frac{(\ln 2)t}{351504}}$$

$$t = 352 \text{ min} = 5.86 \text{ h}$$

Because the preparation of Zn-63 requires about 1 hour, the material can be administered anytime during the next five hours according to the dose doubling criterion. The radiocontaminant, Zn-65, can be greatly reduced by using Cu-63 enriched copper (isotopic composition 99.89%). The amount of Zn-65 would be reduced from 0.002% to 0.000007%, the dose to the ovaries at EOB from Zn-65 can be reduced from 0.2 mrad/mCi Zn-63 to 0.0007 mrad/mCi Zn-63, and the useful "shelf-life" extended from 6 to 51 hours. When a separated isotope is used, it is usually recovered and reused to reduce the target cost. Our procedure provides the copper from the target in a 2.5 Molar 200 ml HCl solution from which it should prove possible to electroplate the copper back onto a target disc in order to recycle the target material with very high efficiency.

The expected uses for zinc-63 include as high priority areas, its direct use in humans as discussed above for nutritionally oriented studies of zinc trace metal metabolism, as a no-carrier-added label for neurotransmitter and other receptor binding ligands, and as a label for monoclonal antibodies.

(1) Lederer, M.C. and Shirley, V.S. Table of Isotopes, 7th Ed., New York, John Wiley and Sons, 1978, p.195.
(2) Dahl, J.R. and Tilbury, R.S., Int. J. Appl. Radiat. Isotop., 23, 431 (1970).
(3) Kraus, K.A. and Moore, G.E. J. Am. Chem. Soc. 75, 1460 (1953).
(4) Washburn, L.C., Sun, T.T., Byrd, B.L. et al. In Radiopharmaceuticals II. New York, Society of Nuclear Medicine, 1979, pp. 767-777.
(5) Feigl, F. and Anger, U. Spot Tests in Inorganic Analyses. Elsevier, New York, 1972, p.205.
(6) Loevinger, R. and Berman, M. MIRD Pamphlet No. 1, Revised, New York, Society of Nuclear Medicine, 1976.
(7) Bigler, R.E. Radiopharmaceutical Dosimetry Symposium, Cloutier, J.L., Snyder, W.S. and Watson, E.E. (Eds.), HEW Publ. 76-8044, 1976, pp. 221-224.

This work was supported in part by the National Institutes of Health, National Heart, Lung and Blood Institute Grant RO1 HL 22371; National Cancer Institute Grant 5 PO1 CA 29502 and 5 T32 CA 09022; U.S. Department of Energy Contract EE-77-S-02-4268; and the NIH, National Cancer Institute Core Grant CA 08748.

PRODUCTION OF HIGH-PURITY ^{77}Kr

G. Blessing, K. Suzuki, He Youfeng, S.M. Qaim, and G. Stöcklin.
Institut für Chemie 1 (Nuklearchemie), Kernforschungsanlage Jülich GmbH, D-5170 Jülich, FRG.

The positron emitter ^{77}Kr [$T_{1/2}$ = 1.2 h] is of interest as a precursor for the 56 h ^{77}Br, and also finds application in lung ventilation studies using conventional γ-cameras and in regional cerebral perfusion studies using positron emission computed tomography. It can be produced via proton- and deuteron-induced reactions on bromine, or via ^{3}He- and α-particle induced reactions on selenium. The (p,xn)- and (d,xn)-reactions on bromine have been well investigated (cf. 1-6). They lead to high yields of ^{77}Kr; the product, however, is strongly contaminated with ^{79}Kr ($T_{1/2}$ = 34.9 h). This work describes a study of the production of high-purity ^{77}Kr via ^{3}He-particle induced nuclear reactions on enriched ^{76}Se and ^{77}Se.

Excitation functions were measured for the first time (7) for the reactions $^{76}Se(^{3}He,2n)^{77}Kr$, $^{77}Se(^{3}He,3n)^{77}Kr$ and several competing reactions up to a ^{3}He-particle energy of 36 MeV. Both of these reactions were found to be very suitable for the production of ^{77}Kr at a compact cyclotron, the former in the energy range of 25→15 MeV and the latter 36→22 MeV.

For production purposes metallic ^{77}Se (94.38 % enriched) is used as target material. A 100 μm thick layer of ^{77}Se is obtained on an Al-sheet by melting at 250 °C and careful spreading. Due to the low m.p. of hexagonal selenium (217 °C), a special rotating target system was developed (8) for irradiations in which the incident particle beam falls at a grazing angle of 19°. The Al-backing is cooled at the back by circulating water at 4 °C.

A degassing technique for the separation of radiokrypton from irradiated ^{77}Se was developed and the effects of release temperature and time were investigated. The removal of radiokrypton follows in two steps, one at ∿ 100 °C and the other at ∿ 220 °C.

Using highly-enriched ^{77}Se-metal as a target material, an irradiation time of about 1 h at a nominal ^{3}He-particle beam current of 15 μA, and a heating time of 14 min at 250 °C, about 60 mCi of ^{77}Kr (at EOB) are produced. The total loss of ^{77}Se after irradiation and removal processes is < 1 %, and the same target is reused for successive production runs. The levels of ^{76}Kr and ^{79}Kr impurities in ^{77}Kr are < 0.35 % (at EOB). Gas chromatographic analysis showed no radiochemical impurities.

(1) Qaim S.M., Stöcklin G. and Weinreich R., Int. J. appl. Radiat. Isotopes, 28, 947 (1977).
(2) Houdayer A.J., Meyer E. and Yamamoto Y.L., Int. J. Nucl. Med. Biol., 4, 83 (1977).
(3) Diksic M., Galinier J.-L., Marshall H. and Yaffe L., Int. J. appl. Radiat. Isotopes, 28, 885 (1977).
(4) Lundqvist H., Malmborg P., Langström B. and Na Chiengmai Suparb., Int. J. appl. Radiat. Isotopes, 30, 39 (1979).
(5) Nozaki T., Iwamoto M. and Itoh Y., Int. J. appl. Radiat. Isotopes, 30, 79 (1979).
(6) De Jong G., Brinkman G.A. and Lindner L., Int. J. appl. Radiat. Isotopes, 30, 188 (1979).
(7) He Youfeng, Qaim S.M. and Stöcklin G., Int. J. appl. Radiat. Isotopes, 33, 13 (1982). See also references cited therein.
(8) Suzuki K., Blessing G., Qaim S.M. and Stöcklin G., Int. J. appl. Radiat. Isotopes, in press.

INVESTIGATION OF ^{123}I AND ^{125}I YIELDS VIA DECAY OF RADIOXENONS PRODUCED IN SALT TARGETS

J. W. Barnes, M. A. Ott, K. E. Thomas, P. M. Wanek, G. E. Bentley, F. J. Steinkruger, and H. A. O'Brien, Jr., Medical Radioisotopes Research Group, Los Alamos National Laboratory, Los Alamos, NM 87545

A study designed to determine the optimum parameters for the production of ^{123}I using the 800 MeV proton beam at LAMPF has been initiated. The principal strategy is to form 2.1-hr ^{123}Xe in an appropriate target, isolate the radioxenon as rapidly as practical after end-of-bombardment, allow ^{123}Xe to decay to ^{123}I, transfer the remaining xenon away from the growth chamber, and recover the radioiodine. The major interference arises from the simultaneous production of 16.8-hr ^{125}Xe, which decays to 60-d ^{125}I. Thus in attempting to maximize the ^{123}I yield but minimize the ^{125}I contamination, the appropriate combination of irradiation and growth periods must be determined. The production variables being studied include: 1) target material; 2) irradiation time; and 3) xenon-to-iodine growth period.

The target materials studied to date include CsCl and CsI. Previous experience with the targets in the production of 36-d ^{127}Xe led to the adoption of an encapsulation system consisting of copper cylinders with welded end pieces. By leaving a small void space at the top, we observed that about 98% of the radioxenon is in this space, presumably released from the target matrix by radiation-induced heating. Thus the xenon can be removed from the container following irradiation by a cryopumping technique within a five minute period.

In the experiments that have been completed thus far, we have irradiated 11 CsCl targets and 1 CsI target for 2- and 4-hr periods. Following an approximately 45-minute period from EOB to start of cryopumping, growth periods of 2, 4, and 6 hours were studied. These data are shown in Table 1, from which the following conclusions can be drawn. The iodide atoms in CsI do not contribute to the ^{123}Xe yield at this energy; because the subsequent ^{123}I yield is reduced by the same amount (35%) as the number of Cs atoms in the target. The average yield of ^{123}I increases by 23% by increasing the growth period from 2 to 4 hours. An increase in irradiation time from 2 hr to 4 hr results in a 55% increase in ^{123}I yield.

No attempt was made in these preliminary studies to maximize production of ^{123}I. Instead we chose a fixed geometry of convenient dimensions to study other parameters. Thus it is inappropropriate to attempt to compare our results with those at other institutions at this time.

We have encountered sufficient variability in the measured ^{125}I contamination to indicate that we must pursue additional development in this area. It appears, however, that the percentage of ^{125}I contamination following a 2-hr irradiation and 2-hr growth period is in the range of 0.2% to 0.5% at the end of the growth period. We saw no increase in this following a 4-hr growth, but we have only one successful experiment under these conditions. Increasing the irradiation time from 2 hours to 4 hours, followed by a 4-hr growth period, resulted in a 41% increase in the ^{125}I contamination. Again, however, this observation is based on a single experiment.

We have studied the oxidation state of radioiodine using an ascending paper chromatographic technique (85% methanol, 15% water with 90 minute developing time). At 1 hr and 24 hr after the end of the growth period, four peaks were observed at R_f values of 0.02, 0.25, 0.45, and 0.75. The identities of the species at the first two R_f values are yet unknown, while the latter two correspond to IO_3^- and I^-, respectively. At 48 hr, only two peaks at 0.02 and 0.75 were observed. Because

the peaks at 0.02 and 0.25 contain unmeasured amounts of ^{121}Te, it is not possible to quote the exact amount of I^-; however, the data show that is is greater than 91% of all other species. We are currently studying anion chromatography techniques that will hopefully be as useful as was the case in the analysis of $^{77}Br^-$.

Although significant progress has been made to date, continued developmental studies are required before large-scale production of ^{123}I can commence. In addition to the planned studies indicated above, we will explore the use of different target materials ($BaCl_2$, CsF, etc.) and other irradiation stations in the Isotope Production Facility where the proton beam is known to be enlarged. A new target encapsulation system will be required to maximize the number of target atoms in the proton beam. Finally, we have begun preliminary design of a targeting system that will permit on-line collection of spallogenic xenon during irradiation.

Table 1. ^{123}I Yields From CsCl and CsI Targets

	Tgt. Wt. (Cs Wt.) (g)	μA·hrs	^{123}I (mCi)	Tgt. Yield (Cs Yield) (mCi/μA·h/g) x 10^3
2 hr I x 2 hr G				
CsCl	30.8 (24.3)	795	69	5.62 (7.10)
	31.3 (24.6)	1050	116	7.04 (8.96)
	28.7 (22.7)	518	120	16.1 (20.4)
	30.1 (23.8)	860	75	5.77 (7.29)
	32.4 (25.6)	530	60	6.98 (8.84)
	21.1 (16.7)	895	67	7.06 (8.92)
CsI	39.5 (20.2)	470	42	4.54 (8.87)
2 hr I x 4 hr G				
CsCl	21.1 (16.7)	825	76	8.69 (11.0)
2 hr I x 6 hr G				
CsCl	22.0 (17.4)	909	43	4.28 (5.41)
4 hr I x 4 hr G				
CsCl	31.6 (25.0)	1389	148	13.5 (17.1)

I = Irradiation; G = Growth Period

PRODUCTION AND RADIOCHEMICAL SEPARATION OF ^{92}Tc AND ^{93}Tc FOR PET

R.M. Lambrecht and S.M. Montner.
Department of Chemistry, Brookhaven National Laboratory, Upton, NY 11973.

This is the first report of the production and rapid radiochemical separation of ^{92}Tc by liquid-liquid extraction for use as a radiopharmaceutical, although ^{92}Tc has been separated by other methods for nuclear studies (1-8) where strict requirements for an injectable solution were not considered. ^{92}Tc has physical properties ($T_{1/2}$ = 4.44m, β^+ = 4.1 MeV, 100%) which are appropriate for use of the radionuclide in combination with PET. The radionuclide should be suitable for PET measurement of the trapping of $^{92}TcO_4^-$ by the thyroid, and of cardiac ejection fraction. Further considerations are required to design ^{92}Tc-labeled compounds that can be related to specific physiological processes. Developments in ^{99m}Tc chemistry may in many instances be applicable to ^{92}Tc or ^{93}Tc.

The ^{92}Mo(p,n)^{92}Tc nuclear reaction was studied with ^{92}Mo of 97.37% and 98.27% isotopic enrichments using 15 MeV protons at either the BNL 60" cyclotron or the Tandem Van de Graaff. The production rate of ^{92}Tc was 75 ± 14 μCi/μA mg cm^{-2} at saturation for $^{92}MoO_3$ targets of 26-39 mg cm^{-2}. The radionuclidic purity was > 98.9% at EOB. Table 1 summarizes the radionuclidic impurities relative to ^{92}Tc.

Table 1. Radionuclidic impurities at EOB relative to 1 mCi of separated ^{92}Tc

Nuclide	$t_{1/2}$	Reaction	(μCi/mCi^{92}Tc)
^{93}Tc	165m	^{92}Mo(p,γ)	< 1.2
^{93m}Tc	43.5m	^{92}Mo(p,γ)	< 1.9
^{94}Tc	293m	^{94}Mo(p,n)	< 0.5
^{94m}Tc	52.5m	^{94}Mo(p,n)	< 6.6
^{95}Tc	20.0h	^{95}Mo(p,n)	< 0.3
^{96m}Tc	51.5m	^{96}Mo(p,n)	< 0.2

The production of ^{93}Tc ($t_{1/2}$ = 165m, β^+ = 13%) by the ^{92}Mo(p,γ) reaction was observed at Ep < 9 MeV. The relative cross sections for production of ^{93}Tc, ^{93m}Tc and ^{92}Tc have been determined to be 25:127:1 (8). ^{93}Tc is potentially useful if a longer-lived positron emitting Tc radionuclide is required.

The radiochemical separation of ^{92}Tc from ^{92}Mo was based on references (9,10). The choice of solvents for the liquid-liquid extraction was based on earlier investigations (11,12). The irradiated $^{92}MoO_3$ was removed from the Al capsule and dissolved in 6 N NaOH and 1 N NaCl containing a few drops of H_2O_2. The NaCl served to 'salt-out' the $^{92}TcO_4^-$ and to retard emulsion formation. A device was designed to affect the remote transfer and radiochemical separation using methyl ethyl ketone extraction, and back extraction with $CHCl_3$ and 0.9% NaCl solution. The radiochemical separation was optimized to 90% in 9 min from EOB. The final solution was passed through a millipore filter and assayed by tlc as $^{92}TcO_4^-$. Mo and Al contamination in the final solution was < 0.7 μg/mL and 0.2 ppm, respectively as determined by colorimetric and atomic absorption methods, respectively.

The original solution was acidified and the ^{92}Mo was precipitated with H_2S. The ^{92}Mo was recovered as the oxide in > 97% yield by heating the $^{92}MoS_3$ in air at 600°C for 4-6 hr. A fully automated radiochemical separation system is presently being debugged.

This research was carried out at Brookhaven National Laboratory, in part, under contract with the U. S. Department of Energy and supported by its Office of Basic Energy Sciences and also by the Office of Health and Environmental Research.

(1) Van Lieshout, R., Monaro, S., Vingiani, G.B., and Morrinaga, H., Phys. Lett. 9, 164 (1964).
(2) De Lange, J.C., Kamermans, R., Vis, R.D., Van Poelgeest, A., and Verheul, H., Nucl. Phys. A258, 141 (1976).
(3) Cochavi, S., McDonald, J.M., Fossan, D.B., Phys. Rev. 3, 1352 (1971).
(4) Poppe, C.H., Grimes, S.M., Anderson, J.D., Davis, J.C., Dunlop, W.H., and Wong, C., Phys. Rev. Lett. 33, 856 (1974).
(5) Tanase, M., J. Radioanal. Chem. 41, 23 (1977).
(6) Kundu, D.N., and Pool, M.L., Phys. Rev. 74, 1775 (1948).
(7) Moore, C.F., Hoffmann, G.W., Fitch, J.F., and Coker, W.R., Phys. Rev. 6C, 1391 (1972).
(8) De Jesus, A.S.M., Rautenbach, W.L., Nucl. Phys. A138, 626 (1969).
(9) Lathrop, K.A., In "Radiopharmaceuticals from Generator-Produced Radionuclides, pp. 39-52, Vienna, IAEA (1971).
(10) Anwar, M., Lahtrop, K., Rosskelly, D., and Harper, P.V., J. Nucl. Med. 9, 298 (1968).
(11) Gerlit, J.B., Proceedings of the 1st International Conference on the Peaceful Uses of Atomic Energy, Geneva, 1955, Vol. 7, pp. 145-151, United Nations, New York, 1956.
(12) Boyd, G.E., and Larson, Q.V., J. Phys. Chem. 64, 988 (1960).

CYCLOTRON PRODUCTION OF RUTHENIUM-97 (NCA) WITH 67.5 MeV PROTONS ON RHODIUM TARGETS

M.C. Lagunas-Solar, M.J. Avila, N.J. Navarro, and P.C. Johnson.
Crocker Nuclear Laboratory (CNL), University of California, Davis, CA 95616 USA.

Because of its desirable nuclear and chemical properties, Ru-97 has already been recognized as a potential label in radiopharmaceutical preparations. Ru-97 (2.88 d) decays by electron capture (100%) with the 216 keV (86%) and 324 keV (11%) gamma rays being its principal emissions. Several methods for the production of Ru-97 have been reported based upon cyclotron and reactor methods (1-6). The reported yields have been rather small. The reactor techniques produce low-specific activity Ru-97 of no-value in radiopharmaceutical synthesis. Comparetto and Qaim (5) used a 36 MeV ^{3}He-beam at 50 μA on natural molybdenum, and reported that ^{97}Ru-yields of about 3 mCi/h can be obtained. Ku et al., in 1978 (7) reported a method able to provide yields of about 100 mCi/day Ru-97 with a 200-MeV proton spallation reaction in Rh-103 targets. This source of Ru-97 has been used for the synthesis of Ru-97-DTPA (8) and Ru-97-PIPIDA [N,α-(p-isopropylacetanilide) iminoacetic acid] (9). These compounds have been reported to have promising applications for imaging the cerebrospinal fluid and the hepatobiliary system. However, the fact that Ru-97 is recognized as a "spallation product" has limited its broader use and consideration for clinical research.

During the investigation of Rh-103 targets for the production of Rh-101m (10), using a 67.5 MeV proton beam, Ru-97 was observed among several other Pd, Rh, and Tc isotopes. This prompted the investigation of cyclotron methods for its production and separation from Rh targets. Several reactions are energetically possible with 67.5 MeV proton beams on Rh-103 targets. These reactions, and their Q-values, are given in Table 1. Thick-target and cumulative Ru-97 yields (mCi/uAh) were measured in the 67- to 37-MeV proton energy range. The total cross section (mb) for Ru-97 production was then calculated from the yield data. Results of these measurements are given in Table 2, and shown in Figure 1.

Ru-97 yields of 1.36 mCi/uAh are possible if a 67-MeV proton beam is used, allowing the production of about 1 Ci of Ru-97 per day, if beam intensities >30 uA are available. It should be noted that simultaneous production of Ci-levels of Rh-101m (from Pd-101, and also directly made) is also obtained in the Rh target, under the same experimental conditions as defined above (10).

Target radiochemistry was performed by electrolytic-acid dissolution of the Rh target (6-8 h) (see figure 2) from which no-carrier-added Ru-97 of high-radionuclidic purity (>99.5% Ru-97, no other Ru isotopes were detected) is obtained by acid-distillation (30-60 min.) (see Figure 3). This method provides an excellent separation of Ru-97 from Pd and Rh, as seen by inspection of figures 2 and 3. However, the Ru-97 solution contained small, detectable levels (<0.5%) of Tc-95m (61 d), Tc-95 (20.0 h), and Tc-96 (4.35 d). The presence of these Tc isotopes can be minimized by limiting the incident proton energy to ∿ 57 MeV, although at the expense of ∿35% of the Ru-97 yield (∿ 0.9 mCi/uAh with 57-MeV protons, 57- to 42-MeV energy thick Rh target). Radiochemistry methods to separate Ru, Pd, Rh and Tc are also being studied so as to maximize Ru-97 yields.

(1) Comar D. and Crouzel C., Radiochem. Radional. Letters, 27 (5-6), 307 (1976).
(2) Subramanian G. and McAfee J.G., J. nucl. Med., 11, 365 (1970) (Abstract).
(3) Silvester D.J., Helus F. and Maier-Borst W., Proc. Second Int. Symp. on Radiopharmaceutical Chemistry (Abstract B-22) Oxford, England (1978).
(4) Gessner M., Music S., et al., Int. J. appl. Radiat. Isotopes, 30, 578 (1979).
(5) Comparetto G. and Qaim S.M., Radiochimica Acta, 27, 177 (1980).
(6) Lebowitz E., Klotz P., et al., J. nucl. Med., 15, 511 (1981) (Abstract).
(7) Ku T.H., Richards P., et al., Proc. Second Int. Congress of the World Federation of Nuclear Medicine and Biology Washington D.C. (1978) (Abstract).
(8) Oster Z.H., Som P., et al., J. nucl. Med., 22, 269 (1981).
(9) Schachner E.R., Atkins H.L., et al., J. nucl. Med., 22, 352 (1981).
(10) Lagunas-Solar M.C., Avila M.J.,

Table 1. Proton induced reactions for the direct and indirect production of Ru-97 from Rh-103 targets.[1]

Reaction	Q-Value (MeV)
Rh-103(p,7n)Pd-97 (3.3 min)→Rh-97 (31.1 min)→Ru-97	-59.5
Rh-103(p,p6n)Rh-97 (31.1 min)→Ru-97	-53.9
Rh-103(p,2p5n)Ru-97	-49.6
Rh-103(p,2d3n)Ru-97	-45.2
Rh-103(p,^{3}He4n)Ru-97	-41.9
Rh-103(p,pt3n)Ru-97	-41.4
Rh-103(p,dt2n)Ru-97	-38.9
Rh-103(p,2tn)Ru-97	-32.7
Rh-103(p,^{4}He3n)Ru-97	-21.2

[1]Mass assignments were obtained from Nuclear Data Tables, "The 1971 Atomic Mass Evaluations". 9 (4-5) July, 1971.

Table 2. Ru-97 yields and total reaction cross section as a function of proton energy.

Proton Energy[1] (MeV)	Ru-97 Thick-Target (mCi/μAh)	Ru-97 Cumulative Yield (mCi/μAh)	Total Cross Section (mb)
67.1	0.028	0.028	18
66.2	0.033	0.061	21
65.3	0.027	0.088	17
64.3	0.031	0.119	20
63.4	0.034	0.153	22
62.4	0.035	0.188	23
61.5	0.038	0.226	24
60.5	0.040	0.266	25
59.5	0.043	0.309	28
58.5	0.046	0.355	29
57.5	0.055	0.410	36
56.5	0.059	0.469	38
55.5	0.068	0.537	43
54.4	0.070	0.607	45
53.4	0.079	0.686	51
52.3	0.087	0.773	56
51.2	0.082	0.855	52
50.1	0.083	0.938	53
49.0	0.081	1.019	52
47.9	0.079	1.098	51
46.7	0.070	1.168	45
45.5	0.061	1.229	39
44.3	0.046	1.275	30
43.1	0.047	1.312	24
41.9	0.025	1.337	16
40.5	0.015	1.352	9.4
39.2	0.008	1.360	5.1
37.8	0.002	1.362	1.4

[1]Average energy (MeV) calculated at center of each Rh foil. Foil thicknesses were 0.1576 g/cm^{2}.

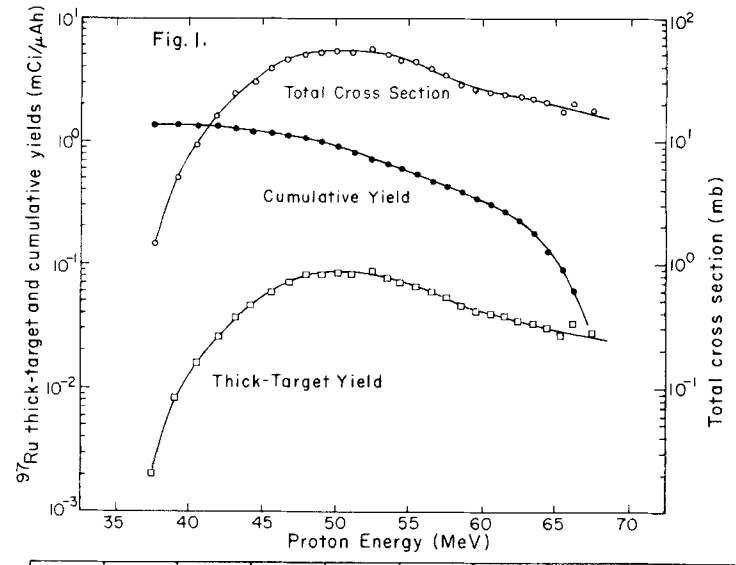
Fig. 1.
Total Cross Section
Cumulative Yield
Thick-Target Yield
^{97}Ru thick-target and cumulative yields (mCi/μAh)
Total cross section (mb)
Proton Energy (MeV)

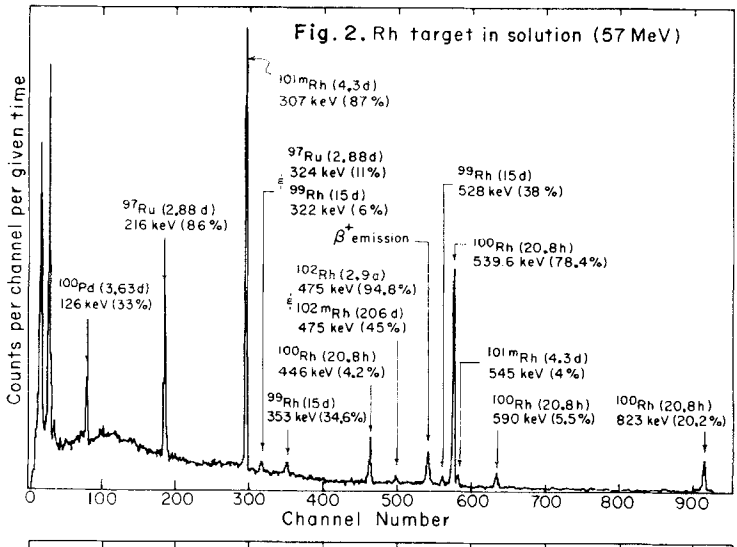
Fig. 2. Rh target in solution (57 MeV)
^{101m}Rh (4.3d) 307 keV (87%)
^{97}Ru (2.88d) 324 keV (11%)
^{99}Rh (15d) 322 keV (6%)
^{97}Ru (2.88 d) 216 keV (86%)
^{99}Rh (15d) 528 keV (38%)
β^+ emission
^{100}Rh (20.8h) 539.6 keV (78.4%)
^{100}Pd (3.63d) 126 keV (33%)
^{102}Rh (2.9a) 475 keV (94.8%)
^{102m}Rh (206d) 475 keV (45%)
^{100}Rh (20.8h) 446 keV (4.2%)
^{101m}Rh (4.3d) 545 keV (4%)
^{99}Rh (15d) 353 keV (34.6%)
^{100}Rh (20.8h) 590 keV (5.5%)
^{100}Rh (20.8h) 823 keV (20.2%)
Counts per channel per given time
Channel Number

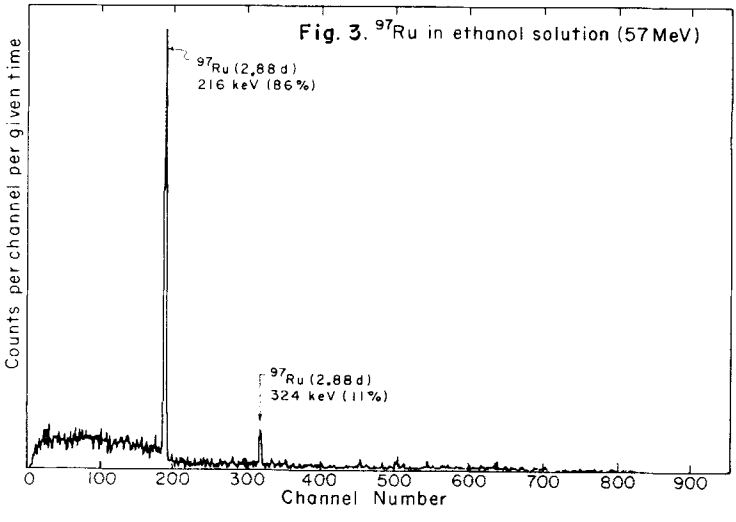
Fig. 3. ^{97}Ru in ethanol solution (57 MeV)
^{97}Ru (2.88 d) 216 keV (86%)
^{97}Ru (2.88 d) 324 keV (11%)
Counts per channel per given time
Channel Number

PRODUCTION OF FISSION MOLYBDENUM ON A TECHNICAL SCALE AT THE NUCLEAR RESEARCH CENTER KARLSRUHE

Sameh A. Ali and H.J. Ache.
Nuclear Research Center Karlsruhe, Institute of Radiochemistry, Postfach 3640, D-7500 Karlsruhe, West Germany.

In the Karlsruhe facility more than one kCi of fission molybdenum of high purity to be used for the preparation of technetium 99m is produced from neutron irradiated targets consisting of highly enriched uranium, which have undergone a short cooling off period after the termination of the irradiation. At this point the total activity of the target is still ca. 100 kCi.

The targets, mainly plates made of UAl_x in an aluminium matrix, are similar to those used in Material Testing Reactor type subassemblies. They are irradiated in a special rig for five to ten days at thermal neutron fluxes between 5×10^{13} and 2×10^{14} n/s cm^2. Following a decay period of at least 12 hours the irradiated material is transferred to the molybdenum production facility in Karlsruhe.

The irradiation fuel element plates are dissolved in sodium hydroxide solution. The aluminium matrix as well as the cesium, strontium, barium, antimony, tellurium, iodine, and molybdenum fission products are dissolved while the krypton and xenon noble gases are released. The non-converted uranium-235 representing more than 99 % of the irradiated amount of uranium-235, the lanthanoids and partly zirconium and ruthenium remain as an insoluble residue.

Because of the extremely high activity and the high content of volatile radioactive fission products and the elevated process temperature required, the dissolution process constitutes a particularly sensitive step. Special remote controlled stainless steel instrumentation and components were developed (1-3) which ensure safe and convenient handling. In a tantalum vessel ammonium rhodanide, tellurium carrier material, sodium sulfite and sulfuric acid are added to the alkaline solution containing the molybdenum after the insoluble residue has been filtered. Addition of potassium iodide accelerates the precipitation of tellurium. After filtration of the tellurium precipitate through a glass wool filter the molybdenum present as the rhodano complex of trivalent and tetravalent molybdenum is fixed on a Chelex-100 colunm (4,5). Chelex-100 is an lonexchanger with funcional nitrilodiacetate groups. It has the property to act as an anion exchanger in highly acidic media and as a cation exchanger in basic media. Its property of acting as an anion-exchanger allows quantitative molybdenum sorption in form of a complex carrying a negative charge. After the column filled with 2M rhodanide and sulfite solution containing sulfuric acid has been washed with pure 2M sulfuric acid and with water, complete elution is carried out by using 1M sodium hydroxide solution. By applying Chelex-100 columns it is possible for the first time to exploit the extremely specific reaction of trivalent and tetravalent molybdenum with rhodanide ions. These anionic species can also be fixed quantitatively on common anionic exchangers, but contrary to the Chelex-100 system, quantitative molybdenum elution is not feasible under practical conditions. The molybdenum elution with sodium hydroxide solution from the Chelex-100 system is exclusively due to the change in the exchange behaviour caused by the medium, namely the transformation of an anion into a cation exchanger and, hence, the repulsion of the negatively charged MoO_4^{--} ions present under these conditions.

The eluted molybdenum is acidified to approximately pH 2 by addition of nitric acid and the molybdenum is adsorbed on an aluminium oxide column (6) in order to eliminate corrosion products and traces of tellurium and iodine.

The column is washed with 0.01M nitric acid, water and 0.01M ammonium hydroxide. Molybdenum elution takes place with 1M ammonium hydroxide. The ammonia solution containing molybdenum is evaporated to dryness and in order to eliminate trace amounts of organic substances the molybdenum is sublimed from a platinum crucible in a quartz vessel at about 850 °C. The sublimed MoO_3 is dissolved in ammonia. After evaporation of the ammonia, sodium hydroxide solution (analytical grade) is added to the solution. The nuclear fuel not burnt up is reprocessed by recycling chemically

the uranium. From the purified uranium new fuel element plates are produced for another irradiation cycle.

To exclude the risk of α-contamination of molybdenum, nuclear fuel recycling is performed in a hot cell specially equipped for this purpose. The main feature of the purification process is the absorption of uranium on a Levextrel column. The efficiency of this recently developed exchange material depends on the presence of TBP incorporated in the solid matrix (7). In this way, the proven extraction properties of TBP are utilized while the drawbacks of liquid/liquid extraction are avoided at the same time, such as fire hazard and the usual difficulties in handling organic solvents. Uranium back-extraction is performed similar to the Purex process with dilute nitric acid. After the uranium is precipitated with ammonium hydroxide and the combustion of the organic components of the filtered ammonium diuranate precipitate the resulting U_3O_8 is transferred to fuel element fabrication.

The U_3O_8 is transferred into UAl_3 via the intermediate step of UF_4 fabrication by melting with aluminium powder in a ceramic furnace at 1350 °C. After remelting and homogenization of the alloy the brittle mass is pulverized, fragmented, mixed with Al-powder and sintered into a matrix. The fuel pellet is fitted into an aluminium frame consistent with the usual framing technique and covered on both sides with Al-sheet. After the aluminium sheets enclosing the fuel have been stitched, the frame is heated to about 500 °C and rolled to the desired size in several steps. The plates formed in this fashion are ready for another irradiation.

(1) Sameh, A. Ali, Jung W., DE-GM 7143037 (1972).
(2) Sameh, A. Ali, Sauermann K., and Jung W., DE-GM 7331934 (1973).
(3) Sameh, A. Ali and Sauermann K., DE-AS 2306592 (1981).
(4) Sameh, A. Ali, Knapp J. and Reinhardt J., DE-PS 2610948 (1974).
(5) Sameh, A. Ali, Knapp J. and Reinhardt J., DE-PS 2758783 (1980).
(6) Tucker W.D., Greene M.W. and Murrenhoff A.P., A.P. Atom Praxis 5, (1963).
(7) Kroebel R., Meyer A., Levextrel, A New Resin for "Extract Elution", I.Chem. E. Symposium No. 42, (1975).

SHORT-LIVED POSITRON EMITTERS FROM RADIOISOTOPE GENERATORS

Y. Yano and T.F. Budinger.
Rm. 222, Donner Laboratory, Lawrence Berkeley Laboratory, University of California, Berkeley, California 94720 U.S.A.

Radioisotope generators provide an alternative to the generally expensive and often unavailable cyclotron production of positron emitters for positron emission tomography (PET). Although the labeling of specific metabolic substrates is not possible, sufficient diversity exists in the in vivo distribution of positron emitters obtained from generators, (Table 1).

In the Sr-82/Rb-82 generator, the 25 day Sr-82 parent is produced by spallation reaction of medium energy protons on a molybdenum target (1). The 76 sec Rb-82 daughter is obtained by elution from a precision flow controlled alumina column generator (2), Fig. 1, to measure myocardial blood perfusion (3) and blood brain barrier changes in brain tumors (4). The present Rb-82 generator has been evaluated in several hundred patient studies over the past 3 years. Figure 2 shows the consistent delivery of the desired Rb-82 activity over a period of several months from a typical loading of 200 mCi of Sr-82 on the alumina column. Rb-82 elutions can be done as often as every 10 min. The breakthrough of radioactive Sr ranges from 10^{-8} to 10^{-6} for hundreds of elutions with 2% saline at pH 8-9. Because of its short half life and high extraction by the myocardium, Rb-82 permits repeated myocardial perfusion studies with 20 mCi of Rb-82 for each study which provides good statistical sampling while minimizing the radiation dose to the patient. The generator is an ideal system for repeated elutions of sterile pyrogen free Rb-82 over a period of several months.

The $^{122}Xe/^{122}I$ generator is a convenient source of the positron emitter 3.6 min I-122 which is separated cryogenically from its 20 hr Xe-122 parent (5). Rapid iodination chemistry is being studied to label amphetamine analogues with I-122 to measure brain blood flow with PET (6). Many mCi of Xe-122 can be produced by the $^{127}I(p,6n)^{122}Xe$ reaction.

A Ga-68 generator using SnO_2 as the support medium for the 275 day Ge-68 parent and 1.0 N HCl as the eluent solution provides $^{68}Ga^{+3}$ directly in the eluate (7). We are evaluating a commercial version of this system (NEN)* for Ge-68 breakthrough, SnO_2 breakthrough*, and labeling chemistry of $^{68}Ga^{+3}$ to transferrin and other compounds.

The $^{128}Ba/^{128}Cs$ generator is presently under development to utilize the 3.8 min Cs-128 positron emitter which has about one-half the extraction of Rb-82 into the myocardium.

Positron-emitters from these four generator systems have a potential for expanding the role of PET in the clinical practice of nuclear medicine. They can be used in conjunction with regionally supplied cyclotron produced fluorine-18 fluorodeoxyglucose, for example, to conduct a comprehensive study of flow and metabolism.

ACKNOWLEDGMENT: This work was supported by the Director, Office of Energy Research, Office of Basic Energy Sciences, Biology and Medicine Division of the U.S. Department of Energy under Contract No. W-7405-ENG-48.

*H. Moore, T.J. Hanrahan, New England Nuclear, Billerica, Massachusetts.

(1) Grant P.M., O'Brien H.A. Jr., and Kahn M., J. Inorg. Nucl. Chem., 37, 413-417 (1975).
(2) Yano Y., Cahoon J., and Budinger T.F., J. Nucl. Med. 22, 1006 (1981).
(3) Budinger T.F., Yano Y., Derenzo S.E., J. Nucl. Med. 20, 603 (1979).
(4) Yen C.K., Yano Y., Budinger T.F., Friedland R.P., Derenzo S.E., and Huesman R.H., "Brain Tumor Evaluation Using Rb-82 and Positron Emission Tomography", J. Nucl. Med., In press (1982).

(5) Richards P., and Ku T.H., Int. J. Appl. Radiat. Isot., 30,250 (1979).
(6) Braun G., Shulgin A.T., and Sargent III T., J. Labelled Compd. Radiopharmaceut., 14, 767 (1978).
(7) Loch C., Maziere B., and Comar D., J. Nucl. Med. 21, 171 (1980).

Table 1. GENERATORS FOR POSITRON EMITTERS

Parent	Half-life	Decay Mode(%)	Daughter	Half-life	Decay Mode(%)	Gammas MeV(%)
Fe-52	8.3 h	β^+(56),EC(44)	Mn-52 m	21.1 m	β^+(98),EC(2)	1.43(100)
Zn-62	9.1 h	β^+(18),EC(82)	Cu-62	9.8 m	β^+(100)	0.59(22)
Ge-68	275 d	EC(100)	Ga-68	68 m	β^+(88),EC(12)	1.08(3.5)
Sr-82	25 d	EC(100)	Rb-82	75 s	β^+(96),EC(4)	0.78(9)
Te-118	6.0 d	EC(100)	Sb-118	3.5 m	β^+(75),EC(22)	1.23(3)
Xe-122	20.1 h	EC(100)	I-122	3.5 m	β^+(100)	0.56(14)
Ba-128	2.43 d	EC(100)	Cs-128	3.8 m	β^+(51),EC(49)	0.44(27)

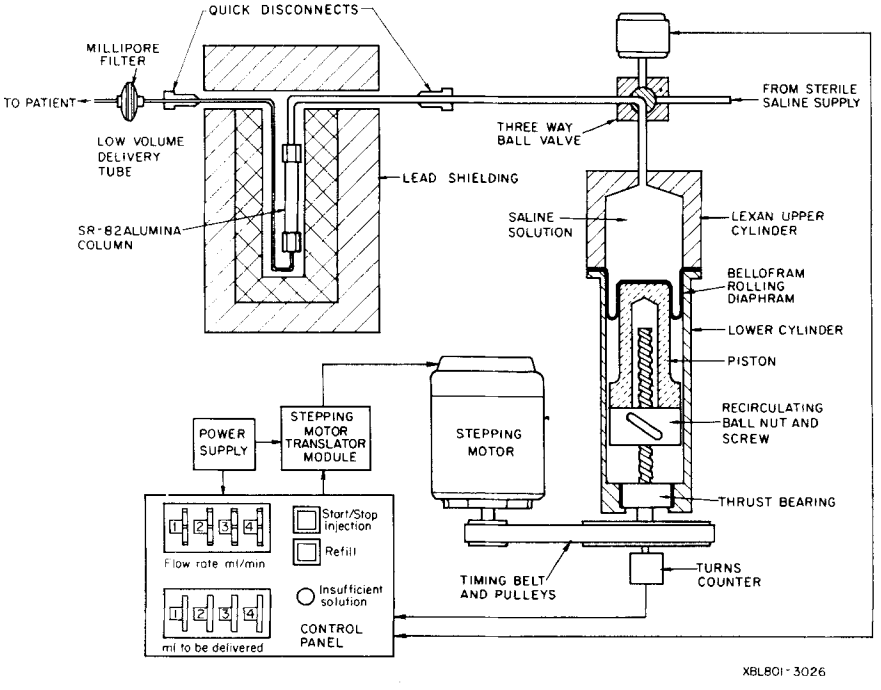

Figure 1. Precision flow-controlled Rb-82 generator with stepping motor drive and micro processor control for bolus or constant infusion studies.

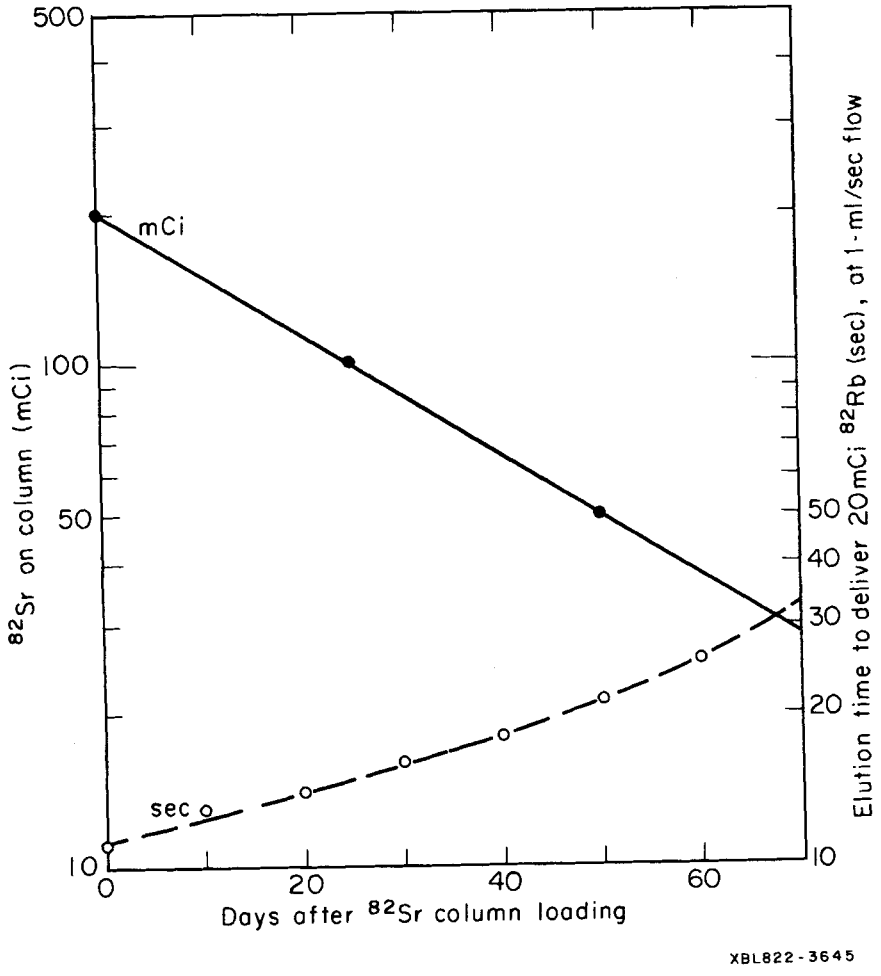

Figure 2. The consistent delivery of 20 mCi of Rb-82 for each elution over 70 days as a function of length of elution time in sec relative to the decay of 25 day Sr-82.

DEVELOPMENT AND USE OF THE Hg195m-Au195m GENERATOR FOR FIRST PASS RADIONUCLIDE ANGIOGRAPHY OF THE HEART

R. Bett, J.G. Cuninghame, H.E. Sims, H.H. Willis, AERE Harwell, Didcot, Oxon, England.
D.S. Dymond, W. Flatman, D.L. Stone, St. Bartholomew's Hospital, London, England.
A.T. Elliott, Western Infirmary, Glasgow, Scotland.

The suitability of the radionuclide pair Hg-195m-Au-195m as a generator was first noted by Lebowitz and Richards in 1974 (1) and its development for medical purposes such as first pass angiography was reported by some of the authors of this paper in 1980 (2,3). The 30.5s half life of Au-195m limits the radiation dosages to the patient while making it possible to do repeat studies at short (3m) intervals without the problem of residual background radiation associated with Tc-99m radiopharmaceuticals. The relatively long (40h) half life of the Hg-195m parent gives a reasonable "shelf-life" of 4-5 days for the generator. We now report on the further development of the generator to the point where it is in fairly regular use in the study of left heart haemodynamics of human patients using the standard intra-venous injection technique for first pass cardiac studies(4).

Since gold is mono-isotopic, the best production reaction from the point of product purity is Au-197(p,3n)Hg-195m. However, Hg-195m has a spin of 13/2+ and there were doubts as to whether a reasonable yield of such a high spin isomer could be obtained by means of a (p,3n) reaction. Results obtained from ALICE evaporation code (5), however, predicted a cross section of 900mb at 25-30 MeV bombarding energy and this encouraged us to start a programme of practical irradiations. Irradiations are now carried out with 34 MeV protons on a helium-cooled 0.5mm thick gold metal target, this energy giving the best compromise between yield and purity. The beam energy is reduced by ~8 MeV in passing through the target, giving a yield of Hg-195m of ~ 4.6mCi/μA/h at end of bombardment; 10-20 μA beams are normally used. The only significant radioactive contaminant is Hg-197m (~ 3.5% at e.o.b.); this is not a problem since it decays to stable Au-197.

Separation of Hg-195m from the irradiated target is straight forward. The Au target is dissolved in concentrated HNO_3/HCl(20ml) + 50μg Hg carrier and NO_3^- is removed by boiling with more HCl. Au is then extracted with amyl acetate and discarded. The aqueous solution is neutralised to pH5 with sodium acetate. The yield is ~ 90% of the Hg-195m produced in bombardment.

The extracted Hg-195m is adsorbed on to suitable column material to form the generator. The material originally used (3) was vicinal dithiocellulose (VDTC), first developed for environmental purposes (6). With 10mM NaCN as eluant this gives an elution efficiency of 10-20% of the Au daughter; note, however, that the Au-195m activity in the eluate was only 5-10% of the Hg-195m activity on the column since only 47% of the Hg-195m decays through Au-195m. The breakthrough of Hg-195m was such that the Au-195m was contaminated with it to the extent of 1-2% by activity.

The original columns contained 10-20mCi of Hg-195m and on scaling them up to 50-100mCi difficulties were experienced with radiation damage after a day or so. An examination of alternative column materials led to a choice of thiopropyl sepharose 6B (7). Advantages of this material over VDTC are

a) It is a commercial product whereas VDTC must be prepared by the user. b) Its elution efficiency is about twice that of VDTC. c) It is not so subject to radiation damage. Fig.1 shows its elution efficiency (ratio of Au-195m activity in eluate to Au-195m activity available on the column expressed as a percentage) as a function of NaCN concentration and Fig. 2 shows elution efficiencies for 1 and 2.5mM NaCN as a function of elution volume. Columns now in use contain ~80mg (0.2ml) of sepharose. 0.6ml of 2.5mM NaCN is used as eluant and this gives an elution efficiency of 30%. If desired, 80% of the activity can be injected in 0.4ml by discar the first 0.2ml. Contamination of the eluant by Hg-195m is < 0.01%. Radiation damage to the column is eliminated by storing it when not in use under 2.5mM NaCN containing a radical scavenger such as 2% $NaNO_3$. Before use the $NaNO_3$ is removed by flushing the column with 10ml of 2.5mM NaCN. We are investigating the possible use of physiologically acceptable substances as radical scavengers in the place of $NaNO_3$.

Animal studies with the generator using rabbits, a greyhound and a pig have been carried out with the following results. a) The eluate is apyrogenic and sterile. b) Heart rate, arterial pressure and central venous pressure showed no changes during the administration. c) Plasma and red cell cyanide levels and plasma thiocyanate levels are within the normal range for non-smoking humans, even though 20ml of eluate was administered (the dose for one measurement on a human is 0.4ml). d) Hg levels in the body were negligible.

Au-195m has been used for non-invasive cardiac studies in patients and the results have been compared with those using the standard radio-pharmaceutical, Tc-99m pertechnetate. Diagnostic cardiac images from intravenous administration of 15-20mCi of Au-195m have been identical to the Tc-99m images and assessment of cardiac function has proved highly reproducible. Radiation dosages to the upper arm are 2mR/mCi for Au-195m and the total body dose is 0.02mR/mCi for Au-195m compared to 10mR/mCi for Tc-99m pertechnetate.

The preliminary medical aspects of this work, including details of results on humans (17 cases by 1st February 1982) will be fully reported in a paper to be presented in Paris next week. (8)

(1) Lebowitz E., Richards P., Seminars in Nuclear Medicine, 257 (1974).
(2) Bett R., Coleman G.L., Cuninghame J.G., Sims H.E., Brit. Pat. Appl. No. P8035352 dated 4 Nov. 80.
(3) Bett R., Coleman G.H., Cuninghame J.G., Sims H.E., Elliott A.T., Stone D.L., Nuc. Med. Commun., 2,75 (1981).
(4) Dymond D.S., Jarritt P.H., Britton K.E., Spurrell R.A.J., Br. Heart J., 41,68 (1979).
(5) Blann M., Plasil F., Phys. Rev. Lett. 24,103 (1972).
(6) Marchant W., Environ. Sci & Tech., 8,993 (1971).
(7) Pharmacia Chemicals Ltd.
(8) Dymond D.S., Elliott A.T., Stone D.L., Flatman W., Bett R., Cuninghame J.G., Sims H.E., Willis H.H., 3rd World Cong. of Nuc. Med. and Biol., Paris, Aug. 1982.

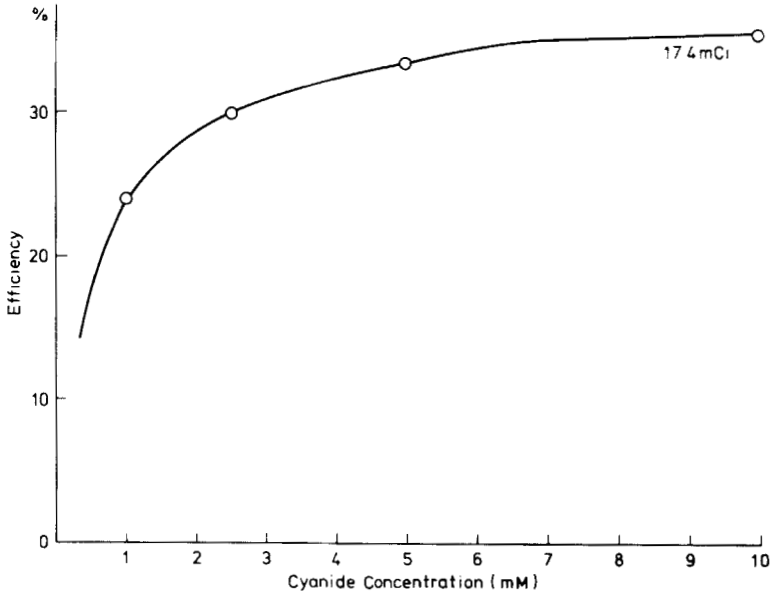
%
30
20
10
0
Efficiency
17·4mCi
1
2
3
4
5
6
7
8
9
10
Cyanide Concentration (mM)

Fig 1

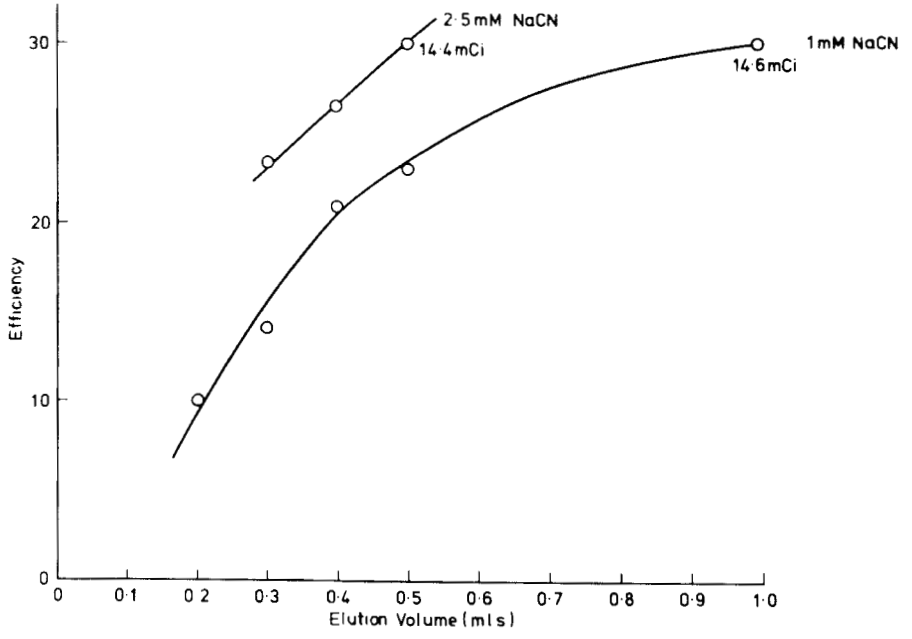
30
20
10
0
Efficiency
2·5mM NaCN
14·4mCi
1mM NaCN
14·6mCi
0
0·1
0·2
0·3
0·4
0·5
0·6
0·7
0·8
0·9
1·0
Elution Volume (mls)

Fig. 2

^{178}W-^{178}Ta GENERATOR: A STUDY OF THE CHROMATOGRAPHIC BEHAVIOUR OF TUNGSTEN AND TANTALUM ON INORGANIC ADSORBENTS

R.D. Neirinckx, A. LeBlanc, M. Vogel, J. Trumper, J.L. Lacy, and P.C. Johnson.
Squibb Institute for Medical Research, New Brunswick, N.J. 08903.

Because of potential in-space utilization of a ^{178}W-^{178}Ta generator on board the Space Lab. an effort has been made to extend the useful life of the ^{178}Ta generator as well as to substitute a more radiation resistant inorganic adsorber for the organic anion-exchanger presently used (1). Therefore, a study of the chromatographic behaviour of tungsten and tantalum was carried out by batch equilibration studies of a ^{178}W-^{178}Ta mixture or ^{182}Ta between inorganic adsorbents and various complexing and non-complexing eluents. The inorganic adsorbents that were evaluated are SnO_2, Al_2O_3, ZrO_2, TiO_2, $TiO_2 \cdot H_2O_2$, Fe_2O_3, polyantimonic acid, CrO_3, MnO_2, chromium phosphate, titanium phosphate, zirconium phosphate, tin phosphate, molybdenyl ferrocyanide, zirconium ferrocyanide, ferric ferrocyanide.

The complexants that were evaluated are fluoride, citrate, tartrate and oxalate. The most promising results were obtained with fluoride containing eluents. A summary of the K_D values of W and Ta between MnO_2 and a 1% NaF solution as a function of pH is shown in Fig. 1. The observed minimum in the adsorption of both tantalum and tungsten is just above the point of zero charge (PZC pH 2.8) of MnO_2. This indicates the desorption of anionic complexes from a cation exchanger. In 1% NaF solutions the tantalum species present are TaF_6^-, TaF_7^{2-} and hydroxo fluoride compounds of complex structure (2,3,4). At higher pH values the stability of the complexes decreases rapidly in favor of hydrolyzed species, which could explain the increasing tantalum adsorption at increasing pH above the PZC.

The K_D values obtained with the inorganic adsorbents, eluted with a pH 6 1% NaF solutions are summarized in Table 1. The $K_{D_W}/K_{D_{Ta}}$ ratio for these systems do not lend themselves to the development of a suitable ^{178}Ta generator.

Most other adsorbent/complexing eluent combination adsorbed tantalum more strongly than tungsten, with K_D values for both tungsten and tantalum declining with increasing pH.

The following conclusions can be drawn from these experiments:

1. The kinetics of adsorption and desorption of tantalum and tungsten are very slow, leading to large discrepancies in K_D values obtained by adsorption or desorption procedures.

2. In the absence of complexing agents the earth acid tantalum forms very stable hydrolyzed compounds (5) that strongly absorb to almost all inorganic exchangers over a wide pH range. Hydrolysis with the hydration water of the adsorbent may be the reason for the strong tantalum binding.

3. Complexing agents are effective at desorbing tantalum from inorganic exchangers. However, solubility of the adsorbents and desorption of tungsten are obstacles that must be overcome on the way to a ^{178}W-^{178}Ta generator based on inorganic adsorbents.

Table 1

K_D values for W and Ta between inorganic adsorbents and aqueous solutions, containing 1% NaF (equil. time = 10')

Adsorbent	K_D			
	W		Ta	
	adsorption	desorption	adsorption	desorption
stannic oxide	260	1,600	73	800
Tin-phosphate	7	85	7	50
titanium oxide	60	450	90	700
zirconium oxide	10	410	13	1,500
zirconium phosphate	7	140	4	100
copper ferrocyanide	8	27	20	60

(1) Neirinckx R.D., Jones A.G., Davis M.A., Harris G.I., and Holman, B.L., J. Nucl. Med., 19, 514 (1978).

(2) Pakholkov, V.S., and Suntsov A.S., Zh. Prikl. Khi., 49, 737 (1976).

(3) Pakholkov V.S., and Suntsov A.S., Zh. Prikl. Khim., 52, 1484 (1978).

(4) Laskorin B.N., Vodolazov L.S., Fedulov Y.N., Schishkina E.G. and Petrenko V.I., Zh. Neorg. Khim., 24, 3082 (1979).

(5) Strelow F.W.E., and Van der Walt T.N., Anal. Chem., 47, 2272 (1975).

Fig. 1

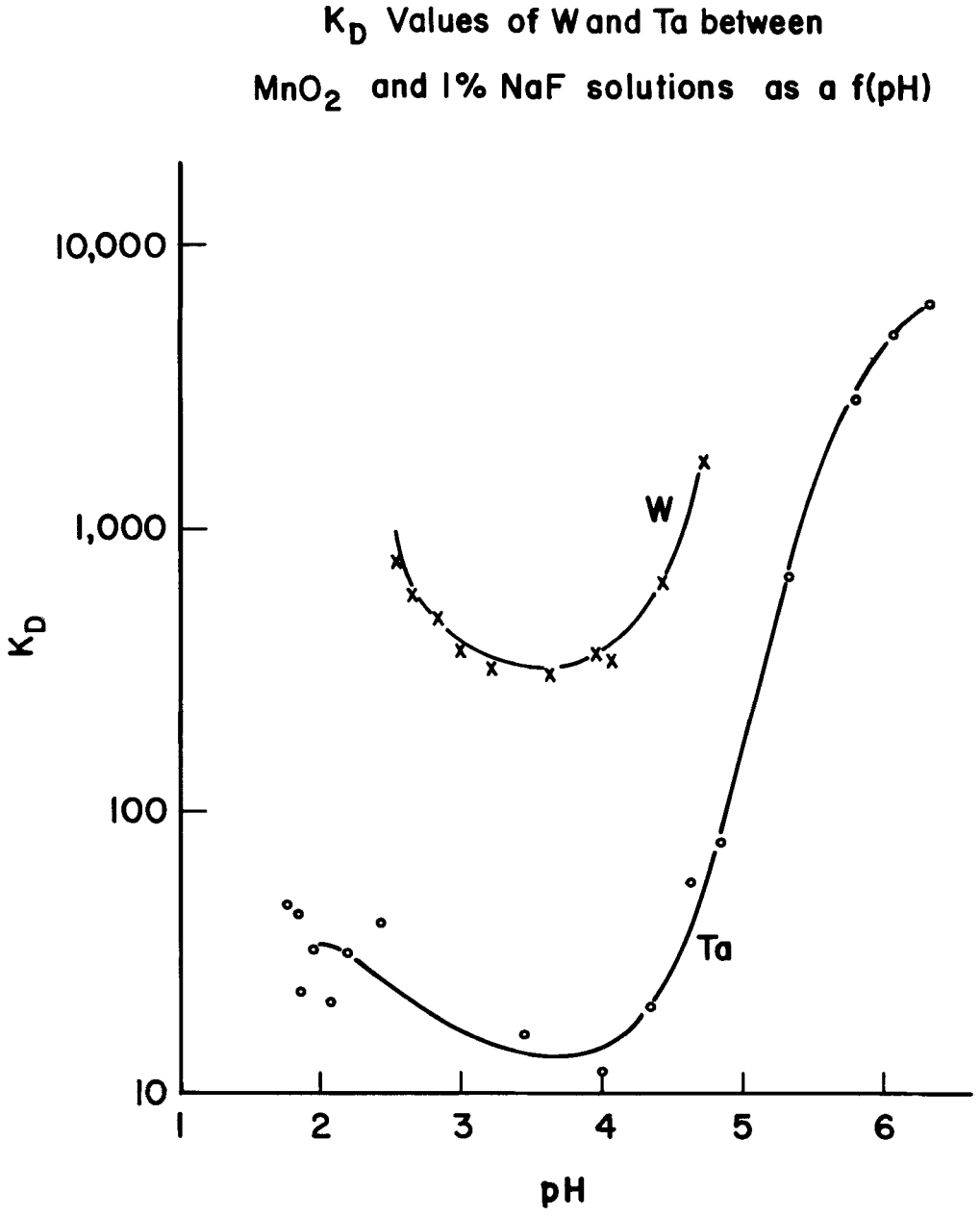
K_D Values of W and Ta between
MnO_2 and 1% NaF solutions as a f(pH)
10,000
1,000
100
10
K_D
W
Ta
1
2
3
4
5
6
pH

A Ba-128 (2.42 d) →Cs-128 (3.62 min.,β+ 61%) GENERATOR SYSTEM FOR PET STUDIES TARGETRY AND RADIOCHEMISTRY METHODS

M.C. Lagunas-Solar, F.E. Little, and H.A. Moore.
Crocker Nuclear Laboratory, University of California, Davis, CA 95616 USA.

Cesium-128 (3.62 min.,β+ 61%, EC 39%) has potential applications in positron-emission tomography (PET) applications, particularly for imaging the myocardium and, or for the assessment of regional blood flow. Other radionuclides used for this latter purpose although using conventional imaging devices, include Cs-129 (1),K-43 (2),Rb-81 (3) and Tl-201 (4). Cyclotron production methods (targetry and radiochemistry) for its production based upon the Cs-133(p,6n)Ba-128 (2.42 d) Cs-128 (3.62 min.) nuclear reaction (Q = -43.98 MeV), were studied.

Cross sections (mb) for the production of Ba-128 (2.42 d), Ba-131 (11.7 d), Cs-129 (32.35 h) and Cs-132 (6.47 d) were calculated from data on induced radioactivities measured on thin - CsCl disc targets, and covering the 67.0- to 36.4-MeV proton-energy range. In addition, thick-target yields (mCi/μAh) were also calculated. These results are given in Table 1.

Table 1. Thick-Target Yields (mCi/μAh) and Cross Sections (mb) for Ba-128, Ba-131, Cs-131, and Cs-129 in the 67.0- to 36.4-MeV Proton-Energy Range.

Proton Energy (MeV)	Ba-128(at EOB)†		Ba-131(at EOB)†		Cs-131(at EOB)†		Cs-129(+9.07 h EOB)†	
	Yield	Cross Section	Yield	Cross Section	Yield	Cross Section	Yield	Cross Section
67.0	354.6	268	20.3	74	51.4	104	547.6	230
65.9	376.4	277	24.3	86	68.1	134	705.7	288
64.8	405.2	298	27.5	98	69.1	136	792.1	324
63.7	373.2	260	22.3	75	67.0	125	795.6	309
62.6	360.0	259	30.8	107	74.3	143	934.3	374
61.4	294.4	213	28.8	101	73.3	142	953.1	383
60.2	232.6	164	25.4	87	70.2	132	967.6	379
59.0	215.5	153	26.2	90	70.4	133	1049.6	413
57.7	180.8	130	31.4	109	75.4	145	1169.8	468
56.6	123.9	88	34.4	118	73.8	140	1168.1	460
55.3	64.3	48	32.6	118	70.0	140	1091.8	453
54.0	49.1	34	34.3	113	75.8	139	1151.0	438
52.7	25.0	17	36.2	120	81.8	150	1144.8	438
51.4	16.8	12	34.8	122	69.5	134	885.5	356
49.9	14.0	10	36.8	121	68.9	125	781.7	294
48.5	11.2	8	37.2	132	69.4	137	593.8	244
47.2	n/d *	--	45.1	163	78.2	156	494.9	205
45.8	n/d	--	47.9	172	72.2	143	308.7	128
44.3	n/d	--	53.6	193	73.9	148	173.7	72
42.8	n/d	--	51.9	182	56.4	110	80.9	33
41.3	n/d	--	67.0	237	65.8	129	56.8	23
39.8	n/d	--	88.7	309	68.9	133	56.8	23
38.1	n/d	--	131.2	445	76.3	143	76.5	30
36.4	n/d	--	168.6	593	71.6	139	104.8	42

*n/d = not detected (†) EOB = end-of-bombardment

The Ba-128-Cs-128 parent-daughter system is in transient equilibrium and the short-lived Cs-128 daughter reaches a maximum a short time (t = 36 min.) after a freshly purified Ba-128 fraction is prepared. Cesium-128 is also short lived enough to allow for sequential studies to be conducted. Furthermore, the 2.42 d Ba-128 parent radioactivity is sufficiently long-lived making Cs-128 available during a span of several days. Because of these characteristics, a transportable generator system was designed, built, and tested allowing a short-lived Cs-128 positron emitter to be taken and used at locations distant from a cyclotron facility.

By summation of the thick-target yields as given in Table 1, for the 67- to 54.0-MeV proton-energy range, the yield of Ba-128-Cs-128 (transient equilibrium) was measured as 3.1 mCi/μAh at EOB, with a 2.32 g/cm^2-thick CsCl target.

Target-radiochemistry using ion-exchange methods allowed the preparation of a transportable generator-type system from which high-radionuclidic purity, radiopharmaceutical quality, no-carrier-added Cs-128, in a 0.9 NaCl pH ∿9 (32.35 h) are also obtained, as given in Table 1. Cross-section data suggest that the Cs-129 is mostly produced from the decay of both Ba-129m (2.13h) and Ba-129 (2.20 h). This allows for the production of high-purity Cs-129 also in a 0.9 NaCl pH ∿9 elution form, provided that the proper radiochemical manipulations are made in the system shown in Figure 1. The efficiency of the generator system is evident when a gamma-ray spectrum of a loaded generator column (Figure 2) is compared with the gamma-ray specta of a Cs-128 eluent solution (Figure 3) obtained utilizing the system shown in Figure 1. By utilizing these methods, current combined cyclotron and linear-accelerator capabilities can generate curie-levels of Ba-128 for use in Ba-128-Cs-128 generator systems for clinical research applications.

(1) Yano Y., Van Dyke D., Budinger T.F., et al. J. nucl. Med. 11, 663 (1970).
(2) Zaret B.L., Strauss H.W., Martin N.D., et al. N. Engl. J. Med. 288, 809 (1973).
(3) Berman D.S., Salel A.F., DeNardo G.L., and Mason D.T. Circulation 52, 619 (1975).
(4) Lebowitz E., Greene M.W., Fairchild R., et al. J. nucl. Med. 16, 151 (1975).
(5) Lambrecht R.M., Gallagher B., Wolf A.P., and Bennett G.W., Int. J. appl. Radiat. Isotopes 31, 343 (1980).

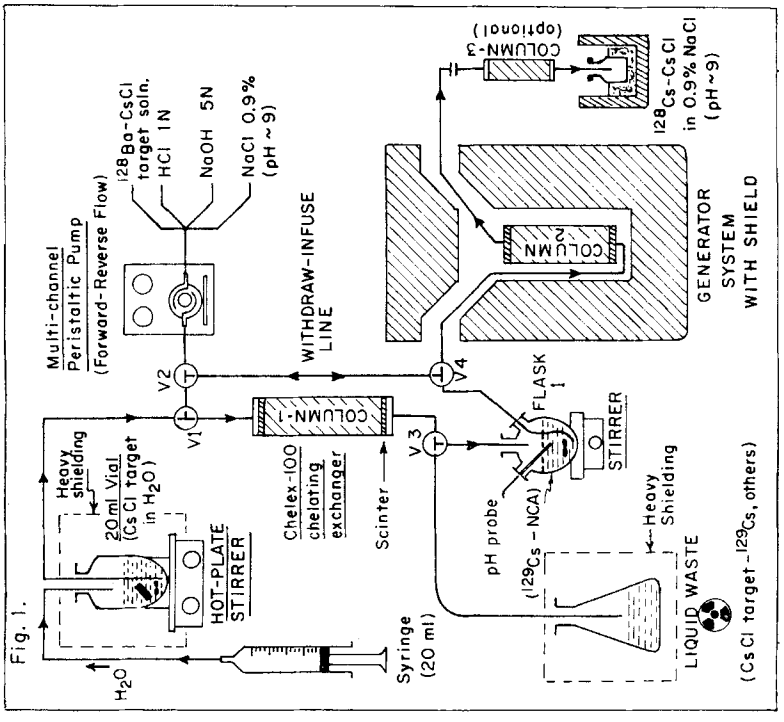
Fig. 1.
Multi-channel Peristaltic Pump (Forward-Reverse Flow)
^{128}Ba-CsCl target soln.
HCl 1N
NaOH 5N
NaCl 0.9% (pH ~ 9)
WITHDRAW-INFUSE LINE
Heavy shielding
20 ml Vial (^{128}Cs Cl target in H_2O)
HOT-PLATE STIRRER
Chelex-100 chelating exchanger
COLUMN-1
Scinter
V1
V2
V3
V4
FLASK 1
STIRRER
pH probe
(^{129}Cs – NCA)
Heavy Shielding
LIQUID WASTE
(^{128}Cs target – ^{129}Cs, others)
Syringe (20 ml)
H_2O
COLUMN-2
COLUMN-3 (optional)
^{128}Cs-Cs Cl in 0.9% NaCl (pH ~ 9)
GENERATOR SYSTEM WITH SHIELD

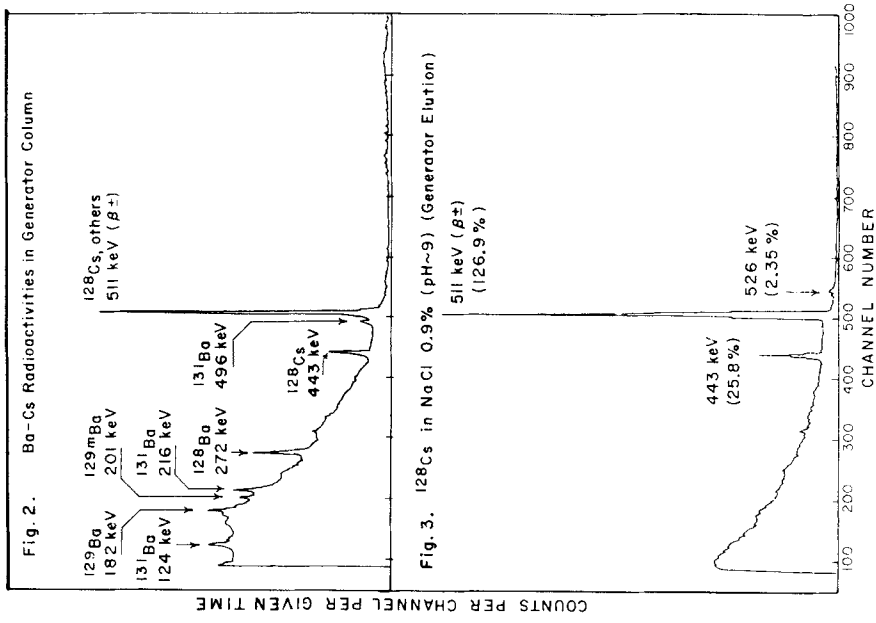
Fig. 2. Ba-Cs Radioactivities in Generator Column
^{129}Ba 182 keV
^{131}Ba 124 keV
^{129m}Ba 201 keV
^{131}Ba 216 keV
^{128}Ba 272 keV
^{131}Ba 496 keV
^{128}Cs 443 keV
^{128}Cs, others 511 keV (β±)
Fig. 3. ^{128}Cs in NaCl 0.9% (pH~9) (Generator Elution)
511 keV (β±) (126.9 %)
443 keV (25.8%)
526 keV (2.35 %)
COUNTS PER CHANNEL PER GIVEN TIME
CHANNEL NUMBER
100 200 300 400 500 600 700 800 900 1000

TECHNETIUM-99M RADIOPHARMACEUTICALS STRUCTURE-ACTIVITY RELATIONSHIPS

R. Münze.
Zentralinstitut für Kernforschung Rossendorf, 8051 Dresden, PF 19, DDR.

At present technetium-99m radiopharmaceuticals are prevailing in routine nuclear medical practice by reason of the favourable nuclear decay characteristic of Tc-99m. The development of compounds which possess higher organ and function specifity is a challenge to modern radiopharmacology and technetium coordination chemistry. Further success depends on more information on chemical structures biodistributions and possible localizing mechanisms of those compounds. In the past many experiments carried out with technetium-99 model substances revealed a high complexity of the chemical reactions between reduced technetium species and appropriate ligand molecules with regard to oxidation states, ligand-metal stoichiometries and polynuclear complex formation in aqueous solutions.

The most important property of the technetium coordination compounds is their kinetic stability against ligand exchange with components in the plasma space. This enables the design of numerous in vivo stable technetium labelled substances with very different chemical structures which are meeting the conditions for specific interactions with biostructures and the adjustment of molecular sizes, ionic charges, and solubilities which are relevant for transport and biodistribution processes.

Most prominent oxidation states in Tc-99-radiopharmaceuticalls are Tc(V), Tc(IV), and Tc(III).

Tc(V) is predominantly stabilized by ligands having soft donors like-S^- and-Se^- as TcO^{3+}, with charged hard donors ($-O^-$, $-COO^-$) as TcO^{3+}, $TcOOH^{2+}$ or $Tc(OH)_2{}^{3+}$, and by hard neutral donors like > NH, $-NH_2$, ⩾ N as $TcO_2{}^+$ centres. Many medically interesting compounds like the Tc(V)hydroxycarboxylato-, Tc(V)dithiolato-, Tc(V)aminothiolato-, Tc(V)pyridino-, Tc(V)diamino-, and Tc(V)cyclam chelates belong to these groups.

Tc(IV) is mainly stabilized as hard $Tc(OH)_2{}^{2+}$ or $TcOOH^+$ centres by hard donor ligands like hydroxycarboxylates, aminopolycarboxylates, phosphates, and phosphonates. These compounds are subject to condensation reactions conducting to poly(homo- and hetero-) nuclear coordination polymers. Many important radiopharmaceuticals like the boneseeking agents are members of that group.

Tc(III) is stabilized by multidentate ligands which are able to shield the metal centre against fast oxidation and hydrolysis.

A further group of medically interesting Tc(III) compounds are the

arsine and phosphine complexes with exchangeable auxiliary ligands. Most of the technetium radiopharmaceuticals are anionic compounds particularly those which have negatively charged ligands. These substances are confined in the plasma space and excreted via glomerular filtration if no special localization mechanism operates. Such a mechanism could be the ligand exchange with biostructures which possess stronger ligator groups than the ligands in the radiopharmaceutical. Ligand exchange seems to be responsible for the high kidney and infarct uptake of the Tc(V) hydroxycarboxylates and tetracycline chelates. Another mechanisms is proposed for the bone and infarct uptake of the phosphate and phosphonate chelates. It is supposed that non required free ligator moities of the coordinated ligand interact with calcium sites in the target tissue. This is supported by the discovery of non phosphorous osteotropic technetium chelates (oxobis-meso-dimercapto-succinato technetate(V), dihydroxo bis d-tartratotechnetate(IV), oligomeric technetiumcitrate complexes) which have free carboxylate and hydroxy groups fitting to coordinate with calcium sites.
In particular cases (substituted iminodiacetic acid chelates for scanning the hepatobiliary tract, Benzoylthioacetamido chelates for kidney function studies) certain stereochemical similiarities with endogeneous substances like bilirubin and hippuric acid can be utilized in the design of function specific technetium radiopharmaceuticals.
More recently neutral (oxinato and thiolato) and cationic (arsine, phosphine, and amine) complexes were prepared in order to get technetium compounds which are able to penetrate vascular and cellular membranes. The usefulness of such substances presupposes an appropriate localizing mechanism either by biotransformations, ligandexchange or interactions with cellular or membranal biostructures resulting in the immobilization of the radioactive label.
A further promising approach is the functionalization of large biomolecules by chelating moities.

PHYSIOCHEMICAL AND STRUCTURAL CORRELATIONS DESCRIBING THE EXCRETION OF HIDAs

A. D. Nunn. Squibb Institute for Medical Research, Georges Road, New Brunswick, New Jersey 08903.

The correlations required for the development of quantitative structure distribution relationships (QSDRs) can be divided into two groups; in one instance, in vivo distribution is correlated with physiochemical data, in the other it is correlated with chemical structure. This paper reports biological data on a series of Tc-99m HIDA complexes. These data have been correlated with the lipophilicity, protein binding and ligand structure of the complexes.

We have synthesized twenty six different HIDA ligands. Tc and other metals have been complexed with some of the ligands in an attempt to elucidate the structure of the metal-HIDA complexes. The Tc-99m complexes of some of them have also been synthesized and their biodistributions determined.

We report here the use of reverse phase HPLC to determine the lipophilicity of the ligands defined in terms of the capacity factor, log k' where -

$$\log k' = \log \frac{V_R - V_M}{V_M}$$

V_R = retention time of ligand

V_M = retention time of unretained sample (acetone)

In addition to log k' values, theoretical lipophilicities were calculated using the substituent hydrophobic constants,(π), tabulated by Hansch and Leo (2). The theoretical lipophilicity of the unsubstituted ligand (phenyl HIDA) was set at zero.

The relationships shown in Fig. 1 allow the prediction of lipophilicity of a HIDA from $\Sigma\pi$ values tabulated by Hansch et al. Three groups of linearily related ligands are obtained when log k' for a ligand is plotted against $\Sigma\pi$. These groups are based on the degree of substitution of the ortho position. Ortho substituents exhibit lower lipophilicities than predicted by $\Sigma\pi$. For example, diortho substituted derivatives are not retained twice as long as the corresponding mono para substituted derivative. If the octanol/water partition coefficients obtained by Molter and Kloss (3) are plotted against $\Sigma\pi$ values, the same linearly related groups of ligands are obtained.

The effect of substitution position on the lipophilicity of the ligands is paralleled by the effect of substitution position on the albumin binding of the Tc-HIDA complexes. Previous work (1) has shown that ortho substituents produce negligible albumin binding whereas para substitutents cause binding proportional to chain length.

A linear relationship is obtained if the renal clearance of the Tc-complexes is plotted against the lipophilicity of the ligand. This relationship encompasses both unsubstituted and diortho substituted ligands but not the mono substituted ligands. As the lipophilicity increases the renal clearance decreases. At the same time the hepatic clearance increases. Thus, contrary to the opinions of Molter and Kloss (4) lipophilicity and protein binding can be used to predict the in vivo distribution of Tc-HIDAs.

The hepatocellular transit times of a Tc-99m complex could not be predicted from either the ligand's lipophilicity or the degree of protein binding of the complex.

The single SDR we have found is that substituents in the ortho position contribute less to the overall lipophilicity than theory predicts. This leads to less protein binding and hence higher renal clearance. The proximity of the ortho positions to the remainder of the molecule suggests that substituents in these positions may be shielded from the environment. Thus the reduced lipophilicity exhibited by ortho substituents may be caused by steric effects.

The identification of these effects is hampered by a lack of knowledge of the

exact conformation of metal-HIDA complexes. We have been unable to determine the complete structure of Tc-HIDA, but we have observed an intermediate which is formed during both carrier and no-carrier-added synthesis. The IR spectrum of the intermediate contains a Tc=O stretch whereas that of the final product does not. The intermediate is probably not due to a partially reduced technetium center as Cr^{3+}-HIDA synthesis shows a similar intermediate and final product.

The information obtained from this work has been used to develop a third generation HIDA (5) which has improved in vivo characteristics in man. In addition some understanding of the general requirements for hepatic and renal clearance of all types of radiopharmaceuticals has been obtained.

(1) Nunn A.D., J. Lab. Comp. Radiopharm., 18, 155 (1981).
(2) Hansch C. and Leo A., "Substituent constants for correlation analysis in chemistry and biology", Wiley, N.Y. (1979).
(3) Molter M. and Kloss G., J. Lab. Comp. Radiopharm., 18, 56 (1981).
(4) Molter M. and Kloss G., J. Lab. Comp. Radiopharm., 18, 196 (1981).
(5) Nunn A.D., Loberg M.D., Conley R.A. and Schramm E., J. nucl. Med., 22, 51 (1981).

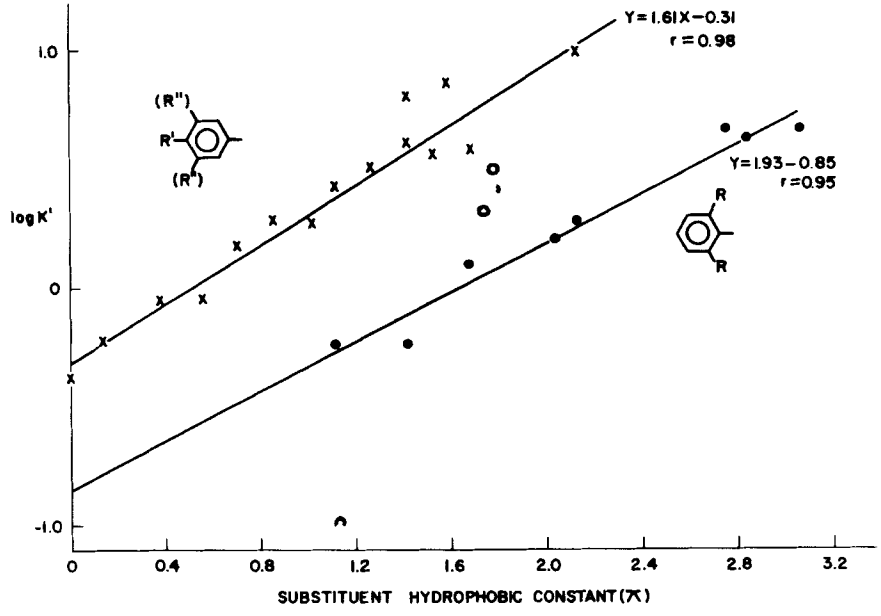

Fig. 1 - Retention by reverse phase HPLC vs. Σπ for various HIDA ligands. X = 2,6 - H,H; ● = 2,6 - R,R; O = 2,6 - R,H

THE MYOCARDIAL UPTAKE AND BIODISTRIBUTION OF KIT FORMULATED, ^{99m}Tc-LABELLED CATIONIC COMPLEX, $Tc(dmpe)_2Cl_2^+$

M.N. Eakins, K.A. Glavan, J.F. Kronauge, R.D. Neirinckx, and M. LaTegola Graff.
Squibb Institute for Medical Research, Georges Road, New Brunswick, N.J. 08903.

Cationic ^{99m}Tc complexes have been recently shown to localize in normal myocardium (1,2). The advantage of using ^{99m}Tc as a radiolabel over ^{201}Tl, the current agent of choice for myocardial imaging, would lie in its lower cost, shorter half-life and better nuclear properties for imaging. However, these advantages are placed beyond the scope of a normal hospital radiopharmacy when the preparation of the ^{99m}Tc-complex is elaborate and requires a chromatographic step for purification (1).

To overcome this problem a lyophilized kit has been developed (3) which, upon addition of generator-produced $^{99m}TcO_4^-$ in 0.9% NaCl solution and heating, produces a cationic technetium complex, ^{99m}Tc-$Tc(dmpe)_2Cl_2^+$ in > 90% purity as assessed by HPLC. Tissue distribution of the complex has been obtained in rat, rabbit, monkey and dog. Rabbits and dogs were also imaged with a gamma camera connected to a computer to obtain time-activity curves for the heart, liver and kidneys.

The in-vivo distribution of ^{99m}Tc-complex in rat, rabbit, dog and monkeys characterized by a rapid blood clearance and localization of the activity in the liver, kidneys and heart (Table 1). The heart to tissue ratios obtained can be compared with the published values for ^{201}Tl chloride (Table 2). The heart to blood ratio for the ^{99m}Tc-complex ranges from 6 in the monkey to 20 in rat while ^{201}Tl ratios range from 34 to 38.

The myocardial clearance of the ^{99m}Tc-complex in rabbit and dog is biexponential as shown in Figure 1. The fast component is presumably due to the washout of vascular activity while the slower component ($T_{\frac{1}{2}}$ dog = 95 minutes; $T_{\frac{1}{2}}$ rabbit = 135 minutes) is presumed to be due to washout from myocardial cells. The washout of ^{201}Tl from the myocardium is slower with half-lives of 4.4 to 7 hours being reported (4,5).

In the 4 species examined, the activity in the liver ranged from 9.5 to 23.4% of the injected dose (%ID) at 20 to 30 minutes after injection (Table 1) with the bile being the preferred route of excretion. Thus in the rat the liver activity was between 11 and 13%ID up to 12 hours after injection and fell to 8%ID 24 hours after injection.

The high adrenal uptake in rats (Table 1) is noteworthy, not from a possible imaging capability since the washout is rapid ($T_{\frac{1}{2}}$ = 60 minutes) but because it provides a possible insight into the drug's mechanism of uptake. By comparing the structure, charge and biological distribution of $Tc(dmpe)_2Cl_2^+$, bretylium and iodobenzylguanidines (6,7), it is conceivable that the observed myocardial and adrenal uptake of these three compounds is by the same carrier-mediated process. However, no direct proof is yet available to sustantiate this hypothesis.

(1) Deutsch E., Glavan K.A., Sodd V.J., Nishiyama H., Furguson D.L., and Lukes S.J., J. Nucl. Med. 22, 897 (1981).

(2) Deutsch E., Bushong W., Glavan K.A., Elder R.C., Sodd V.J., Scholz K.L., Fortman D.L., and Lukes S.J., Science 214, 85 (1981).

(3) Neirinckx R.D., Glavan K.A., Kronauge J.F., and Eakins M.N. Abstract 4th International Symposium on Radiopharmaceutical Chemistry.

(4) Bradley-Moore P.R., Levowitz E., Greene M.W., Atkins H.L., and Ansari A.N. J. Nucl. Med. 16, 156 (1975).

(5) Gewirtz H., O'Keefe D.D., Pohorst G.M., Strauss H.W., McIlduff J.B. and Daggett W.M. Circulation 58, 215 (1978).

(6) Korn N., Buswink A., Yu T., Carr E.A., Carroll M. and Counsell R.E. J. Nucl. Med. 18, 87 (1977).

(7) Wieland D.M., Wu J., Brown L.E., Mangner T.J., Swanson D.P. and Beierwaltes W.H. J. Nucl. Med. 21, 349 (1980).

(8) Schachner E.R., Oster Z.H., Cicale N.R., Sacker D.F., Som P., Atkins H.L. and Brill A.B. Eur. J. Nucl. Med. 6, 585 (1981).

(9) Hamilton G.W., Narahara K.A., Yee H., Ritchie J.L., Williams D.L. and Gould K.L. J. Nucl. Med. 19, 10 (1978).

Table 1

Tissue distribution of ^{99m}Tc-$Tc(dmpe)_2Cl_2^+$ in rat, rabbit, dog and monkey at 30 minutes

	% Injected Dose			
	Rat[a]	Rabbit	Dog	Monkey
Heart	1.61 ± 0.49	1.56 ± 0.34	4.48 ± 0.31	1.30
Liver	11.43 ± 2.60	9.46 ± 2.57	18.53 ± 4.21	23.40
Kidneys	7.33 ± 1.42	11.32 ± 3.10	7.58 ± 0.69	2.34
Blood (per g)	0.10 ± 0.01	0.012± 0.004	0.0037 ± 0.0008	0.0139
Muscle (per g)	0.24 ± 0.06	0.017± 0.007	0.0053 ± 0.0011	0.0124
Adrenal (per g)	3.74 ± 1.12	0.056± 0.008	0.145 ± 0.012	
n	6	4	4	1

[a]20 minutes

Table 2

Heart to tissue ratios for ^{99m}Tc-$Tc(dmpe)_2Cl_2^+$ in rat, rabbit, dog, and monkey at 30 minutes compared with ratios for ^{201}Tl chloride.

	Rabbit ^{99m}Tc	Rat[a] ^{99m}Tc	Rat[b] ^{201}Tl	Beagle Dog ^{99m}Tc	Dog[c] ^{201}Tl	Monkey ^{99m}Tc
Blood	17	20	34	16	38	6
Lung	2	1	3	6	2	1
Liver	2	2	3	1	2	0.4
Muscle	12	9	9	11	6	7
n	4	6	6	6	4	1

a 20 minutes; b reference 8; c reference 9. Ratio of % injected dose per gram of heart to % injected dose per gram of tissue.

Fig. 1

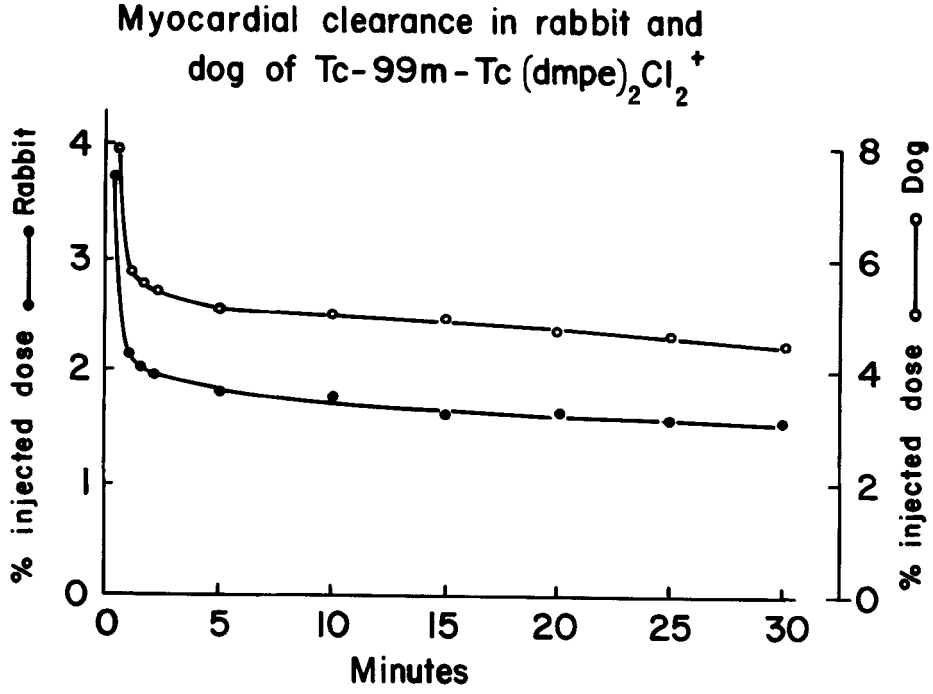
Myocardial clearance in rabbit and dog of Tc-99m-Tc (dmpe)2Cl2+
% injected dose Rabbit
% injected dose Dog
0
1
2
3
4
0
2
4
6
8
0
5
10
15
20
25
30
Minutes

RELATIONSHIPS BETWEEN CHEMICAL STRUCTURE AND BONE LOCALIZATION PROPERTIES OF Tc-99m MONOPHOSPHATES AND MONOPHOSPHONATES

T.S.T Wang, R.A. Fawwaz, and P.O. Alderson. College of Physicians and Surgeons, Columbia University, New York, N.Y. 10032.

Technetium 99m chelated monophosphates amd monophosphonates have been studied for bone localization (1,2,3,4). The purpose of this study was to evaluate a series of structurally related organic monophosphates and monophosphonates in order to determine the relationship between their structure and their bone localization. The compounds were labeled with Tc-99m in the presence of $SnCl_2$. The final pH of the complex was 7.0-7.4. Labeling efficiencies were determined by ITLC with acetone and 85% methanol systems.

Tissue distribution studies were done in rats (n=3 each group) at two hours after iv administration of tracer. The data revealed that only compounds 5,6,8,9,10 and 15 achieved relatively high femur/blood ratios (cts/g.). These results suggest that (1) compounds that can form the most stable five or six membered chelating rings with Tc-99m have the best bone localization; (2) compounds that can only form poorly overlapped four or seven membered rings with the metal yield much lower femur/blood ratios; (3) the CH_2, O, and NH groups are isosters; and (4) that the carbonyl group may play an essential role for resonance stabilization of monophosphates and monophosphonates.

(1) Citrin D.L., Bessent R.G. and Greig W.R., J. nucl. Med., 15, 1110 (1974).
(2) Nelson M.F., Melton R.E. and Van Wazer, J. nucl. Med., 16, 1043 (1975).
(3) Hosain P., Spencer R.P., Ahlquist K.J. and Sripada P.K., J. nucl. Med., 19, 530 (1978).
(4) Kung H.F., Ackerhalt R. and Blau M., J. nucl. Med., 19, 1027 (1978).

Chemical Structures and Femur/Blood Ratios of Monophosphates and Monophosphonates

	Chemical Structure		Femur/Blood/g.* at 2 hrs post-injection
1.	NaH_2PO_4	Sodium biphosphate	1.57±0.33
2.	R—CH_2—OH	Hydroxymethyl phosphonic acid	0.97±0.28
3.	R—CH_2—Cl	Chloromethyl phosphonic acid	1.04±0.26
4.	R—CH_2—NH_2	Aminomethyl phosphonic acid	1.24±0.47
5.	R—CH_2—C(=O)—OH	Phosphonoacetic acid	5.75±1.25
6.	R—CH(CH_3)—C(=O)—OH	Phosphono-2-propionic acid	5.22±1.41
7.	R—C(CH_3)$_2$—C(=O)—OH	Phosphono-t-butyric acid	1.11±0.36
8.	R—O—C(=O)—NH_2	Carbamyl phosphate	6.57±1.71
9.	R—NH—C(=O)—NH_2	Carbamyl iminophosphonate	6.71±1.12
10.	R—O—C(=O)—CH_3	Acetyl phosphate	5.03±0.98
11.	R—O—CH(OH)—COOH	Phosphoglycolic acid	1.18±0.34
12.	R—O—CH(—CH_2OH)—COOH	2-Phosphoglyceric acid	0.81±0.32
13.	R—O—C(=CH_2)—COOH	Phosphoenol Pyruvic acid	1.26±0.29
14.	R—O—CH_2—C(=O)—CH_2OH	Dihydroxyacetone phosphate	0.67±0.09
15.	R—C(=O)—OH	Phosphonoformic acid	6.87±1.37

R = HO—P(=O)(OH)—

* Mean±s.d.

SYNTHESIS AND EVALUATION OF NEW Tc-99m LABELED IODINE SUBSTITUTED ACETANILIDO IMINODIACETATES

G. Subramanian, R. F. Schneider, J. G. McAfee, T. Feld, E. Palladino, and C. Zapf-Longo and F. D. Thomas.

S.U.N.Y., Upstate Medical Center, 750 E. Adams Street, Syracuse, NY 13210.

Earlier Tc-99m hepatobiliary agents (1-4) were mostly IDA derivatives of alkyl-substituted acetanilides. Recently(5) it was shown that bromine substituted on the aromatic ring of 2, 4, 6-trimethylacetanilide considerably altered the biodistribution.

We synthesized iodine substituted 2,6-dimethyl, 2,6-diethyl, 2,4,6-trimethyl and bromine substituted 2,4,6-trimethyl acetanilides and prepared their corresponding IDA derivatives.

Iodine substitution was performed by the method of Suzuki(6). Bromination was carried out at room temperature by adding an equimolar quantity of bromine to a chloroform solution of the chloroacetanilide and stirring for 2-3 days. The chloroform was evaporated and the residue suspended in ethanol/water containing sodium metabisulfite, filtered and purified by recrystallization from petroleum ether. The structure of the compounds were verified by IR, NMR and other standard analytical techniques.

Both the iodination and bromination resulted in substitution at the 3 position on the aromatic ring. The biodistribution of the Tc-99m complexes was performed in rabbits (3-4 kgs) fasted overnight. The results are shown in the Table compared with data previously published(2) on non-halogen substituted compounds.

These data indicate that heavy halogen substitution on the aromatic ring of these compounds reduces urinary excretion, and hastens blood and hepatic clearance rates. For example for 2,6-diethyl derivative the urinary excretion decreased from 7.2% to 1.4% when iodinated. Similar results were noted for others. With the trimethyl derivatives almost identical distribution results from iodine or bromine substitution.

Iodine substitution on the meta position of the aromatic ring of 'HIDA' compounds should provide hepatic imaging agents of superior quality. However further evaluation is needed before these compounds can be recommended for clinical use.

(1) Chervu, L.R., Nunn, A.D., Loberg, M.D. Sem. Nucl. Med. 12,5(1982)
(2) Subramanian, G., McAfee, J.G., Henderson, R.W. Proc. 15th International Meeting of Society of Nuclear Medicine, Groningen, 1977. Editors M. Moldring et al F. K. Schaltauer, Verlag, Stuttgart: 1978; pp. 136-139
(3) Molter, M., Kloss, G. Lab. Compounds Radiopharm. 18,56(1981)
(4) Chiotellis, E., Varvarigov, A. Int. J. Nucl. Med Biol. 7,1(1980)
(5) Nunn, A.D. J. Nucl. Med. 22,5(1981)
(6) Suzuki, H. Org. Synthesis. 51,94(1971)

BIODISTRIBUTION OF ^{99m}Tc LABELED SUBSTITUTED ACETANILIDE DERIVATIVES OF IDA IN RABBITS
PRECENT INJECTED DOSE IN WHOLE ORGAN - AVERAGE VALUES FOR 3-6 ANIMALS EACH

COMPD	BLOOD				LIVER				GIT+GB				URINE			
	5'	15'	30'	60'	5'	15'	30'	60'	5'	15'	30'	60'	5'	15'	30'	60'
DIMETHYL	13.2	3.5	2.4	1.3	31.1	9.8	2.9	1.0	31.3	69.7	74.9	78.8	0.5	5.2	10.0	10.3
IODO DIMETHYL	3.6	1.7	0.4	0.9	21.4	6.0	1.2	0.9	62.7	81.6	90.1	86.0	1.0	2.4	2.3	5.9
DIETHYL	7.4	2.6	1.3	2.2	37.2	21.9	3.3	1.8	29.5	56.9	80.8	81.1	1.8	3.6	3.9	7.2
IODO DIETHYL	3.3	1.7	0.9	0.8	46.7	19.0	5.1	1.6	39.4	70.7	88.1	90.1	0.3	1.2	0.9	1.4
TRIMETHYL	7.9	3.4	2.7	2.5	32.3	10.6	1.7	1.0	29.5	68.0	81.8	81.2	1.8	3.3	5.1	8.1
IODO TRIMETHYL	3.1	0.7	0.4	0.4	35.8	6.3	2.4	0.7	50.9	85.2	90.8	92.7	0.1	0.3	0.3	0.7
BROMO TRIMETHYL	1.6	0.7	0.2	0.5	22.9	4.0	0.5	0.5	67.0	87.7	93.6	92.3	0.3	0.6	0.4	1.3

MECHANISM OF RED BLOOD CELL LABELING WITH ^{99m}TECHNETIUM-PERTECHNETATE AND THE ROLE OF CATION PUMPS AT RBC MEMBRANE ON DISTRIBUTION AND BINDING OF Sn^{2+} AND ^{99m}TECHNETIUM WITH MEMBRANE PROTEINS AND HEMOGLOBIN

M.K. Dewanjee, S.A. Rao, and J.T. Penniston.
Division of Nuclear Medicine and Biochemistry, Mayo Clinic and Mayo Foundation, Rochester, Minnesota 55905, U.S.A.

Permeability of anions and cations in red blood cell (RBC) and presence of Na^+-K^+-ATPase and Ca^{2+}-ATPase on cation transport had been extensively studied (1-5). Although ^{99m}Tc-labeled RBC is routinely used (6,7) for evaluation of ventricular function by sequential administration of tin (II)-pyrophosphate (Sn-PP) and ^{99m}Tc-pertechnetate, their transport via RBC membrane and the role of cation pumps, membrane glycoproteins, and hemoglobin on the binding of Sn^{2+} and ^{99m}Tc are poorly understood. In the past we demonstrated the similarity of binding of Cr^{3+} and oxotechnetium (TcO^{3+}) cation with beta chain of hemoglobin (8,9) and studied the pharmacology of Sn^{2+}-complexes (10). We have recently studied the effect of Sn^{2+}, $^{99m}TcO_4^-$, CrO_4^{2-}, and VO_4^{3-} ions on ATP hydrolysis by ATPases by radiometric assay. There is some similarity of the binding of oxovanadium and oxotechnetium cation with hemoglobin (5,9).

Distribution of ^{99m}Tc and ^{113}Sn in in vitro and in vivo labeled RBC of dogs was determined by labeling, hypotonic lysis, membrane filtration, ultracentrifugation, dissolution of labeled membrane proteins in 1% sodium dodecyl sulfate and gel filtration chromatography of membrane proteins and hemoglobin. The difference in the distribution of ^{99m}Tc and ^{113}Sn on membrane proteins and hemoglobin in in vitro and in vivo labeled RBC is shown in Table 1.

RBC maintains intracellular Na^+ and Ca^{2+} balance by ATP hydrolysis via ATPases. γ-^{32}P-ATP (0.1 nCi/n mole) was used as substrate for Na^+-K^+-ATPase (porcine cortex: 14.38 µg) and Ca^{2+}-ATPase (human RBC:1.75 µg) ATP hydrolysis was carried out at 37° C for 30 minutes in presence of Sn^{2+} and anions (50-400 µM). The reaction was stopped with silicotungstic acid, and phosphomolybdate complex was formed after addition of ammonium molybdate; ^{32}P-labeled phosphomolybdate was extracted with benzene: isobutanol (1:1) and beta radioactivity was measured with a liquid scintillation counter by adjustment of lower level discrimminator for avoiding low energy ^{99g}Tc-beta radioactivity.

Anions e.g. $^{99g}TcO_4^-$, MnO_4^-, CrO_4^{2-} permeate by diffusion and no ATP hydrolysis is demonstrated in Figs. 1 and 2. Sn^{2+} ion stimulates ATP hydrolysis in presence of both enzymes (Fig. 3), suggesting that this cation might be pumped out of RBC like Ca^{2+}, once it diffuses inside red blood cells.

(1) Deuticke B., Naturwissenschaften, 57, 172-179 (1970).
(2) Rothstein A., Cabantchik Z.I., Knauf P., Fed. Proc., 35, 3-10 (1976).
(3) Sachs J.R., Knauf P.A., and Dunham P.B., "The Red Blood Cell", Academic Press, New York (1975).
(4) Barrabin H., Garrahan P.J., and Rega A.F., Biochim. Biophys. Acta., 600, 796-804 (1980).
(5) Cantley L.C., and Aisen P., J. Biol. Chem., 254, 1781-1874 (1979).
(6) Atkins H. L., Eckelman W.C., Klopper J.F., and Richards P., Radiology, 106, 357-360 (1973).
(7) Pavel D.G., Zimmer A.M., and Patterson V.N., J. Nucl. Med., 18, 305-308 (1977).
(8) Pearson H.W., Blood, 22, 218-230 (1963).
(9) Dewanjee M.K., J. Nucl. Med., 15, 703-707 (1974).
(10) Dewanjee M.K. and Wahner H.W., Radiology, 132, 711-716 (1979).

TABLE 1. DISTRIBUTION (%) OF ^{99m}Tc & ^{113}Sn IN RBC AND PLASMA

	In Vitro (30 min.)		In Vivo (30 min.)	
	^{99m}Tc	^{113}Sn	^{99m}Tc	^{113}Sn
RBC membrane	58 ± 9	0.6 ± 0.2	29 ± 5	1 ± 1
Hemolysate	40 ± 7	1.4 ± 0.5	64 ± 7	2 ± 1
Plasma proteins	2 ± 1	98 ± 3	7 ± 1	14 ± 5

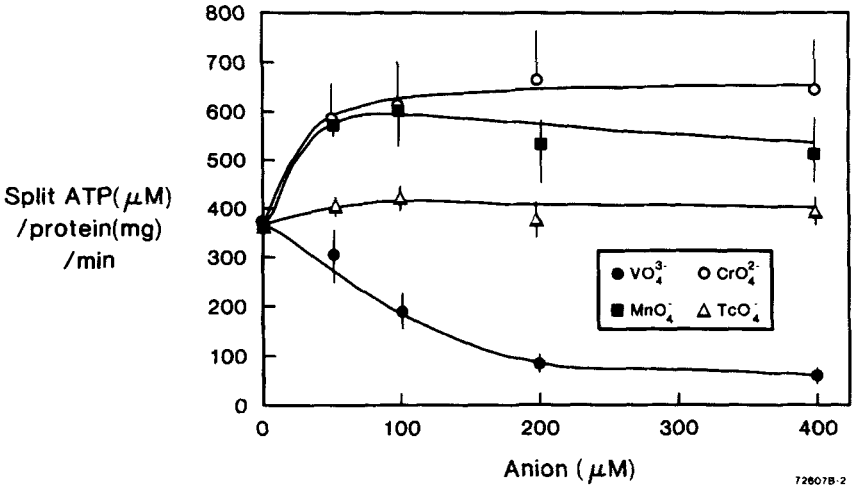

Fig. 1 Effect of anions on ATP hydrolysis with Na^+-K^+-ATPase (Porcine cortex)

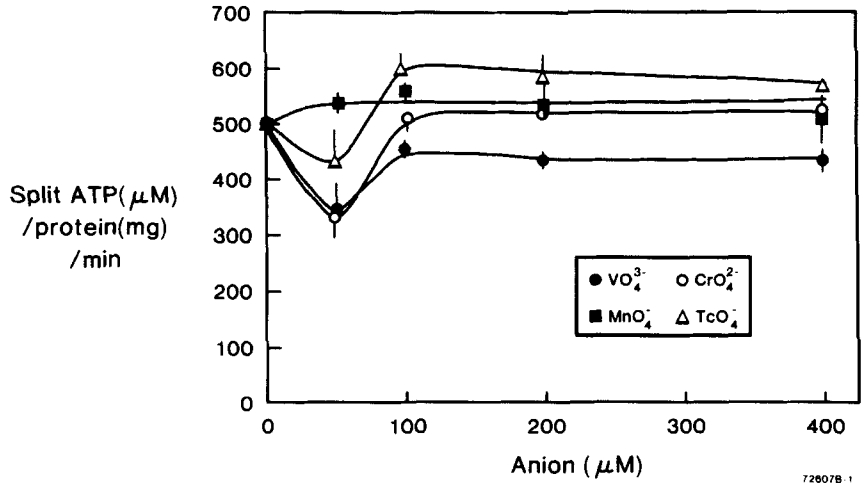

Fig. 2 EFFECT OF ANION ON Ca^{2+} - ATPase (Porcine Cortex) (RADIOMETRIC ASSAY)

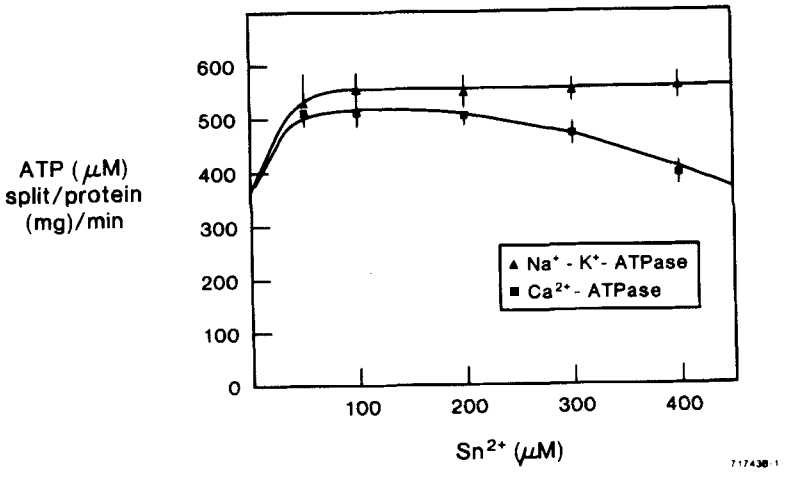

Fig. 3 Effect of stannous ion on ATP hydrolysis with Ca^{2+}-ATPase and Na^+-K^+-ATPase (Radiometric assay)

TETRASULFOPHTHALOCYANINE LABELLED WITH ^{99}Tc, ^{99m}Tc AND ^{67}Ga

J.E. van Lier and J. Rousseau.
Department of Nuclaer Medicine, University of Sherbrooke Medical Center, Sherbrooke, Quebec, J1H 5N4, Canada.

Porphin analogs have a long and controversial history as potential tumor seeking molecules. Over five decades ago the first reports appeared suggesting their potential as tumor visualizing agents through their combined fluorescence and tumor affinic properties (1). Mixed acetic and sulfuric acid derivatives of hematoporphyrin were introduced in the early sixties and the successful detection of neoplasm of the uterian cervix was reported with such analogs (2). However, tissue distribution studies with the ^{14}C- and ^{3}H-labelled products revealed a much higher uptake in the liver, kidneys and spleen than in the tumor (3). Similar discrepencies were reported concerning the tumor seeking properties of tetraphenyl-porphin sulfonate derivatives, even though the successful delineation of human cerebral tumor with the corresponding ^{57}Co labelled derivatives has been reported (4). More recent studies on a series of meso-substituted porphyrins labelled with ^{57}Co revealed a correlation between overall charge and tumor uptake of such complexes with certain derivatives attaining better tumor to blood ratios than ^{67}Ga citrate, although tumor to liver ratios were less favorable (5).

Another class of compounds which mimic the naturally occurring porphyrins are phthalocyanines. They consist of four benzisoindole nuclei fused via nitrogen bridges, and they form stable chelates with metal ions and metal oxides. Metallophthalocyanines are obtained either by condensation of phthalic acid with a bivalent metal cation or by exchange of a metal ion with the central ion of lithium phthalocyanine (6). Uranyl tetrasulfo-phthalocyanine (UO_2-TSPC) was prepared by the latter method and shown to accumulate in brain tumors (7). Although the synthesis of a number of other metallo-TSPC complexes has been described, no further studies on the potential diagnostic applications of analogous γ-emitting complexes have been reported. As a result we prepared both the ^{99m}Tc- and ^{67}Ga-labelled tetrasulfophthalocyanines and evaluated their tissue distribution pattern and tumor uptake in experimental animals.

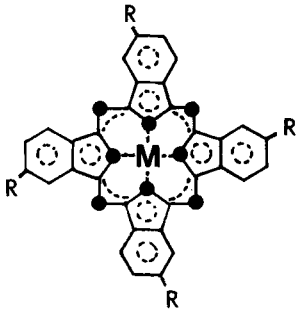

•: nitrogen atom

PC: phthalocyanine M = H_2 R = H

TSPC: tetrasulfo-PC M = H_2 R = SO_3^-

Tc-TSPC: M = Tc R = SO_3^-

Ga-TSPC: M = Ga R = SO_3^-

The chemistry of the Tc-TSPC was studied with the corresponding chelates prepared with the long-lived ^{99}Tc-isotope. Substitution of the central hydrogen atoms in H_2-TSPC by ^{99}Tc-species of different oxidation states gave unsatisfactory results and accordingly we adapted the condensation method for the synthesis of a stable Tc-TSPC complex. Pertechnetate was prepared by dissolving ^{99}Tc metal in nitric acid. The reaction mixture was neutralized, dried and dissolved in an aqueous solution containing hydroxylamine, 3-sulfophthalic acid, urea, ammonium chloride and a trace of molybdate as a catalyst. After water was evaporated at 90°C, the temperature of the mixture was increased to 260°C to allow condensation to occur. Hydroxylamine was choosen as a reducing agent since it decomposes at these elevated temperatures without leaving a residue. The black reaction mixture was suspended in dry methanol, filtered and washed thoroughly with methanol to yield a crude ^{99}Tc-TSPC preparation as a black, water soluble powder with a specific activity of 2.6 mCi/g. Extensive chromatography on ion exchange resin and silica gel gave three blue-green coloured components with ^{99}Tc-TSPC characteristics. Spectral, specific activity and combustion analysis indicated that the major, blue product contained one mol of Tc per mol of TSPC, whereas the spec. act. of the two minor, more polar, green complexes corresponded to about 2 mol of TSPC per mol of ^{99}Tc. In both types of complexes the Tc ion is most likely bonded to three adjacent pyrrole nitrogens and situated above the plane of the TSPC ring system, or sandwiched between two TSPC molecules. The same products were obtained with the short-lived ^{99m}Tc-isotope for *in vivo* studies.

The ^{67}Ga-TSPC complex was readily obtained by direct labelling of the empty H_2-TSPC. Yields of up to 80% based on ^{67}Ga incorporation were obtained, depending on pH, temperature and incubation time. Optimal reaction conditions included a pH of 4.1 and heating for 1 hr at 80°C. Both ^{99m}Tc- and ^{67}Ga-TSPC were found to be stable *in vivo* with distinctly different distribution patterns as compared to the free metal isotopes. With a view towards enhancing its organ selectivity, we are presently working on chemical modifications of the TSPC moeity.

(1) Korbler J., Strahlentherapie 41, 510 (1931).
(2) Lipson R.L., Pratt J.H., Baldes E.J., et al., Obstet. Gynec. 24, 78 (1964).
(3) Gomer C.J. and Dougherty T.J., Cancer Res. 39, 146 (1979).
(4) Winkelman J., Rubenfeld S. and McAffee J., J. Nuclear Med. 5, 462 (1974).
(5) Wang T.S.T., Fawwaz R.A. and Tomashefsky P.,"Radiopharmaceuticals, structure-activity relationships", R.P. Spencer, Ed., Grune and Stratton, New York, 1981, p. 225.
(6) Jackson A.H., "The Porphyrins, vol. I", D. Dolphin, Ed., Academic Press, New York, 1978, p. 374.
(7) Frigerio N.A., U.S. Patent no. 3,027,391, March 27, 1962.

MULTILAMELLAR DSPC LIPOSOMES: VESICLES WITH IMPROVED STABILITY

P.W. Gallagher and M.R. Zalutsky,
Department of Radiology, Harvard Medical School, Boston, MA 02115.

Particulate carriers labeled with α-or β-emitting nuclides such as ^{211}At, ^{188}Re and ^{165}Dy might be useful for both radiotherapy of well-defined lesions via catheter-directed delivery and selected irradiation of isolated body spaces. Recent results with one such particulate, an astatine-211-tellurium colloid, have demonstrated that this approach is highly effective in the treatment of experimental malignant ascites (1). Liposomes are a potentially useful particulate carrier for *in vivo* use, because they are fabricated from biodegradable phospholipids, can be produced in a wide variety of sizes and can in principle be used to entrap any water or lipid soluble radiochemical. Their utility as particulate carriers for radiotherapy will be dependent upon the development of vesicles that are stable and impermeable *in vivo* so that irradiation of normal tissue due to leakage of radioactivity from the vesicle will be minimized. In addition, the liposome must be of sufficient size to prevent its migration as an intact particle from potential target sites.

In an effort to meet these requirements, we have investigated the *in vitro* and *in vivo* stability of multilamellar vesicles (MLV) composed of distearoylphosphatidylcholine (DSPC). Multilamellar vesicles were studied, because they are potentially less permeable than unilamellar vesicles, and since they are larger, their leakage as intact vesicles should be less. DSPC (phase transition temperature Tc = 56°C) was used because recent studies suggest that liposomes fabricated from phospholipids which are solid at physiological temperature have increased retention of their aqueous contents in the presence of serum (2,3).

Multilamellar liposomes were prepared by a variation of the method of Bangham and coworkers (4). Approximately 15 μmoles of DSPC were dissolved in chloroform and evaporated under vacuum. The lipid film was then lyophilized to remove any remaining solvent. About 1 ml of phosphate buffered saline (PBS) containing $^{99m}TcO_4^-$ was then added to the lipid layer, and after heating to 64°C, the mixture was vortexed periodically for 10 min. After an additional 30 min incubation at 64°C, the liposomes were separated from unencapsulated $^{99m}TcO_4^-$ by centrifugation at 50,000g followed by repeated centrifugation at 1000g in order to remove unilamellar vesicles.

With this procedure, 12-14% of the $^{99m}TcO_4^-$ added in the aqueous layer was encapsulated in the MLV. The size distribution of the ^{99m}Tc-DSPC liposomes was determined by both light and electron microscopy using latex spheres of known diameter as standards. The majority of the liposomes were 1-4 μm in diameter.

The *in vitro* stability of ^{99m}Tc-DSPC liposomes was determined by dialysis at 37°C against PBS, 50% fetal calf serum, and 50% synovial fluid. The half times for leakage of ^{99m}Tc activity from the vesicles (Table 1) was less than those reported by Allen (2) for the leakage of calcein from unilamellar vesicles of various compositions, and also less than those reported by Espinola (5) for the leakage of ^{99m}Tc-DTPA from multilamellar vesicles composed of phosphatidylcholine/cholesterol. The decrease in leakage rate per hour observed at longer time points suggests that it would be beneficial to dialyze the liposomes for 6-12 hr prior to *in vivo* use.

The biodistribution of ^{99m}Tc-DSPC multilamellar liposomes so treated was investigated in mice and rabbits. Following intravenous injection, the majority of the activity in both species was found in the lungs, liver, and spleen as would be expected for particles of this size. In the mouse, the activity in these organs was 37%, 33%, and 3.24%, respectively at 30 min post injection clearing to about half these values at 24 hr. In order to study the leakage rate from an isolated body space, the disappearance of ^{99m}Tc activity from the knee was measured following the injection of ^{99m}Tc-DSPC liposomes into the synovial capsule of two rabbits. The knee is an ideal site for study because of the potential for treating rheumatoid arthritis via radiation synovectomy. The average leakage rates determined by serial gamma camera imaging were 2.4% at 1 hr, 13% at 8 hr and 31% at 24 hr. The tissue distribution of ^{99m}Tc activity leaked from the knee (Table 2) indicates that most of the activity which leaked had been excreted at 24 hr. This suggests that one advantage of using liposomes as particulate carriers for radiotherapy is that the radiation absorbed dose to blood forming organs such as the spleen and bone marrow, tissues that normally accumulate small particulates, could be minimized by incorporating the radionuclide within the liposome in a chemical form which is rapidly excreted.

The application of liposomes as radiotherapeutic agents will require the use of radioisotopes with short half lives and vesicles with even greater stability. Experiments are now in progress to investigate the effect on vesicle stability of variables such as the nature of the phospholipid head group and the molecular weight of the entrapped radiochemical.

(1) Bloomer, W.D., McLaughlin, W.H., Neirinckx, R.D., et al., Science, 212, 340 (1981).

(2) Allen, T.M., Biochim. Biophys. Acta, 640, 385 (1981).

(3) Mauk, M.R., Gamble, R.C. and Baldeschwieler, J.D., Science, 207, 309 (1980).

(4) Bangham, A.D., Standish, M.M. and Watkins, J.C., J. Mol. Biol., 13, 238 (1965).

(5) Espinola, L.G., Beaucaire, J., Gottschalk, A. and Caride, V.J., J. Nucl. Med., 20, 432 (1979).

Table 1. Leakage of ^{99m}Tc activity from multilamellar vessicles composed of DSPC

Medium	% Leakage				Leakage
	6 hr	12 hr	24 hr	48 hr	half time
PBS	20	26	35	42	>76 hr
Serum (50%)	29	36	44	56	36 hr
Synovial fluid (50%)	30	40	48	61	28 hr

Table 2. Tissue distribution of ^{99m}Tc activity in the rabbit following injection of ^{99m}Tc-DSPC multilamellar liposomes

Tissue	% injected dose	
	Intrasynovial injection, 24 hr	Intravenous injection, 9 hr*
liver	1.24	39.51
spleen	0.006	3.02
lungs	0.067	23.27
kidneys	0.36	1.79
bladder	0.07	0.03
urine	4.53	0.73
thyroid	0.02	0.01
whole body	15.7+	85.0

*Since activity does not leave the knee as a bolus, an i.v. injection at 9 hrs, the half time at which activity leaked from the knee over 24 hrs, was used for comparison.

+Excluding activity in injected knee.